GROUP 19

Oil-Well Monitoring System

EEL 4915 – Senior Design II

Louis Bengston
Jimit Shah
Kaleb Stunkard

Sponsored by Harris Corporation

Contents

List of Figures

List of Tables

Chapter 1: Project Definition

1.1 Executive Summary

Hydrocarbons and their derivatives are a vital energy source for the world. This energy source must be managed effectively. Failure to do so often results in severe economic and environmental damage. Oil spills/leaks still remain an area of hydrocarbon management that needs improvement. The Gulf of Mexico alone is home to 27,000 abandoned oil well heads. Currently, there is no monitoring system in place to detect oil leakage from these abandoned wells. A system with the ability to actively prevent, monitor and respond to oil spills is desperately needed.

A small army of engineers has been assembled to develop such a system. A plethora of oil detection senor packages can be developed to detect underwater oil leaks. However, all of these packages require power. Obtaining useful electrical energy in the middle of the ocean is not an easy task. Nature provides three main sources of convertible energy. These include: solar, wind, and waves. A mechanical energy team has decided to design and build a hydro turbine to power a generator. Deep water ocean waves will move water over the turbine causing it to rotate. The wave generator will be placed on a large buoy that is tethered to the underwater apparatus. Several factors influence the magnitude, direction and frequency of waves. Thus, ocean waves fluctuate at random. The latter directly impacts the output of the generator. The output of the generator will be a signal of variable voltage, current and frequency. Such a signal can't be used by any electronic components. Additionally, the generator is only efficient if it operates above a particular RPM. Thus, the electrical energy from this generator must be efficiently managed, converted and stored for use by the remaining components of the system.

The team analyzed, designed, built and tested a low cost power management circuit. The AC signal was first converted to high voltage DC. A step down DC-to-DC converter brought the DC voltage down to a usable level. Also, the circuit utilized effective control mechanisms to automatically adjust the load based on input voltage. Excess power was stored in a battery. A charging circuit was integrated into the design to allow the charging of a 12V battery. Lastly, it was designed to withstand harsh weather conditions in the gulf coast.

1.1.1 Hardware Components

All of the main hardware components were designed on a printed circuit board (PCB). These components include:

- Input Circuit (AC-DC)

- Buck Converter (DC-DC)
- Controller
- Charging Circuit

The PCBs will be housed inside a weatherproof enclosure.

1.1.2 Software Components

The software components were split into two main sections. PC Software will be used to interact with and reprogram the digital controllers. The controller itself will also run software that will perform some basic arithmetic.

1.2 Motivation

Energy management solutions have gained significant ground in recent years. With the push for going green, obtaining maximum energy efficiency is in high demand. The electrical engineering group contributed valuable research into advanced power electronics. Hopefully the design has a significant positive impact on the clean-energy movement. The group also looks forward to representing the United States, the University of Central Florida, and Harris Engineering Corporation.

1.3 Goals

Harris Engineering Corporation will be using this system as part of their oil detection monitoring system. Therefore, success was determined by meeting the following goals outlined below:

1. Maximize the energy supplied from the wave generator.
2. Charge lead-acid battery.
3. Protect against battery overcharging.
4. Operate over a range of 80 to 150 rpm.
5. Operate when the generator output voltage is less than the battery voltage.
7. Allow controller to monitor and control the system.

1.4 Objectives

1.4.1 Hardware

The hardware objectives start with specifying the inputs and outputs of the system. The wave generator's output will be used as the input to the system. The system's output will be connected to a battery and sensor package. The system's goal is to transfer the power from the input to the output in the most efficient

manner possible. Efficiency will be verified by connecting the system to a computer. All of the electronic components will be fitted onto a single PCB. The objectives above will be accomplished while maintaining a low parts cost.

1.4.2 Software

The software objectives are limited to PC software and controller software. The PC software will be used to program and monitor the system. Having a PC interface simplifies the development process while providing excellent logging capabilities. The onboard controller software will run a simple algorithm to monitor input voltage and disable the buck converter circuit when voltage drops below a set threshold.

1.5 Requirements and Specifications

1.5.1 General Specifications

Harris Corporation has assigned four groups: three mechanical engineering groups and one electrical engineering group to be a part of this project. The mechanical engineering groups together will be in charge of development of turbine, buoy and the sensor package. The electrical engineering group has been assigned to make sure that the necessary power is supplied to the system.

The hardware must meet the requirements as stated by Harris Corporation. According to these requirements, the system must meet the following:

- Efficiently convert a varying AC signal to a conditioned DC voltage.
- Develop an energy storage method which can continuously deliver power to the sensors.
- Design an automated generator load control system which can optimize the load control for varying input forces and generator RPM's.
- Create a GPS system which can determine and relay the buoy position for a given time.
- Must be able to work in high and low pressure environment.
- Suitable for dry and under water environment.

1.5.2 Hardware

Ginlong Generator Specifications — A Ginlong generator (Model #GL-PMG-500A) is ready to be used to develop wave energy. The electrical specifications of this generator are shown in Table 1.1.

Electrical Specifications	
Rated Output Power(W)	500
Rated Rotation Speed (RPM)	450
Rectified DC Current at Rated Output (A)	20
Required Torque at Rated Power	14.8
Phase Resistance (Ohm)	5
Output Wire Square Section (mm^2)	4
Output Wire Length (mm)	600
Insulation	H Class
Generator configuration	3 Phase star connected AC output
Design Lifetime	>20 years

Table 1.1: Electrical Specifications of Ginlong Generator

Because the generator will be turned by wave energy harnessed through a uniquely designed turbine system, it is expected that the rotations per minute of the generator will vary significantly. No load will be placed upon the generator at startup, but the load control circuitry will ultimately be responsible for maintaining the steadiest possible rotation in the generator. Figure 1.1 shows the power (W) and voltage (V) outputs for the Ginlong generator as functions of rotation speed (RPM). The power output is very low and grows very slowly for low rotation speeds, but at higher rotation speeds, the power output begins to climb more rapidly. The voltage output has an approximately linear relationship with rotation speed, where the voltage in volts is equal to one tenth of the rotation speed in RPM.

Sensor Power Requirements — Sensor power requirements needed to be met in an efficient manner. The sensor package was the most critical part of the project since this package was responsible for detecting the presence of oil in water. According to the sensor team, they used a Wi-Ranger to power the components (sensors, DAQ, etc.). The supply power specification for their project was 12VDC with minimum input current.

Control System — The Control System was comprised of:

- Input Circuit (AC-DC Converter)
- DC-DC Buck Convertor
- PIC microcontroller
- Battery Charging Controller

An **AC-DC Rectifier** was needed to rectify the input AC signal to output DC signal. These were the various requirements for the rectifier:

- Must be able to control a sinusoidal input current
- Maintain input current to be in phase with input voltage
- Variable frequency, voltage and current

- Produce a constant DC signal
- Reduce DC ripple

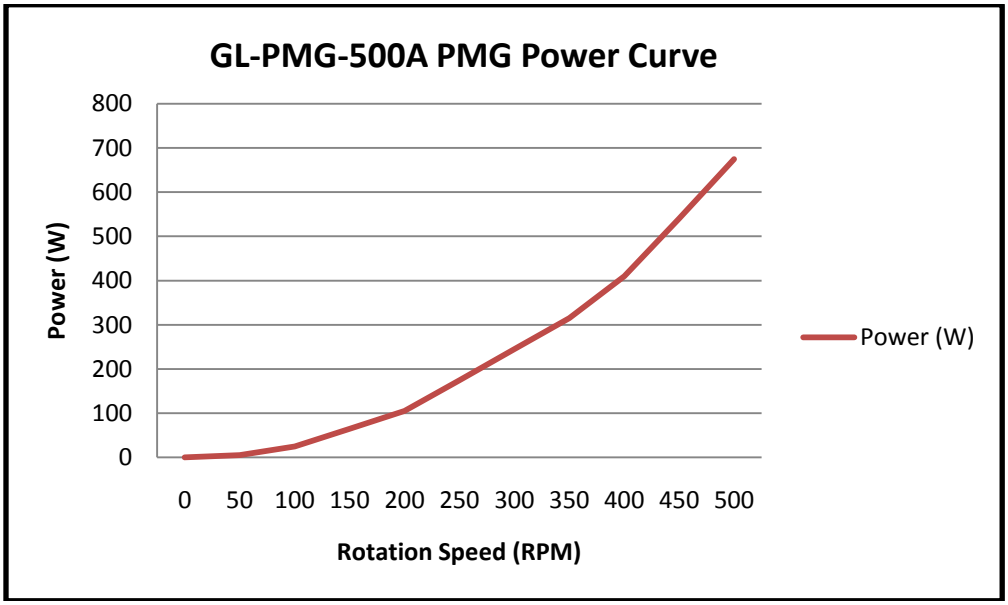

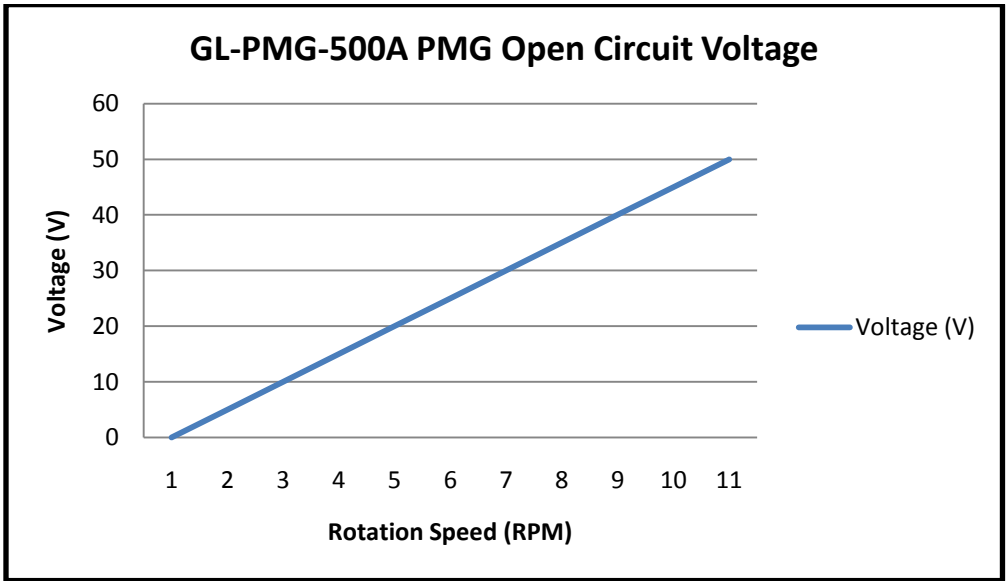

Figure 1.1: Power v. Rotation Speed and Voltage v. Rotation Speed for the Ginlong generator

A **DC-DC Converter** must regulate the input DC signal coming from the input circuit to a constant DC output signal. A major problem in creating such a converter would be its fluctuating output due to the varying nature of the wave speed. Hence, the converter will need to meet or exceed the following expectations:

- Large input voltage capability, up to 60V
- Must be able to produce a constant output voltage of 12V DC to charge the battery.
- Maintain low voltage ripple
- Implement error compensation loop
- Must maintain high efficiency levels

Battery Charging Circuit – An efficient circuit charging design needs to be implemented that can meet or exceed the following requirements:

- Maximize long term charging capacity
- Provide accuracy
- Be able to communicate in various conditions
- Maintain high level efficiency
- Be cost-efficient

1.5.3 System Protection

Since this system was to be placed in volatile conditions, necessary steps needed to be taken to ensure maximum safety. Hence, utmost care was taken while choosing components for the design as they needed to withstand various parameters such as high voltage, power, pressure, etc. If a situation arose such that certain components could pass the threshold of the parameters mentioned above, it was highly likely to cause permanent damage to the system.

In order to protect the system from such drastic conditions, precautions were taken. Protection was implemented in two levels – hardware and software. Also, external protection such as epoxy resin could be used for potting transformers and inductors in order to prevent a short circuit and to maintain a stable, long-lasting life.

1.6 Budget and Financing

Due to the nature of the project, the primary costs were for the components and testing materials. A research lab and certain other facilities were already available for use. These facilities included Amateur Radio Club lab, test rig, hydraulic wave generator simulator, etc. Figure 1 below provides an example of a development kit that the team purchased since the cost of the total package of the kit was less than the individual components.

The total budget provided to the team by Harris Corporation was $2,000. However, the final cost of the team ended up being $1,600.

Chapter 2: Research

2.1 Previous Works and Similar Works

One of the major hurdles in the research for this project stemmed from the fact that the various aspects of the project were split between several groups. It is necessary to research a variety of power related topics – ranging from AC-DC rectification to DC-DC step down conversion to load control – without having immediate access to information from the other groups. Not knowing definitively the specifications of the power produced by the wave generator, or the power requirements of the sensor package, research had to be conducted on a broader range.

In order to facilitate the research, it was determined practical to investigate similar previous works. While the concept of wave-generated power has existed since the 1870's [1], investigations into wave power were drastically reduced in the 1980's in favor of wind power [2]. As a result, there is a significantly greater quantity of more thorough, readily available information regarding wind power than there is for wave power. In light of the design of the wave power generator and anticipated variation in its power generation resulting from the randomness of waves, it is decided reasonable to make a comparison between the wave power provided by this project and the power provided by modern wind power generators. To this end, various aspects of power management in wind power generators were researched, including but not limited to AC-DC conversion, DC-DC step-down conversion, MOSFETs, and op-amps.

2.2 Hardware Research

2.2.1 AC-DC Rectification

The output from the wave generator is known to be AC electric power of variable magnitude. In order to power the sensor package, this needed to be converted to stable DC electric power. To accomplish this, the first aspect that is researched is AC-DC rectification.

Full Wave Bridge Rectification — A simple rectifying circuit is the full wave bridge rectifier, so named for its diode bridge. When the input voltage is positive, two of the diodes are forward biased, while the opposite two are reverse biased, providing a positive output voltage across the resistor. When the input voltage is negative, the diode biases are switched, and a positive output voltage is still produced across the resistor.

While the voltage output for the full wave bridge rectifier is a positive DC voltage, it strongly mirrors the amplitude of the input AC voltage, which is undesirable. It

is also possible to utilize a transformer to reduce the input voltage before it reaches the diode bridge, but an anticipated low maximum power supplied by the wave generator make the necessity for this reduction unlikely.

Three-Phase Full Wave Rectification — A three-phase full wave rectifying circuit, shown in Figure 2.1, is able to provide a more DC output that is closer to a constant value for a three-phase AC input. This is a result of the fact that the phase difference between the three AC waveforms, when fully rectified, is smaller than the wavelength of any one waveform.

The advantage of this circuit is a significant decrease in the DC voltage's dependency on the amplitude of the AC waveform. This would result in a reduced necessity of ripple attenuation for the DC output. However, the three-phase full wave rectifier requires more components than a full wave bridge rectifier. This would make it more expensive and require more space. It also requires a three-phase AC input.

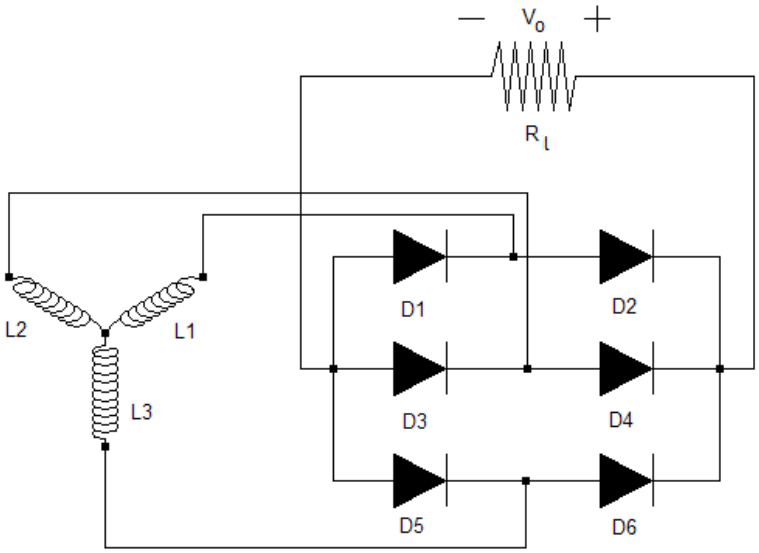

Figure 2.1: Three-Phase Full Wave Rectifier Circuit

VIENNA Rectifier — The VIENNA rectifier is a three-phase, three-level, pulse-width modulation full wave rectifying circuit invented by Johann Kolar [3]. The circuit is shown in Figure 2.2.

The VIENNA rectifier is an extension of the full wave bridge rectifier with a boost converter for a higher DC output. It has a unity power factor [5]. Other potential advantages to the VIENNA rectifier are high power density and low switching losses. The pulse width modulation would also serve to compensate for the variable frequency power produced by the wave generator.

The VIENNA rectifier has been shown to demonstrate a wide variety of features that make it an excellent choice for this project. One of the requirements for any

rectifying circuit utilized is compatibility with the three-phase Ginlong generator. A power factor as close to one as possible is also desired. The rectifier also needs to be able to handle effectively variable amplitude, variable frequency AC voltage input because of the sporadic nature of the waves turning the generator. The VIENNA rectifier is a natural choice in light of its three-phase input, its high power factor, and its ability to rectify a voltage input with variable amplitude and frequency.

The most significant disadvantage of the VIENNA rectifier is that it functions as a two-switch boost rectifier, resulting in a significantly increased output voltage, the value of which depends on the boost ratio. The boost ratio can vary, but it is expected to be approximately 6.4 the input voltage. For a 25V input from the Ginlong generator, this would result in a voltage output from the VIENNA rectifier of 160V. DC-DC step down conversion would be required to compensate for this effect.

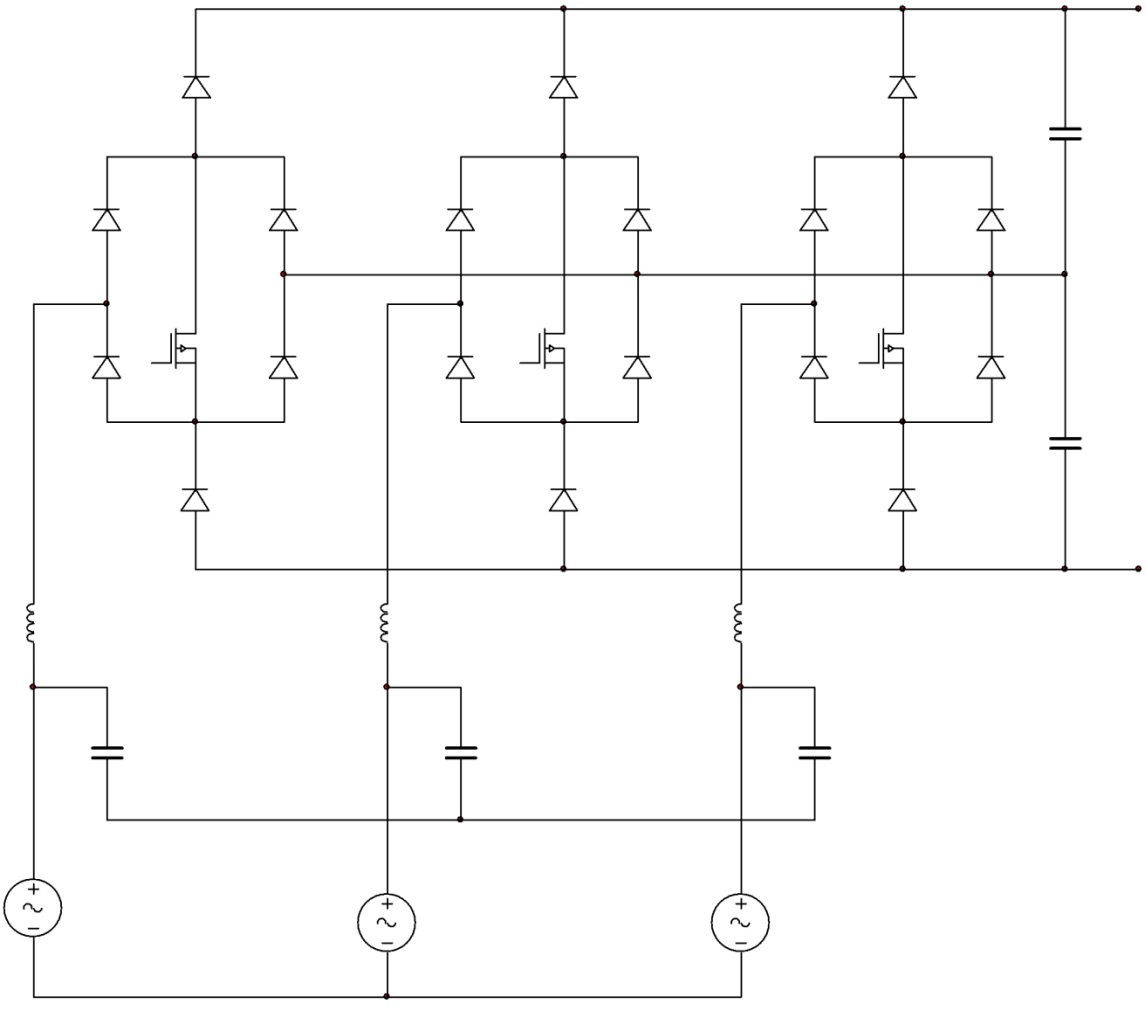

M

Figure 2.2: VIENNA Rectifying Circuit

There are two methods of controlling the VIENNA rectifier: the hysteresis control method and the constant frequency method. A graphical depiction of the hysteresis method of control is presented in Figure 2.3. For this method, upper and lower boundaries for inductor current are set. The current is controlled through a switch to maintain a value between the established boundaries. This method has the disadvantage of complexity, but the advantage of its power harmonics being spread over a large range of frequencies.

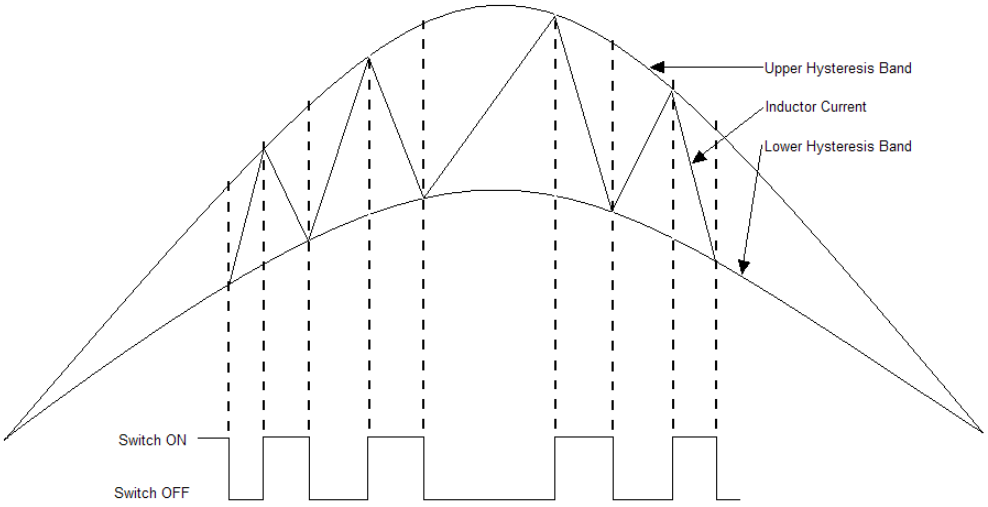

Figure 2.3: Hysteresis Control Method for the VIENNA Rectifier

A graphical depiction of the constant frequency control method is presented in Figure 2.4. For this method of control, the control switch is switched at a constant frequency with varying pulse width.

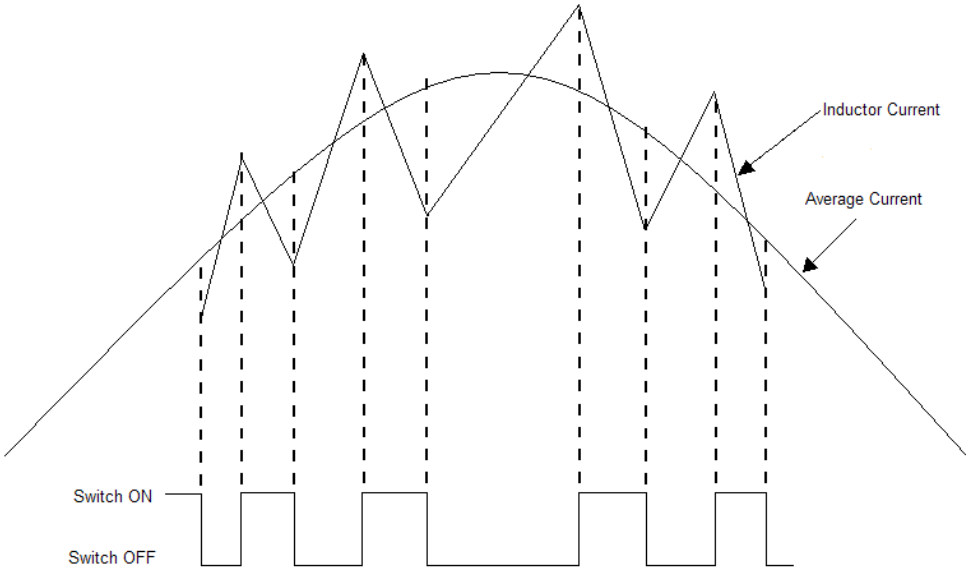

Figure 2.4: Constant Frequency Control Method for the VIENNA Rectifier

Each of these methods has specific advantages and disadvantages that ought to be considered when deciding how best to control the VIENNA rectifier. Table 2.1 considered the comparative advantages and disadvantages to these two methods.

	Control Method	
	Constant Frequency Control	**Hysteresis Control**
Advantages	Easier EMI filtering	EMI distributed over wide spectrum
	Simple control implementation	Inherent current protection
	Single control loop for output voltage and input current	
	Automatically balances output capacitor bank	
Disadvantages	Requires input voltage state sensing	More strict EMI filtering
		Requires input voltage sensing
		Requires extra control loop to balance output capacitor bank
		More complex control algorithm

Table 2.1: Comparison of Control Methods for the VIENNA Rectifier

In general, the VIENNA rectifier boasts a significant number of advantages over alternative rectifying circuits. These advantages include:

- Low input current harmonic distortion
- Three-level output for compatibility with any DC-DC converter
- Low switch count
- Low control effort in terms of quantity of required gate drives
- Compatibility with variable frequency inputs

2.2.2 DC-DC Step Down Conversion

Once the AC power from the wave generator is converted into DC power, it was concluded that it might be necessary to utilize DC-DC step-down conversion to reduce the DC power. In order to accomplish this, various methods of step-down conversion were investigated. These methods, along with applicable benefits and drawbacks, are discussed in this section.

Voltage Divider — A voltage divider is a simple, inexpensive tool that could be used to reduce DC power. For a voltage divider, the output voltage across the

load resistor is given by $V_o = V_i \times \frac{R_l}{R_l + R}$. This voltage divider was not ideal for the project, as it is highly inefficient, resulting in a constant loss of power equal to $100 \times \left(1 - \frac{R_l}{R_l + R}\right)\%$. Also, the circuit itself does not contain any inherent control, so a separate circuit would need to be designed in order to provide control options.

Zener Regulator — A zener regulator has an additional degree of control provided by the zener diode. The zener diode allows current to pass in the reverse direction under certain conditions that would damage regular diodes, and it can be used to control the output voltage. For this circuit, the output voltage is given by $V_o = \frac{R_L(V_i - V_Z - RI_Z)}{R}$. This is not ideal for voltage regulation, because the zener voltage is dependent on the input voltage and on the load.

Series Voltage Regulator — Adding a common collector BJT to the zener regulator results in a series voltage regulator. The presence of the transistor reduces the load on the diode, reducing the fluctuation of zener voltage. This circuit has the capability to regulate a voltage drop with greater stability than the previously discussed regulators, but it is still dependant on the load. All of these regulators also run the risk of overheating if the difference between the input and output voltage is large.

Buck Converter — After researching different DC-DC converters, it was found that a basic voltage divider or a linear regulator would be extremely inefficient due to the power losses associated with it. Additionally, there are ripple currents and high ripple voltage, ΔVo, associated with these circuits. This phenomenon is greatly reduced by using dc-dc step-down converters (buck converter) with topologies that include high switching frequency. Research showed that the two most appropriate buck converter topologies for the design were: Asynchronous buck converter and Synchronous buck converter. The main difference between these two topologies is the difference in its design.

First topology is shown in Figure 2.5. This topology uses a buck convertor with a switch, diode, inductor and a capacitor. The diode in such a design is called a “free-wheeling” diode. This is because the diode eliminates or reduces any sort of fly-back voltage or voltage spikes in the inductive load as a result of sudden voltage drop in the supply voltage or if the supply voltage were to be completely removed.

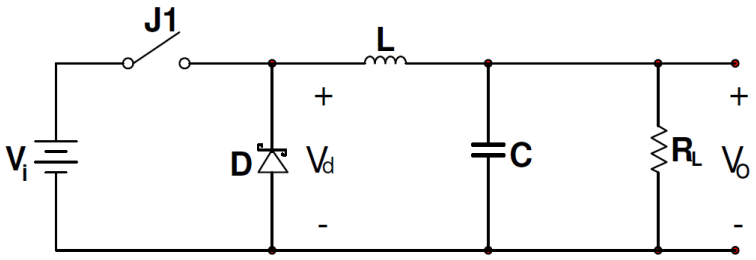

Figure 2.5: Asynchronous Buck Converter

The second topology is shown in Figure 2.6. This topology uses a buck converter with a switch and the inner diode is replaced by another switch. Ideally, this switch would be a semiconductor transistor of type BJT or MOSFET. Generally, MOSFETs are considered to be a better option. This is because BJTs require an input current to turn on and causes offset. BJTs are more desirable for designs requiring fast switching as they lack gate capacitance; although, this is at an expense of lower efficiency. MOSFETs offer better switching frequency, higher efficiency and less complexity. Comparing between PMOS and NMOS, PMOS served as a better option as it is less complex in nature.

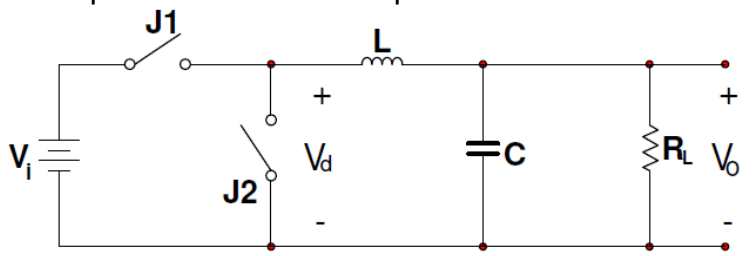

Figure 2.6: Synchronous Buck Converter

Looking at the two topologies, it was critical to determine the most viable design. Table 2.2 provides a detailed comparison between the two topologies:

Comparison	Asynchronous	Synchronous
1. Components	Uses a switch J1 (MOSFET) and diode D (Schottky Key)	Uses two switches J1 and J2 (MOSFETs)
2. Voltage Drop	Low forward voltage drop at the diode	Much lower voltage drop at the MOSFET
3. Power Dissipation	High	Low
4. Switching Losses	Low	Negligible
5. Switching Speed	Slow	Fast
6. Efficiency	High	Higher
7. Total Cost	Less expensive	More expensive

Table 2.2: Comparison of Synchronous versus Asynchronous Converters

A mathematical comparison between the two was made to further clarify the most appropriate topology for the design. Other than cost and complexity of the design, the most important factors that contribute mathematically to determine efficiency included:

1. Duty Cycle (D) should be lower and
2. Output Voltage (V_o) must be higher to eliminate power dissipation losses

Realistic values were used in order to achieve goal-specific results. Accordingly, the parameter values for the design are as follows:

V_i = 0-60V, V_o = 12V, I_o = 2A

Utilizing basic equations for Duty Cycle and Power Loss, we can generate the values for the two topologies. At the given parameters, the voltage drop (V_d) for a Schottky diode is known to be around 0.4V while that for a MOSFET is 0.1V (for low-voltage devices). Table 2.3 shows a comparison of power losses for synchronous and asynchronous buck converters with equal duty cycles.

Topology	**% Duty Cycle (D) V_o/V_i x 100**	**Power Loss $V_d I_o(1-D)$**	**% Power Loss $V_d(1-D)/V_o$**
1. Asynchronous	17.14%	0.66 W	2.76%
2. Synchronous	17.14%	0.25W	0.69%

Table 2.3: Comparison of Power Losses for Synchronous and Asynchronous Buck Converters

Similarly, the efficiency was also compared as ~90% for asynchronous topology and ~94% for synchronous topology[1].

Looking at the comparison, the synchronous buck converter topology was chosen, neglecting its component cost which will be covered by the sponsor.

While the buck converter is a DC-DC step-down converter, combining a buck converter with a DC-DC step-up boost converter results in a buck-boost converter or also known as the SEPIC topology. This circuit was also researched as it can be used either as a step-up converter or a step-down converter, depending upon the duty cycle of the switching transistor.

2.2.3 Battery Charging Circuit

Today, there are lots of high end batteries that require efficient solutions for charging circuits that supply long battery life along with high performance. Hence, there was a need to look at different options for such circuits that can provide innovative ideas to achieve high efficiency along with ideal charging conditions. A proper system needed to be initialized for the project that could meet or exceed

the necessary requirements. After looking closely at the process of designing a charging circuit, the main conflict was to choose between a custom built microprocessor circuit and an off-the-shelf Integrated Circuit (IC). The difference between the two is reviewed below:

An off-the-shelf IC can be easily acquired for low-voltage charging. However, due to unregulated output, it also is responsible for higher accuracy losses during charging period. A custom built microprocessor circuit could be configured to attain voltage regulation at the output which easily eliminates the losses toward charging accuracy. Another advantage of using a custom built circuit is the advantage of adjusting variations of performance levels. This provides the user with larger efficiency results. Although this feature could be available for an off-the-shelf IC, it is also very likely for its price to be significantly higher. The authentication or communication process between the microprocessor and the host system is likely to be much smoother than that between the off-the-shelf IC and the host system. One of the main differences lies in the ability to perform tasks using simple and easier methods. Figure 2.7 shows the charging strategy that was researched by the team. This strategy was then implemented in finding the right fit for a battery charging controller.

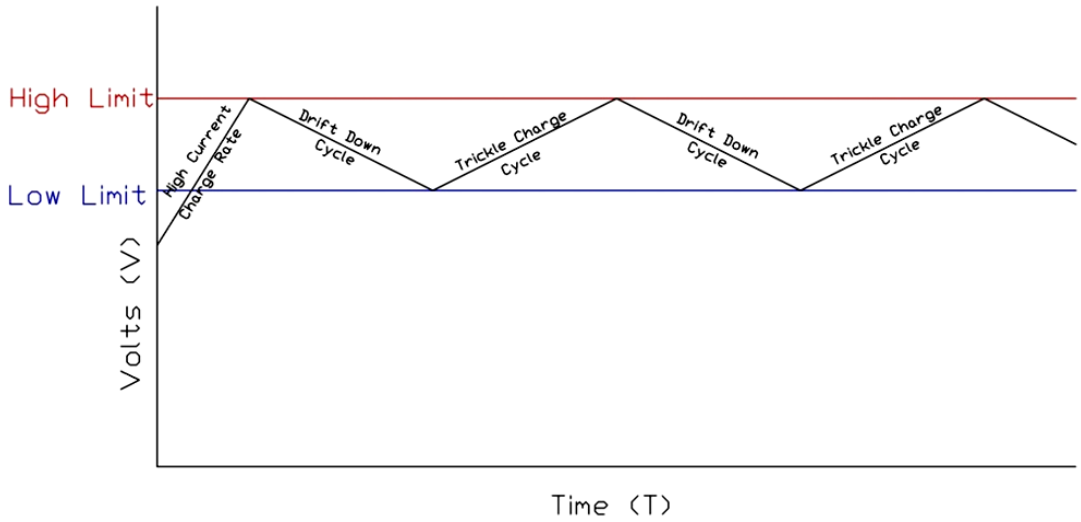

Figure 2.7: Battery Charging Strategy Utilized in Charging Circuit

2.2.4 Analog to Digital Signal Conversion

In order to transfer the power signal from the wave generator to the sensor package, analog to digital signal conversion was researched in case it was necessary to convert the signal from analog to digital. Analog to digital converters, or ADCs, typically consider the analog voltage or current input and convert the magnitude to a digital number. The output is generally a two's compliment binary number. These devices can vary significantly depending on the resolution, or the number of digital values that can be generated for an

analog input. Accuracy errors in ADCs are typically found in the least significant bit of the digital output, and may be the result of an aperture error. This particular error is of significant interest, as it results from clock jitter when converting time dependent analog signals to digital. Because the wave power was expected to vary with time, this error was likely to be encountered in conversion from analog to digital. The significance of the error depends on the resolution; increasing the quantity of bits in the digital output signal decreases the dependence on the least significant bit.

Analog to Digital Converters can be found in various forms. To determine the most suitable and accurate analog to Digital Converter, the first step was to determine the amount of bits required by the design. This could be determined by using Table 2.4 that shows the resolution in ppm and dB for converter systems from 8 bits to 24 bits:

# of Bits	**2^n**	**LSB (FS = 1V)**	**Resolution (%)**	**Resolution (ppm)**	**Resolution (dB)**
8	256	3.91 mV	0.391	3910	48.16
10	1024	977 µV	0.0977	977	60.21
12	4096	244 µV	0.0244	244	72.25
14	16384	61 µV	0.0061	61	84.29
16	65536	15.3 µV	0.00153	15.3	96.33
18	262144	3.81 µV	0.000381	3.81	108.37
20	1048576	954 nV	9.54×10^{-5}	0.954	120.41
22	4194304	238 nV	2.38×10^{-5}	0.238	132.45
24	16777216	59.5 nV	5.95×10^{-6}	0.0595	144.46

Table 2.4: Analog to Digital Bit Resolution

As seen in the table above, high precision can be obtained by choosing the right number of bits. If the system requires a 21 bit converter, it is recommended to use 22 or 24 bit converter. This is just a precautionary measure as it allows the user to design a system that needs more bits, if necessary. An example of a circuit design for an ADC is depicted in Figure 2.8.

This particular circuit design produces an 8-bit binary output from an analog input signal. The analog input is fed to a buffer amplifier at the CON-BNC connector, and the digital output leaves via the ADCV_DATA connector.

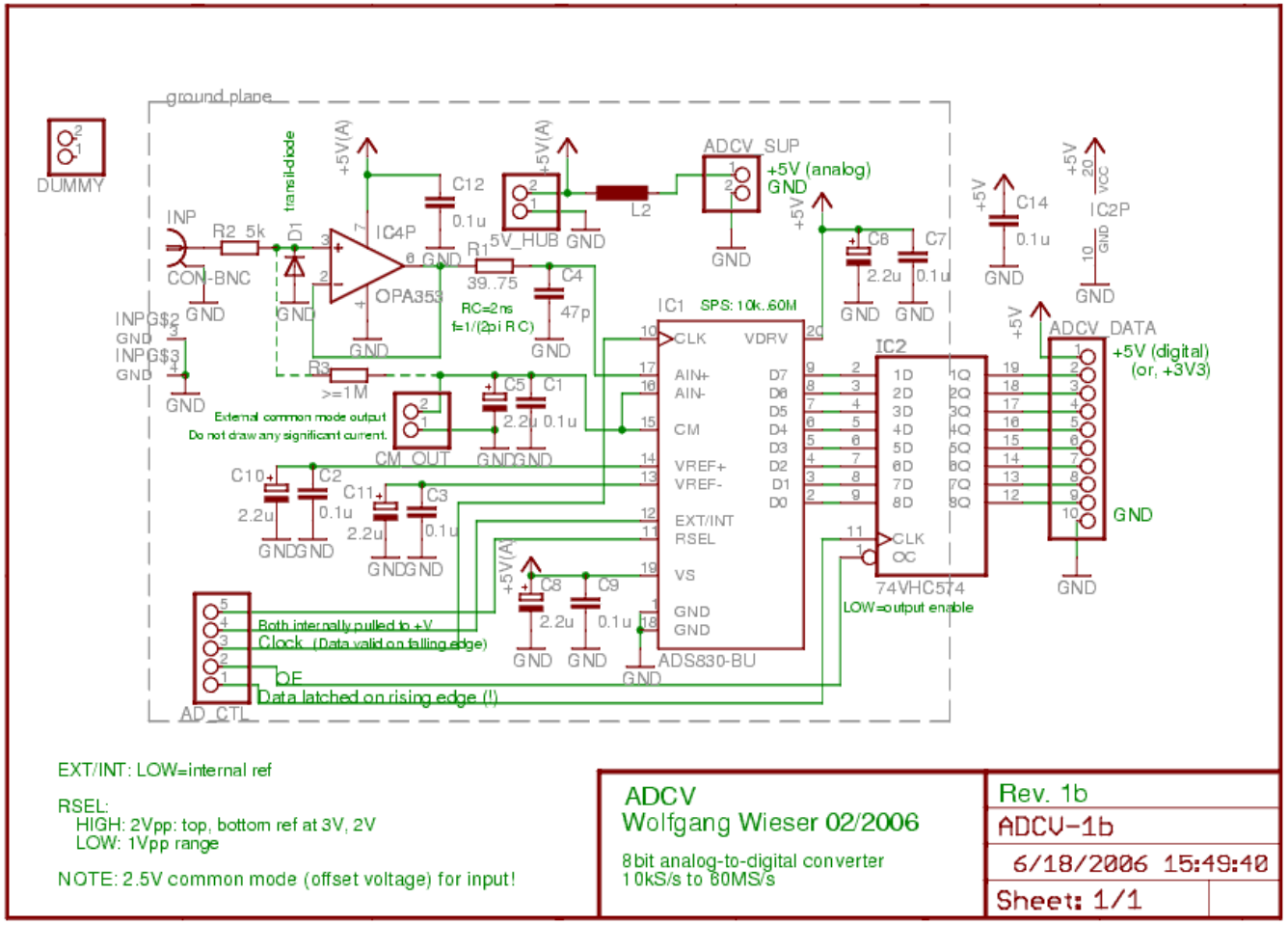

Figure 2.8: 8-bit Analog to Digital Converter Circuit
(Reprinted with permission, as noted at the referenced url [4])

2.2.5 MOSFET Driver

Among the possible devices that could serve as a switch for a buck converter with an LC filter, a metal oxide semiconductor field effect transistor (MOSFET) seemed ideal because of its capacity for high frequency switching, a capability that would improve the buck converter's ability to maintain a consistent output voltage. Several MOSFET drivers were investigated in order to find the best fit for this project, and they are discussed in this section.

The LM5101A 3A High Voltage High-Side and Low-Side Gate Driver from National Semiconductor is able to operate with an input voltage up to 100V, a supply voltage between 7.5V and 14V, and provide 3A of gate drive, with a listed price of $1.35 per unit per thousand [6]. The parameters for this device are given in Table 2.5.

Parameters	**Values**
Topology	Synchronous Buck, Bridge
Input Max Voltage	100 Volt
Supply Minimum	7.5 Volt
Supply Maximum	14 Volt
Peak Sink Current	3 Amp
Peak Source Current	3 Amp
Output Rise Time (tr)	10 ns
Output Fall Time (tf)	10 ns
Bottom Driver Prop Delay	25 ns
Top Driver Propagation Delay	25 ns
Pulse Width Min	50 ns
Quiescent Current	0.2 ma
High Side Drive	Yes
Low Side Drive	Yes
Outputs	2
Low Gate Enable	No
UVLO	Yes
Shut down	No
Internal Boot Diode	Yes
Input Control	Dual, independent
Special Features	TTL type threshold inputs
Reg Type	MOSFET Driver
Temperature Minimum	-40° C
Temperature Maximum	125° C

Table 2.5: Parameters for the LM5101A Driver

The ADP3625 High Speed, Dual, 4A MOSFET Driver from Analog Devices is able to operate with a supply voltage between 4.5V and 18V, providing 4A of

gate drive, with a listed price of $0.88 per unit per thousand [7]. These devices also included internal temperature sensors with overheating shutdown at excessive junction temperatures. The parameters for this device are given in Table 2.6.

Parameters	**Values**
Product Description	High Speed, Dual, 4 Amp MOSFET Driver, inverting A & non-inv B input pins, 4.5V<Vin<18V
V_{in} Range (V)	4.5-18
Peak Drive Current (A)	4
Prop-Delay Rising (ns)	14
UVLO On/Off T-Hold V typ	4.2 / 3.9
Precision Enable	Yes
Over Temperature Protection	Yes
Over Temperature Warning Signal	Yes
Package	8L-MSOP_VD; 8L-SOIC-EP
Temperature Range (Deg C)	-40 to +85
Price* (1000 pcs.)	$0.88

Table 2.6: Parameters for the ADP3625 Driver

The LTC4440-5 series of drivers from Linear Technology is able to operate with an input voltage up to 60V and a supply voltage between 4V and 15V, with an output of 1.1A and a listed price of $2.50 per unit, or $1.75 per unit per thousand [8]. The parameters for this device are given in Table 2.6.

Parameters	**Values**
Maximum Operating TS	60 V
Absolute Max TS	80 V
MOSFET Gate Drive	4 V to 15 V
V_{cc} UV^{+}	3.2 V
V_{cc} UV^{-}	3.04 V
INP Voltage	-0.3 V to 15 V
BOOST Voltage (continuous)	-0.3 V to 85 V
BOOST Voltage (100 ms)	-0.3 V to 95 V
TS Voltage (continuous)	-5 V to 70 V
TS Voltage (100 ms)	-5 V to 80 V
Peak Output Current < 1 µs (TG)	4A
Temperature Range (Deg C)	-40° C to 85° C
Junction Temperature	125° C

Table 2.7: Parameters for the LTC4440-5 Driver

2.2.6 Controllers

A variety of system control options were considered to handle the control portion of the power conversion. Each of the available system controllers possessed costs and benefits that needed to be weighed in order to make the best selection for this project. The costs and benefits of several controller systems are discussed in this section.

Field Programmable Gate Arrays — Field programmable gate arrays, or FPGAs, are integrated circuits that can be programmed by the consumer after manufacture. The ability of an FPGA to be individually programmed is a significant potential benefit, as other controllers programmed during manufacture lack flexibility. Another advantage to the FPGA is the ability to define and simulate the exact code before programming the device. One potential disadvantage is that FPGAs often occupy more space than other controller systems.

Microcontrollers — A microcontroller is a miniature computer built on an integrated circuit. One advantage to a microcontroller is their very small power consumption, particularly while inactive. Microcontrollers contain their own memory that may be field programmable or defined during manufacture. They are also typically very small, which can be a significant advantage when space conservation is an issue. Microcontrollers are also readily available on the market and generally inexpensive.

Digital Signal Processors — Digital Signal Processors, or DSPs, are a variety of microprocessor designed primarily for digital signal processing, but they often provide other features, sometimes serving as microcontrollers. Like embedded microcontrollers, they are small and often, though not invariably, inexpensive.

PIC Microcontrollers — PIC microcontrollers derive their name from Programmable Interface Controller. Some of the many benefits of PIC microcontrollers include low cost, high availability, a large number of users that has resulted in a large quantity of documentation and application notes, C programming capability, low power consumption, and the capability to enter a low-power sleep state. Some of the potential drawbacks include a limited number of instructions, ranging from 35 to 80 or more, or only a single accumulator [9]. These drawbacks do not necessarily apply strictly to all PIC microcontrollers. With a very wide range of available options, a PIC microcontroller can feasibly be obtained for nearly any application desired. A variety of PIC microcontrollers available from Microchip were investigated in order to find the best fit for this project, and they are discussed in this section. The PIC10F222 is an inexpensive, 8-bit static Flash-based microcontroller. It uses 33 single-word / single-cycle 12-bit wide instructions. Some of its features include low power sleep current, in-circuit debugging support, and programmable code protection. The parameters for this device are given in Table 2.8.

Parameters	Values
Program Memory Type	Flash
Program Memory (KB)	0.75
Program Memory KWords	0.5
Self-Write	No
CPU Speed (MIPS)	2
RAM Bytes	23
Max CPU Speed (MHz)	8
Internal Oscillator	4 MHz, 8 MHz
Timers	1 x 8-bit
ADC	2 ch, 8-bit
Temperature Range (deg C)	-40 to 125
Operating Voltage Range (V)	2 to 5.5
Input / Output Pins	4
Pin Count	6
Cap Touch Channels	2
Volume Pricing	$0.39

Table 2.8: Parameters for the PIC10F222 Microcontroller

The PIC16F886 is an inexpensive PIC microcontroller that features on-board EEPROM data memory, an analog comparator, an internal oscillator with selectable 8 MHz – 32 KHz, and programmable on-chip voltage reference. The parameters for this device are given in Table 2.9.

Parameters	Values
Program Memory Type	Flash
Program Memory (KB)	3.5
Program Memory KWords	2
Self-Write	No
CPU Speed (MIPS)	5
RAM Bytes	128
Data EEPROM (bytes)	256
Max CPU Speed (MHz)	20
Internal Oscillator	8 MHz, 32 kHz
Timers	2 x 8-bit, 1 x 16-bit
ADC	4 ch, 10-bit
Comparators	1
Temperature Range (deg C)	-40 to 125
Operating Voltage Range (V)	2 to 5.5
Input / Output Pins	6
Pin Count	8
Cap Touch Channels	3
Volume Pricing	$0.91

Table 2.9: Parameters for the PIC12F683 Microcontroller

The PIC16F886 is an 8-bit Flash-based CMOS PIC microcontroller with features that include self-programming, two comparators, a power saving sleep mode, and in-circuit debugging. The parameters for this device are given in Table 2.10.

Parameters	**Values**
Program Memory Type	Flash
Program Memory (KB)	14
Program Memory KWords	8
Self-Write	Yes
CPU Speed (MIPS)	5
RAM Bytes	368
Data EEPROM (bytes)	256
Max CPU Speed (MHz)	20
Internal Oscillator	8 MHz, 32 kHz
Digital Communication Peripherals	1-A/E/USART, 1-MSSP(SPI/I2C)
Capture/Compare/PWM Peripherals	1 CCP, 1 ECCP
Timers	2 x 8-bit, 1 x 16-bit
ADC	4 ch, 10-bit
Comparators	2
Temperature Range (deg C)	-40 to 125
Operating Voltage Range (V)	2 to 5.5
Input / Output Pins	6
Pin Count	28
Cap Touch Channels	11
Volume Pricing	$1.49

Table 2.10: Parameters for the PIC16F886 Microcontroller

The PIC18F2620 is an 8-bit Flash-based CMOS PIC microcontroller with features that include a failsafe clock monitor, two comparators, run, idle, and sleep modes, and C compiler optimized RISC architecture. The parameters for this device are given in Table 2.11.

Parameters	**Values**
Program Memory Type	Flash
Program Memory (KB)	64
Program Memory KWords	32
Self-Write	Yes
CPU Speed (MIPS)	10
RAM Bytes	3968
Data EEPROM (bytes)	1024
Max CPU Speed (MHz)	40
Internal Oscillator	8 MHz, 32 kHz
Digital Communication Peripherals	1-A/E/USART, 1-MSSP(SPI/I2C)
Capture/Compare/PWM Peripherals	2 CCP

Timers	1 x 8-bit, 3 x 16-bit
ADC	10 ch, 10-bit
Comparators	2
Temperature Range (deg C)	-40 to 125
Operating Voltage Range (V)	2 to 5.5
Input / Output Pins	25
Pin Count	28
Volume Pricing	$4.06

Table 2.11: Parameters for the PIC18F2620 Microcontroller

The dsPIC33FJ16GS504 is a 16-bit digital signal controller with features that include a failsafe clock monitor, two high speed analog comparators, run, idle, and sleep modes, and C compiler optimized instruction set. The parameters for this device are given in Table 2.12.

Parameters	**Values**
Program Memory Type	Flash
Program Memory (KB)	16
Program Memory KWords	32
Self-Write	Yes
CPU Speed (MIPS)	40
RAM Bytes	2048
Data EEPROM (bytes)	0
Max CPU Speed (MHz)	40
Internal Oscillator	7.37 MHz, 32 kHz
nanoWatt Features	Fast Wake/Fast Control
Digital Communication Peripherals	1-UART, 1-SPI, 1-I2C
Analog Peripherals	2-A/D 12x10-bit @ 4000(ksps) 4-D/A 1x10-bit @ 640(ksps)
Timers	2 x 16-bit
16-bit PWM resolutions	16
Motor Control PWM Channels	8
Comparators	4
Temperature Range (deg C)	-40 to 125
Operating Voltage Range (V)	3 to 3.6
Input / Output Pins	35
Pin Count	44
Volume Pricing	$3.42

Table 2.12: Parameters for the dsPIC33FJ16GS504 Microcontroller

The PIC24FJ96GA010 is a 16-bit digital signal controller with features that include a failsafe clock monitor, two high speed analog comparators, run, idle, and sleep modes, and C compiler optimized instruction set. The parameters for this device are given in Table 2.13.

Parameters	Values
Program Memory Type	Flash
Program Memory (KB)	96
CPU Speed (MIPS)	16
RAM Bytes	8192
Internal Oscillator	8 MHz, 32 kHz
nanoWatt Features	Fast Wake/Fast Control
Digital Communication Peripherals	2-UART, 2-SPI, 2-I2C
Analog Peripherals	1-A/D 16x10-bit @ 500(ksps)
Timers	2 x 16-bit
16-bit PWM resolutions	16
Comparators	2
Temperature Range (deg C)	-40 to 85
Operating Voltage Range (V)	2 to 3.6
Input / Output Pins	85
Pin Count	100
Volume Pricing	$3.42

Table 2.13: Parameters for the PIC24FJ96GA010 Microcontroller

The PIC microcontroller was determined to be the most appropriate choice for this project. PIC microcontrollers are readily available with a wide array of available parameters making them a good fit for many applications. They are inexpensive and highly versatile. For the purposes of this project, the 16-bit PIC24FJ96GA010 microcontroller was determined to be the optimal choice. Initially, another microcontroller was going to be used. However, this microcontroller came pre-mounted on an MCU card with the development system used for this project. With repeated experimentation, the device eventually became familiar enough to use. It was found to be more than sufficient for the purposes of the project.

Descriptions for the pin inputs and outputs for the PIC24FJ96GA010 are given in Table 2.14.

Function	Pin Number	I/O	Input Buffer	Description
AN0	25	I	ANA	A/D Analog Inputs
AN1	24	I	ANA	
AN2	23	I	ANA	
AN3	22	I	ANA	
AN4	21	I	ANA	
AN5	20	I	ANA	
AN6	26	I	ANA	
AN7	27	I	ANA	
AN8	32	I	ANA	
AN9	33	I	ANA	

AN10	34	I	ANA	
AN11	35	I	ANA	
AN12	41	I	ANA	
AN13	42	I	ANA	
AN14	43	I	ANA	
AN15	44	I	ANA	
AV_{DD}	30	P	—	Positive Supply for Analog Modules
AV_{SS}	31	P	—	Ground Reference for Analog Modules
BCLK1	48	O	—	UART 1 IrDA Baud Clock
BCLK2	39	O	—	UART 2 IrDA Baud Clock
C1IN-	21	I	ANA	Comparator 1 Negative Input
C1IN+	20	I	ANA	Comparator 1 Positive Input
C1OUT	32	O	—	Comparator 1 Output
C2IN-	22	I	ANA	Comparator 2 Negative Input
C2IN+	23	I	ANA	Comparator 2 Positive Input
C2OUT	33	O	—	Comparator 2 Output
CLKI	63	I	ANA	Main Clock Input Connection
CLKO	64	O	—	System Clock Output
CN0	74	I	ST	Interrupt-on-Change Inputs
CN1	73	I	ST	
CN2	25	I	ST	
CN3	24	I	ST	
CN4	23	I	ST	
CN5	22	I	ST	
CN6	21	I	ST	
CN7	20	I	ST	
CN8	10	I	ST	
CN9	11	I	ST	
CN10	12	I	ST	
CN11	14	I	ST	
CN12	44	I	ST	
CN13	81	I	ST	
CN14	82	I	ST	
CN15	83	I	ST	
CN16	84	I	ST	
CN17	49	I	ST	
CN18	50	I	ST	
CN19	80	I	ST	
CN20	47	I	ST	
CN21	48	I	ST	
CV_{REF}	34	O	ANA	Comparator Reference Voltage Output
EMUC1	24	I/O	ST	In-Circuit Emulator Clock Input/Output
EMUD1	25	I/O	ST	In-Circuit Emulator Data Input/Output
EMUC2	26	I/O	ST	In-Circuit Emulator Clock Input/Output
EMUD2	27	I/O	ST	In-Circuit Emulator Data Input/Output
ENVREG	86	I	ST	Enable for On-Chip Voltage Regulator
IC1	68	I	ST	Input Capture Inputs
IC2	69	I	ST	
IC3	70	I	ST	

IC4	71	I	ST	
IC5	79	I	ST	
INT0	55	I	ST	External Interrupt Inputs
INT1	18	I	ST	
INT2	19	I	ST	
INT3	66	I	ST	
INT4	67	I	ST	
(MCLR)’	13	I	ST	Master Clear (Device Reset) Input. This line is brought low to cause a Reset.
OC1	72	I	ST	Output Compare / PWM Peripherals
OC2	76	I	ST	
OC3	77	I	ST	
OC4	78	I	ST	
OC5	81	I	ST	
OCFA	26	I	ST	Output Compare Fault A Input
OCFB	44	I	ST	Output Compare Fault B Input
OSC1	63	I	ANA	Main Oscillator Input Connection
OSC2	64	O	ANA	Main Oscillator Output Connection
PGC1	24	I/O	ST	In-Circuit Debugger and ICSP Programming Clock
PGD1	25	I/O	ST	In-Circuit Debugger and ICSP Programming Data
PGC2	26	I/O	ST	In-Circuit Debugger and ICSP Programming Clock
PGD2	27	I/O	ST	In-Circuit Debugger and ICSP Programming Data
PMA0	44	I/O	ST/TTL	Parallel Master Port Address Bit 0 Input (Buffered Slave Modes) and Output (Master Modes)
PMA1	43	I/O	ST/TTL	Parallel Master Port Address Bit 1 Input (Buffered Slave Modes) and Output (Master Modes)
PMA2	14	O	—	Parallel Master Port Address (Demultiplexed Master Modes)
PMA3	12	O	—	
PMA4	11	O	—	
PMA5	10	O	—	
PMA6	29	O	—	
PMA7	28	O	—	
PMA8	50	O	—	
PMA9	49	O	—	
PMA10	42	O	—	
PMA11	41	O	—	
PMA12	35	O	—	
PMA13	34	O	—	
PMBE	78	O	—	Parallel Master Port Byte Enable Strobe
PMCS1	71	I/O	ST/TTL	Parallel Master Port Chip Select 1 Strobe / Address Bit 14
PMCS2	70	O	—	Parallel Master Port Chip Select 2 Strobe / Address Bit 15

PMD0	93	I/O	ST/TTL	Parallel Master Port Data (Demultiplexed Master Mode) or Address / Data (Multiplexed Master Modes)
PMD1	94	I/O	ST/TTL	
PMD2	98	I/O	ST/TTL	
PMD3	99	I/O	ST/TTL	
PMD4	100	I/O	ST/TTL	
PMD5	3	I/O	ST/TTL	
PMD6	4	I/O	ST/TTL	
PMD7	5	I/O	ST/TTL	
PMRD	82	I/O	ST/TTL	Parallel Master Port Read Strobe
PMWR	81	I/O	ST/TTL	Parallel Master Port Write Strobe
RA0	17	I/O	ST	PORTA Digital I/O
RA1	38	I/O	ST	
RA2	58	I/O	ST	
RA3	59	I/O	ST	
RA4	60	I/O	ST	
RA5	61	I/O	ST	
RA6	91	I/O	ST	
RA7	92	I/O	ST	
RA9	28	I/O	ST	
RA10	29	I/O	ST	
RA14	66	I/O	ST	
RA15	67	I/O	ST	
RB0	25	I/O	ST	PORTB Digital I/O
RB1	24	I/O	ST	
RB2	23	I/O	ST	
RB3	22	I/O	ST	
RB4	21	I/O	ST	
RB5	20	I/O	ST	
RB6	26	I/O	ST	
RB7	27	I/O	ST	
RB8	32	I/O	ST	
RB9	33	I/O	ST	
RB10	34	I/O	ST	
RB11	35	I/O	ST	
RB12	41	I/O	ST	
RB13	42	I/O	ST	
RB14	43	I/O	ST	
RB15	44	I/O	ST	
RC1	6	I/O	ST	PORTC Digital I/O
RC2	7	I/O	ST	
RC3	8	I/O	ST	
RC4	9	I/O	ST	
RC12	63	I/O	ST	
RC13	73	I/O	ST	
RC14	74	I/O	ST	
RC15	63	I/O	ST	
RD0	72	I/O	ST	PORTD Digital I/O
RD1	76	I/O	ST	
RD2	77	I/O	ST	

RD3	78	I/O	ST	
RD4	81	I/O	ST	
RD5	82	I/O	ST	
RD6	83	I/O	ST	
RD7	84	I/O	ST	
RD8	68	I/O	ST	
RD9	69	I/O	ST	
RD10	70	I/O	ST	
RD11	71	I/O	ST	
RD12	79	I/O	ST	
RD13	80	I/O	ST	
RD14	47	I/O	ST	
RD15	48	I/O	ST	
RE0	93	I/O	ST	PORTE Digital I/O
RE1	94	I/O	ST	
RE2	98	I/O	ST	
RE3	99	I/O	ST	
RE4	100	I/O	ST	
RE5	3	I/O	ST	
RE6	4	I/O	ST	
RE7	5	I/O	ST	
RE8	18	I/O	ST	
RE9	19	I/O	ST	
RF0	87	I/O	ST	PORTF Digital I/O
RF1	88	I/O	ST	
RF2	52	I/O	ST	
RF3	51	I/O	ST	
RF4	49	I/O	ST	
RF5	50	I/O	ST	
RF6	55	I/O	ST	
RF7	54	I/O	ST	
RF8	53	I/O	ST	
RF12	40	I/O	ST	
RF13	39	I/O	ST	
RG0	90	I/O	ST	PORTG Digital I/O
RG1	89	I/O	ST	
RG2	57	I/O	ST	
RG3	56	I/O	ST	
RG6	10	I/O	ST	
RG7	11	I/O	ST	
RG8	12	I/O	ST	
RG9	14	I/O	ST	
RG12	96	I/O	ST	
RG13	87	I/O	ST	
RG14	85	I/O	ST	
RG15	1	I/O	ST	
RTCC	68	O	—	Real-Time Clock Alarm Output
SCK1	55	O	—	SPI1 Serial Clock Output
SCK2	10	I/O	ST	SPI2 Serial Clock Output

SCL1	57	I/O	I^2C	I2C1 Synchronous Serial Clock Input / Output
SCL2	58	I/O	I^2C	I2C2 Synchronous Serial Clock Input / Output
SDA1	56	I/O	I^2C	I2C1 Data Input / Output
SDA2	59	I/O	I^2C	I2C2 Data Input / Output
SDI1	54	I	ST	SPI1 Serial Data Input
SDI2	11	I	ST	SPI1 Serial Data Output
SDO1	53	O	—	SPI2 Serial Data Input
SDO2	12	O	—	SPI2 Serial Data Output
SOSCI	73	I	ANA	Secondary Oscillator / Timer1 Clock Input
SOSCO	74	O	ANA	Secondary Oscillator / Timer1 Clock Output
(SS1)’	23	I/O	ST	Slave Select Input / Frame Select Output (SPI1)
(SS2)’	14	I/O	ST	Slave Select Input / Frame Select Output (SPI2)
T1CK	74	I	ST	Timer1 Clock
T2CK	6	I	ST	Timer2 External Clock Input
T3CK	7	I	ST	Timer3 External Clock Input
T4CK	8	I	ST	Timer4 External Clock Input
T5CK	9	I	ST	Timer5 External Clock Input
TCK	38	I	ST	JTAG Test Clock / Programming Clock Input
TDI	60	I	ST	JTAG Test Data / Programming Data Input
TDO	61	O	—	JTAG Test Data Output
TMS	17	I	ST	JTAG Test Mode Select Input
(U1CTS)’	47	I	ST	UART1 Clear to Send Input
(U1RTS)’	48	O	—	UART1 Request to Send Output
U1RX	52	I	ST	UART1 Receive
U1TX	51	O	DIG	UART1 Transmit Output
(U2CTS)’	40	I	ST	UART2 Clear to Send Input
(U2RTS)’	39	O	—	UART2 Request to Send Output
U2RX	49	I	ST	UART2 Receive
U2TX	50	O	DIG	UART2 Transmit Output
V_{DD}	2,16,37,46,62	P	—	Power Supply for Peripheral Digital Logic and I/O Pins
V_{DDCAP}	85	P	—	External Filter Capacitor Connection (regulator enabled)
V_{DDCORE}	85	P	—	Power Supply for Microcontroller Core Logic (regulator disabled)
V_{REF-}	28	I	ANA	A/D and Comparator Reference Voltage (Low) Input
V_{REF+}	29	I	ANA	A/D and Comparator Reference Voltage (High) Input
V_{SS}	15,36,45,65,75	P	—	Ground Reference for Logic and I/O Pins

Table 2.14: Pin Description for the PIC24FJ96GA010 Microcontroller

The pin layout for this device is shown in Figure 2.9.

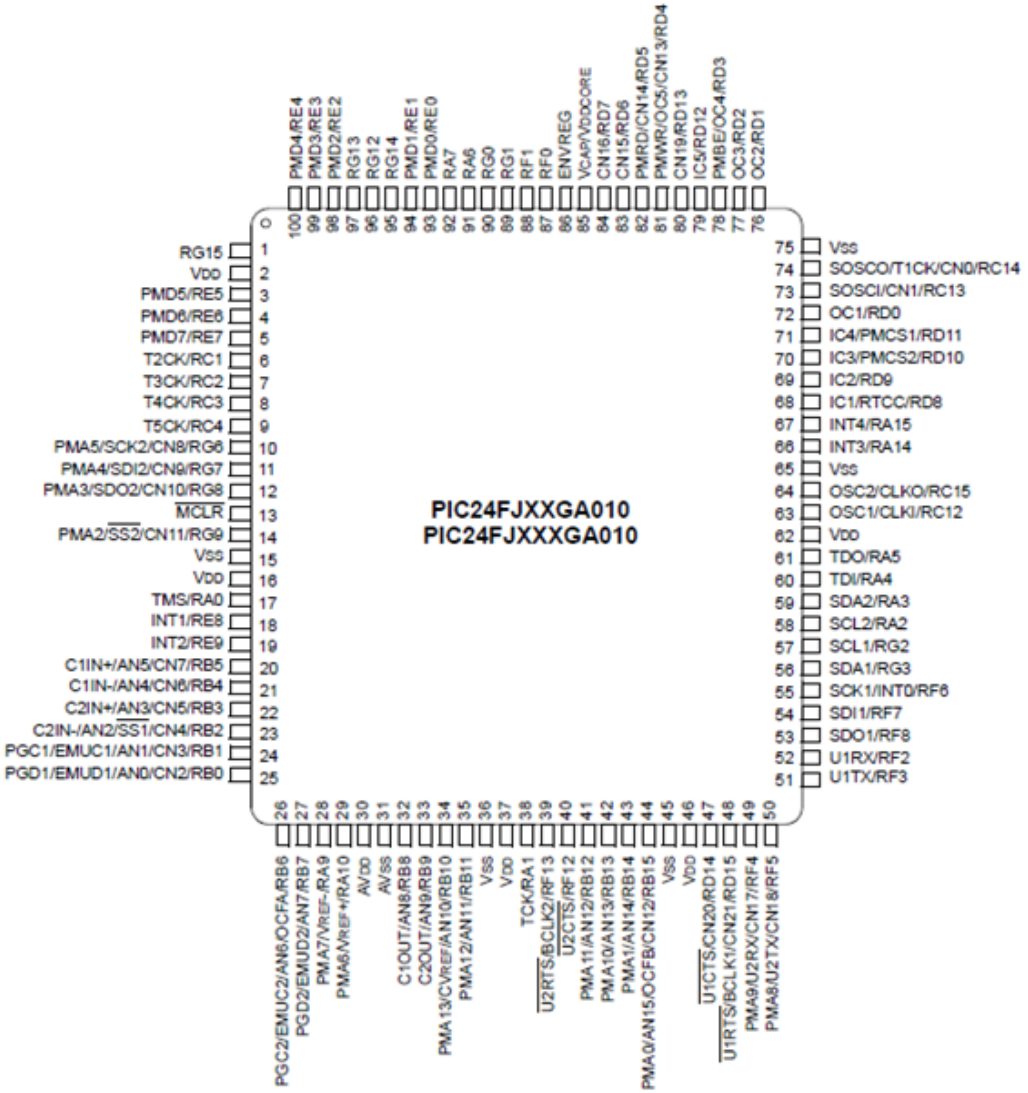

Figure 2.9: Pin Layout for the PIC24FJ96GA010 Microcontroller

Initially, the dsPIC33FJ16GS504 was to be used. Further investigation into the functioning of the dsPIC33FJ16GS504 microcontroller was required in order to ensure that the desired results were achieved, and to protect the microcontroller from potential damage. Microchip provided ample information regarding the proper use of their microcontroller. The basic requirements of the dsPIC33FJ16GS504 microcontroller are further expanded below.

Decoupling Capacitors: Decoupling capacitors are required on every power supply pin. These include the V_{DD}, V_{SS}, AV_{DD}, and AV_{SS} pins. Several factors needed to be considered in choosing the appropriate capacitor. Microchip recommended the use of a ceramic capacitor of 0.1 µF, 10–20 V, with a resonance frequency over 20 MHz. These capacitors should be placed as close

to the pin as possible, preferably within 6 mm on the same side of the board as the device. For the reduction of noise over 10 MHz, a second ceramic capacitor could be added, in parallel with the first, with a capacitance between 0.01 µF and 0.001µF. Figure 2.10 shows the recommended minimum connections for the decoupling capacitors.

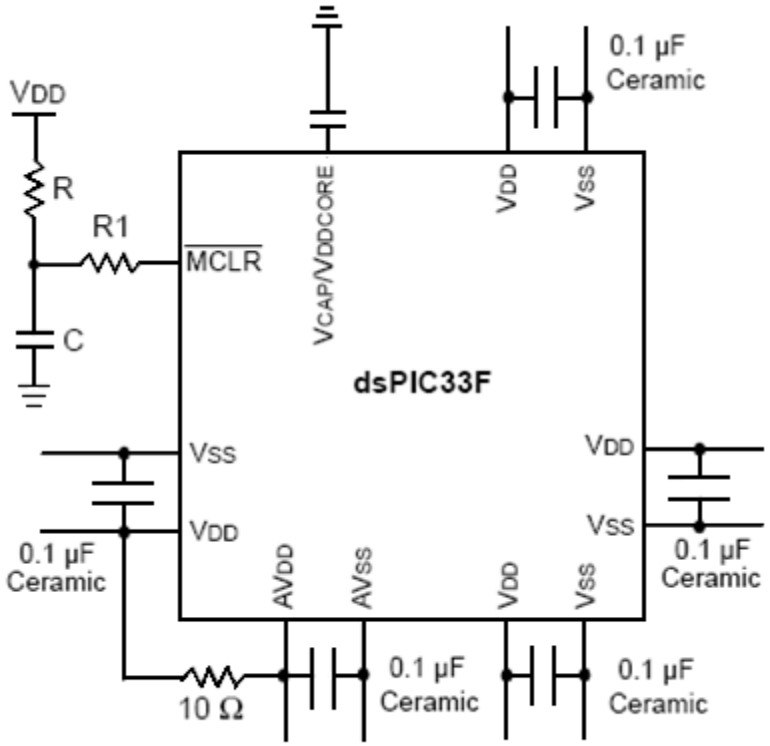

Figure 2.10: Minimum Recommended Connections for Decoupling Capacitors for the dsPIC33FJ16GS504 PIC Microcontroller

Capacitor on Internal Voltage Regulator: For the V_{CAP}/V_{DDCORE} pin, a capacitor with low ESR, under 5 Ω, is needed to make the output voltage on the voltage regulator stable. Microchip recommended a ceramic or tantalum capacitor between 4.7 µF and 10 µF, 16V connected to ground, placed within 6 mm of the pin.

Master Clear Pin: This pin is used for resetting the microcontroller, as well as for programming and debugging. Differing values of resistance and capacitance need to be placed on the pin depending on the current status of the microcontroller. While programming and debugging the microcontroller, Microchip recommends that the capacitance be isolated from the master clear pin. Figure 2.11 shows the recommended connection for the master clear pin.

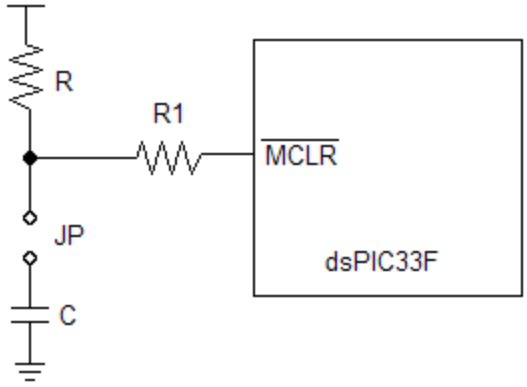

Figure 2.11: Recommended Connection for the Master Clear Pin for the dsPIC33FJ16GS504 PIC Microcontroller

ICSP Pins: In-Circuit Serial Programming pins, such as the PGECx and PGEDx pins, are used for programming and debugging. Microchip advised against the use of pull-up resistors, series diodes, or capacitors in these pins, as this would interfere with the devices' communications for programming and debugging. IN the event that these components are required for the device, they should be removed during programming and debugging.

External Oscillator Pins: The dsPIC33FJ16GS504 microcontroller has both a high-frequency and a low-frequency oscillator. Microchip recommends that the circuit for the oscillator be placed on the same side of the board as the device, within 12 mm of the appropriate oscillator pin. They also suggested placing a grounded copper pour around the oscillator circuitry to separate it from any other nearby circuits. This copper pour needs to be routed to the MCU ground directly, and no power or signal traces should be run through it. Figure 2.12 shows the recommended placement of the oscillator circuit.

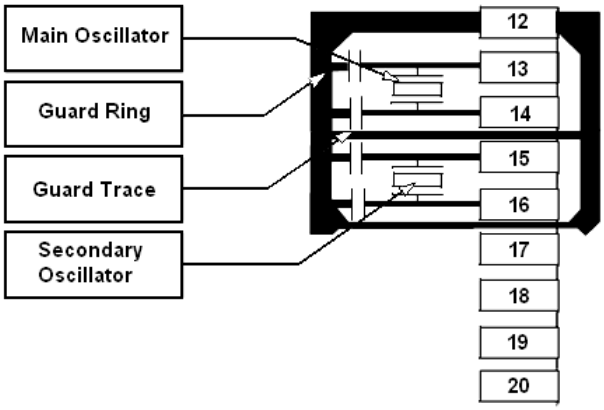

Figure 2.12: Recommended Placement of the Oscillator Circuit for the dsPIC33FJ16GS504 PIC Microcontroller

Oscillator Value Conditions on Device Start-Up: When the device first powers up, if the PLL is enabled and configured, the maximum oscillator source frequency must be constrained between 4 MHz and 8MHz. Otherwise, default settings will violate the device operating speed.

Configuration of Analog and Digital Pins During ICSP Operations: MPLAB ICD 2, ICD 3, or REAL ICE can be used as a debugger to automatically initialize all of the ANx pins as digital. The bits contained in the registers correlating to these A/D input pins that are initialized in this way must not be cleared by user application firmware, or else there will be communication errors between the debugger and the microcontroller. Furthermore, if MPLAB ICD 2, ICD 3, or REAL ICE are used as programmers, the ADPCFG registers must be configured correctly. Only debugging, and not programming, results in these registers being initialized. If the registers are not correctly configured, the A/D pins will be recognized as analog input pins, which could adversely affect the functionality.

Unused I/Os: I/O pins that are not going to be used should either be configured as outputs and driven to a logic-low state, or else connected to a resistor between 1 kΩ and 10 kΩ and connected to V_{SS}.

When the microcontroller is configured correctly, it can be used for a wide range of applications. Figure 2.13 shows the use of a dsPIC33FJ06GS202 microcontroller, in the same family of microcontrollers as the dsPICFJ06GS504, in a synchronous buck converter circuit.

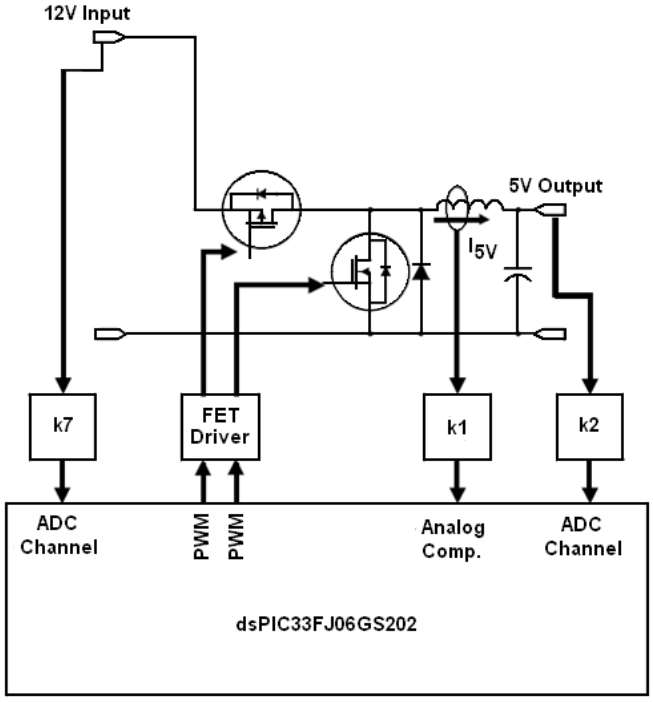

Figure 2.13: Synchronous Buck Converter Circuit with dsPIC33FJ06GS202 PIC Microcontroller

CPU: The CPU module for the dsPIC33FJ16GS504 microcontroller utilizes 16-bit Harvard architecture and a 24-bit instruction word. All instructions for this device are executed in a single cycle except for instructions that alter the program flow, the double-word move instruction, and table instructions. DO and REPEAT instructions can be used for program loops and are interruptible at any time. The CPU features both MCU and DSP instructions, designed for compatibility with C compilers. Figure 2.14 shows a block diagram of the CPU for the dsPIC33FJ06GS202 microcontroller.

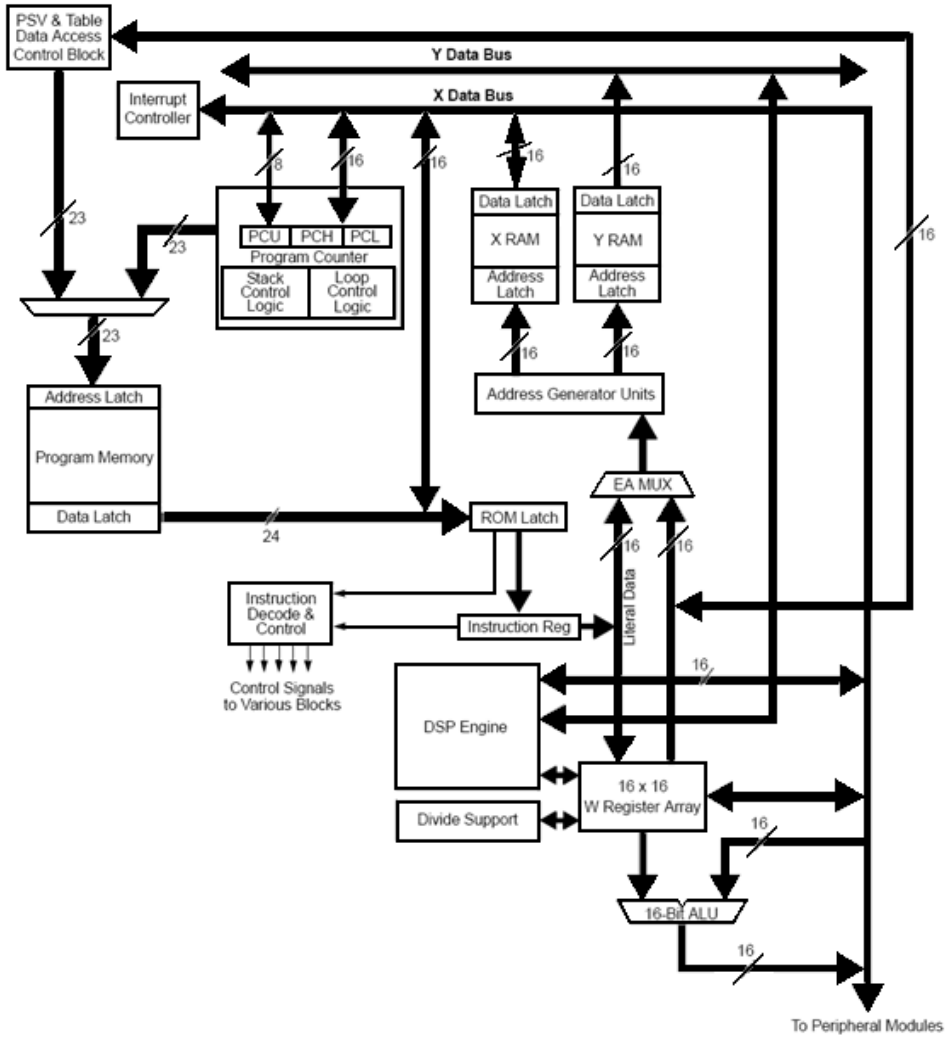

Figure 2.14: CPU Block Diagram for the dsPIC33FJ16GS504 PIC Microcontroller

Figure 2.15 elaborates with a programmer's model for the CPU. Data space can be addressed either as 32K words or as 64 Kb. It is split into two sections which have been designated X and Y data memory, each with an independent Address Generation Unit. MCU instructions operate only through the X AGU, while DSP instructions may operate through the X or Y AGUs. The DSP engine includes a high-speed 17x17-bit multiplier, a 40-bit ALU, two 40-bit saturating accumulators,

and a 40-bit bidirectional barrel shifter that can shift a 40-bit value as many as 16 bits to the right or left in a single cycle.

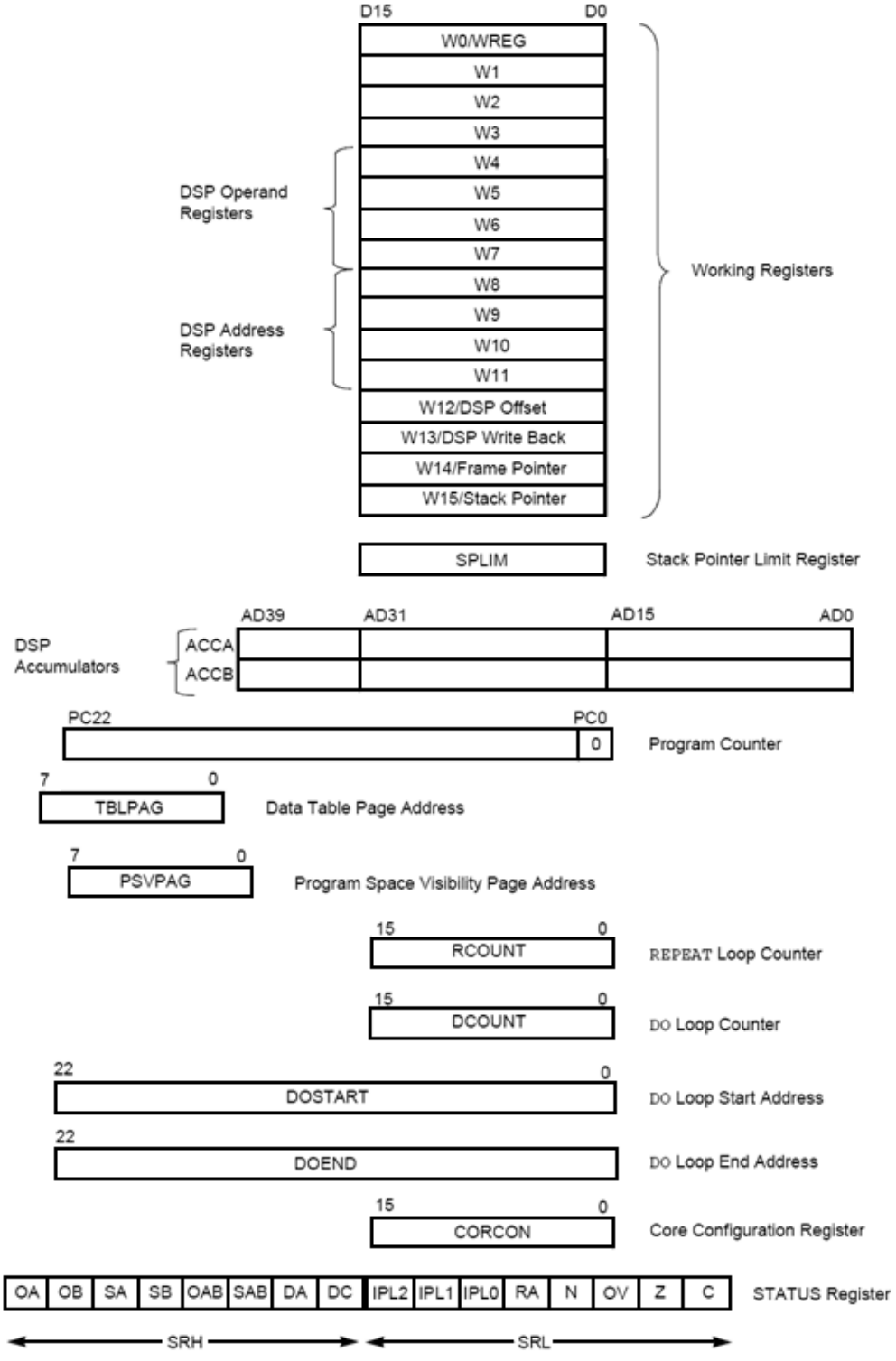

Figure 2.15: CPU Programmer's Model for the dsPIC33FJ16GS504 PIC Microcontroller

Figure 2.16 depicts the designation of the CPU status register. Bit 15 (OA) is the Accumulator A Overflow Status bit, which holds a 1 if accumulator A has overflowed, else a 0. Bit 14 (OB) is the Accumulator B Overflow Status bit, which holds a 1 if accumulator B has overflowed, else a 0. Bit 13 (SA) is the Accumulator A Saturation 'Sticky' Status bit, which holds a 1 if accumulator A is or has been saturated, else a 0. Bit 12 (SB) is the Accumulator B Saturation 'Sticky' Status bit, which holds a 1 if accumulator B is or has been saturated, else a 0. Bit 11 (OAB) is the OA / OB Combined Accumulator Overflow Status bit, which holds a 1 if accumulators A or B have overflowed, else a 0. Bit 10 (SAB) is the SA / SB Combined Accumulator 'Sticky' Status bit, which holds a 1 if accumulators A or B are or have been saturated, else a 0. Bit 9 (DA) is the DO Loop Active bit, which holds a 1 if a DO loop is in progress, else a 0. Bit 8 (DC) is the MCU ALU Half Carry/Borrow bit a carry out form the 4th or 8th low-order bit of the result occurred, else a 0. Bits 7-5 (IPL<2:0>) are the CPU Interrupt Priority Status bits, forming a 3-bit binary bus defining the CPU Interrupt Priority Level ranging from 111 (Level 7) to 000 (Level 0). Bit 4 (RA) is the REPEAT Loop Active bit, holding a 1 if a REPEAT loop is in progress, else a 0. Bit 3 (N) is the MCU ALU Negative bit, holding a 1 if a negative result was obtained, else a 0. Bit 2 (OV) is the MCU ALU Overflow bit, holding a 1 if overflow occurred for signed arithmetic, else a 0. Bit 1 (Z) is the MCU ALU Zero bit, holding a 1 if an operation affecting the Z bit has set it at some point, else a 0 if the most recent operation affecting the Z bit cleared it. Bit 0 (C) is the MCU ALU Carry/Borrow bit, holding a 1 if a carry out occurred from the MSB of the result, else a 0.

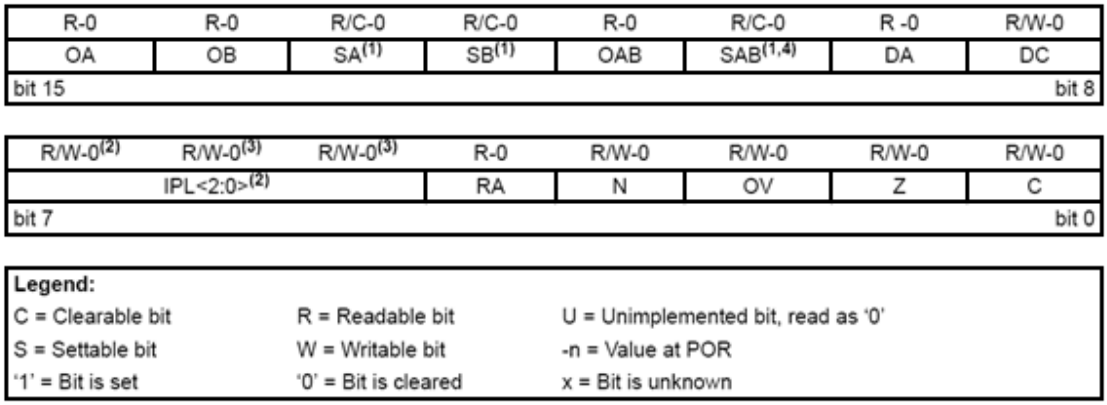

Figure 2.16: CPU Status Register Designation for the dsPIC33FJ16GS504 PIC Microcontroller

Figure 2.17 depicts the designation of the core control register. Bits 15-13 are unimplemented. Bit 12 (US) is the DSP Multiply Unsigned/Signed Control bit, holding a 1 if the DSP engine multiplies are unsigned, else a 0. Bit 11 (EDT) is the Early DO Loop Termination Control bit, where holding a 1 terminates execution of the DO loop at the end of the current iteration, and holding a 0 does nothing. Bits 10-8 (DL<2:0>) are the DO Loop Nesting Level Status bits, which comprise a 3-bit binary bus where the binary value defines the number of active

DO loops, from 111 (7 DO loops active) to 000 (0 DO loops active). Bit 7 (SATA) is the ACCA Saturation Enable bit, which holds a 1 if accumulator A has saturation enabled, else a 0. Bit 6 (SATB) is the ACCB Saturation Enable bit, holding a 1 if accumulator B has saturation enabled, else a 0. Bit 5 (SATDW) is the Data Space Write from DSP Engine Saturation Enable bit, holding a 1 if the data space write has saturation enabled, else a 0. Bit 4 (ACCSAT) is the Accumulator Saturation Mode Select bit, holding a 1 for super saturation of 9.31, else 0 for normal saturation of 1.31. Bit 3 (IPL3) is the CPU Interrupt Priority Level Status bit, which holds 1 if the CPU interrupt priority level is greater than 7, else a 0. Bit 2 (PSV) is the Program Space Visibility in Data Space Enable bit, holding a 1 if program space is visible in data space, else a 0. Bit 1 (RND) is the Rounding Mode Select bit, holding a 1 if conventional biased rounding is enables, else a 0 if convergent unbiased rounding is enabled. Bit 0 (IF) is the Integer or Fractional Multiplier Mode Select bit, which holds a 1 if integer mode is enabled for DSP multiply operations, else a 0 if fractional mode is enabled for DSP multiply operations.

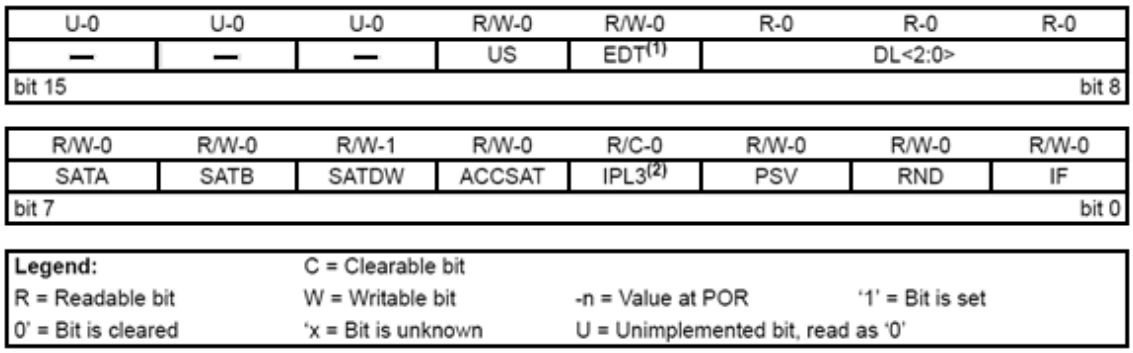

Figure 2.17: Core Control Register Designation for the dsPIC33FJ16GS504 PIC Microcontroller

ALU: The ALU on the dsPIC33FJ16GS504 PIC microcontroller has a width of 16 bits and is able to perform addition, subtraction, bit shifts, and logic operations. It uses 2's compliment for arithmetic operations. The ALU can operate on data from the W register array or from data memory, and ALU output can likewise be written to either of these locations. The ALU is also able to perform the following multiplication operations:

- 16-bit x 16-bit signed
- 16-bit x 16-bit unsigned
- 16-bit signed by 5-bit (literal) unsigned
- 16-bit unsigned x 16-bit unsigned
- 16-bit unsigned x 5-bit (literal) unsigned
- 16-bit unsigned x 16-bit signed
- 8-bit unsigned x 8-bit unsigned

It can also perform the following division operations:

- 32-bit signed / 16-bit signed
- 32-bit unsigned / 16-bit unsigned
- 16-bit signed / 16-bit signed
- 16-bit unsigned / 16-bit unsigned

DSP Engine: The dsPIC33FJ16GS504 utilizes a DSP engine with a 17-bit x 17-bit multiplier, a barrel shifter, and a 40-bit adder/subtractor. Generally, as the microcontroller uses single-cycle instruction flow architecture, the DSP engine and the MCU instruction flow cannot be simultaneously active. DSP engine options can be selected via the CPU Core Control register for multiplication, rounding, or saturation control. Figure 2.18 shows the block diagram for the DSP engine.

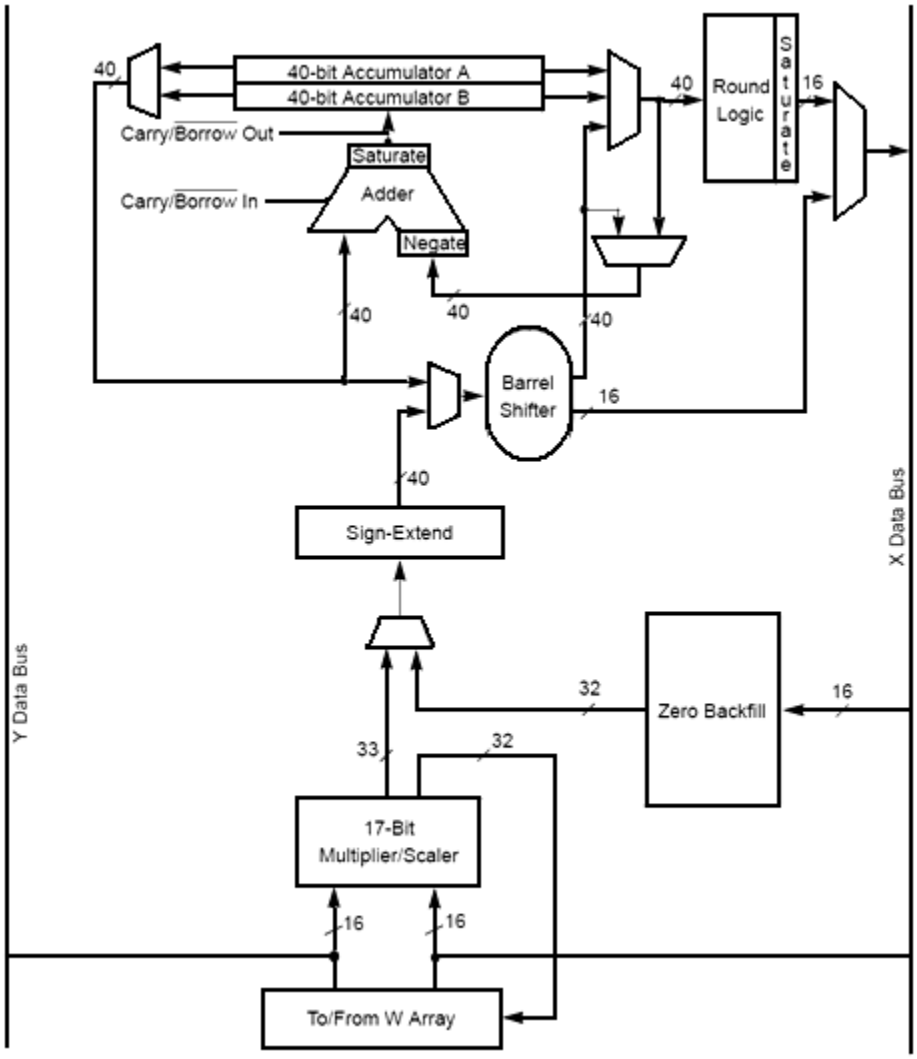

Figure 2.18: DSP Engine Block Diagram for the dsPIC33FJ16GS504 PIC Microcontroller

Memory Organization: The dsPIC33FJ16GS504 microcontroller utilizes distinct program and memory data spaces, permitting access to program memory while code is being executed. Program memory space is accessible only to the lower half of the address range, form 0x000000 to 0x7FFFFF, with the exception of the TBLRD and TBLWT operations. Figure 2.19 shows the program memory map for the device.

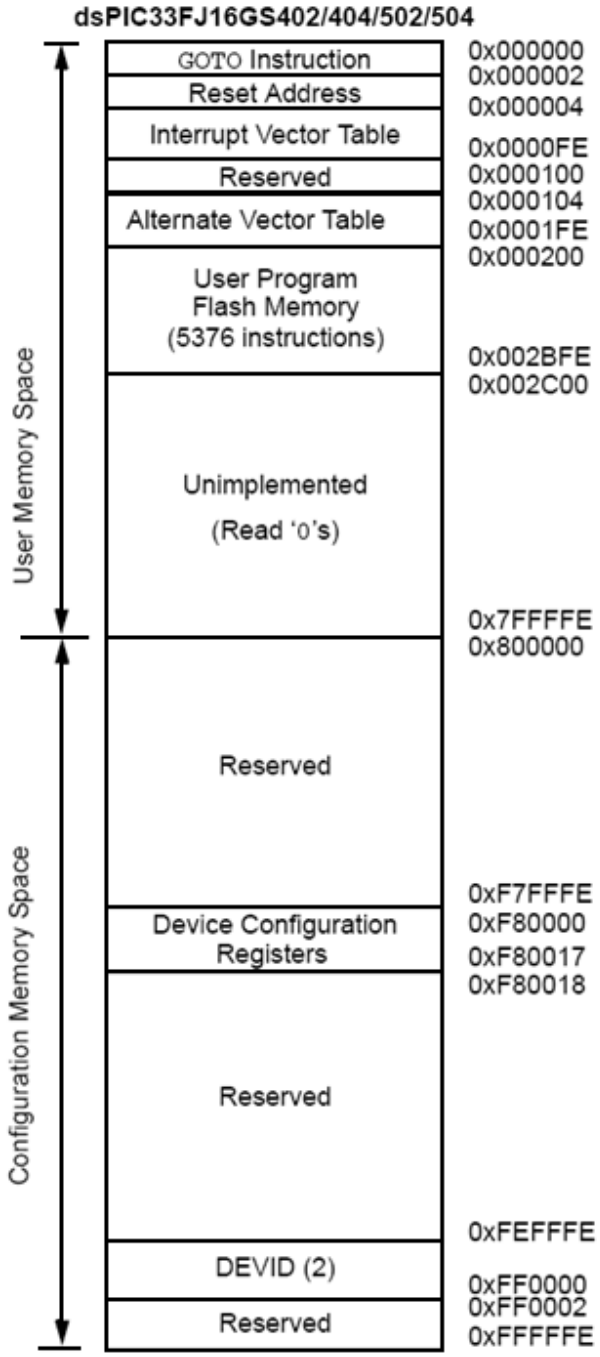

Figure 2.19: Program Memory Map for the dsPIC33FJ16GS504 PIC Microcontroller

Program memory space is separated into word-addressable blocks, each 24 bits wide, which can be interpreted as a lower word and an upper word. The highest byte of the upper word (corresponding to bits 24-31) is never implemented. The addresses between 0x000000 and 0x000200 are held for hard-coded program execution vectors.

Addresses in the data memory space are 16 bits wide and point to data space, resulting in a 64Kb data space. The lower half corresponds to implemented memory addresses and the upper half to the Program Space Visibility area.

Flash Program Memory: The dsPIC33FJ16GS504 microcontroller utilizes internal Flash memory in order to store and execute code. It is possible to read, write, or erase memory during operation of the device. Flash memory can be programmed by either in-circuit serial programming or run-time self-programming. The former makes possible the manufacture of boards with unprogrammed devices that have the digital signal controller programmed immediately before shipping. The latter uses the table read and table write instructions to write program memory data in blocks of 64 instructions.

The device's programming time depends upon the values of the FRC accuracy (which is temperature dependant) and the FRC Oscillator Tuning register. It is given by Equation 2.1.

$$T_{RW} = \frac{T}{7.37\ MHz \times (FRC\ Accuracy)\% \times (FRC\ Tuning)\%} \qquad (2.1)$$

The process of programming the Flash memory entails programming one row at a time, according to the following algorithm:

1. Read eight rows of program memory. Store in data RAM.
2. Update program data in RAM with desired data.
3. Erase the block:
    a. Set NVMOP to 0010 to configure for erase. Set the ERASE and WREN bits.
    b. Write the starting address to be erased into TBLPAG and W.
    c. Write 0x55 to NVMKEY.
    d. Write 0xAA to NVMKEY.
    e. Set WR to start the erase cycle, stalling the CPU. WR is cleared when the erase completes.
4. Write the first 64 instructions from data RAM into program memory buffers.
5. Write the program block to Flash memory:
    a. Set NVMOP to 0001 to configure for programming. Clear the ERASE bit and set the WREN bit.
    b. Write 0x55 to NVMKEY.
    c. Write 0XAA to NVMKEY.
    d. Set WR to start the programming cycle, stalling the CPU

6. Repeat from 4, incrementing TBLPAG, until all 512 instructions have been written to Flash memory.

Oscillator Configuration: The dsPIC33FJ16GS504 microcontroller's oscillator system provides options for both internal and external oscillator clock sources, clock switching between clock sources, and a monitor that detects clock failure and takes certain failsafe measures. Figure 2.20 shows the oscillator system.

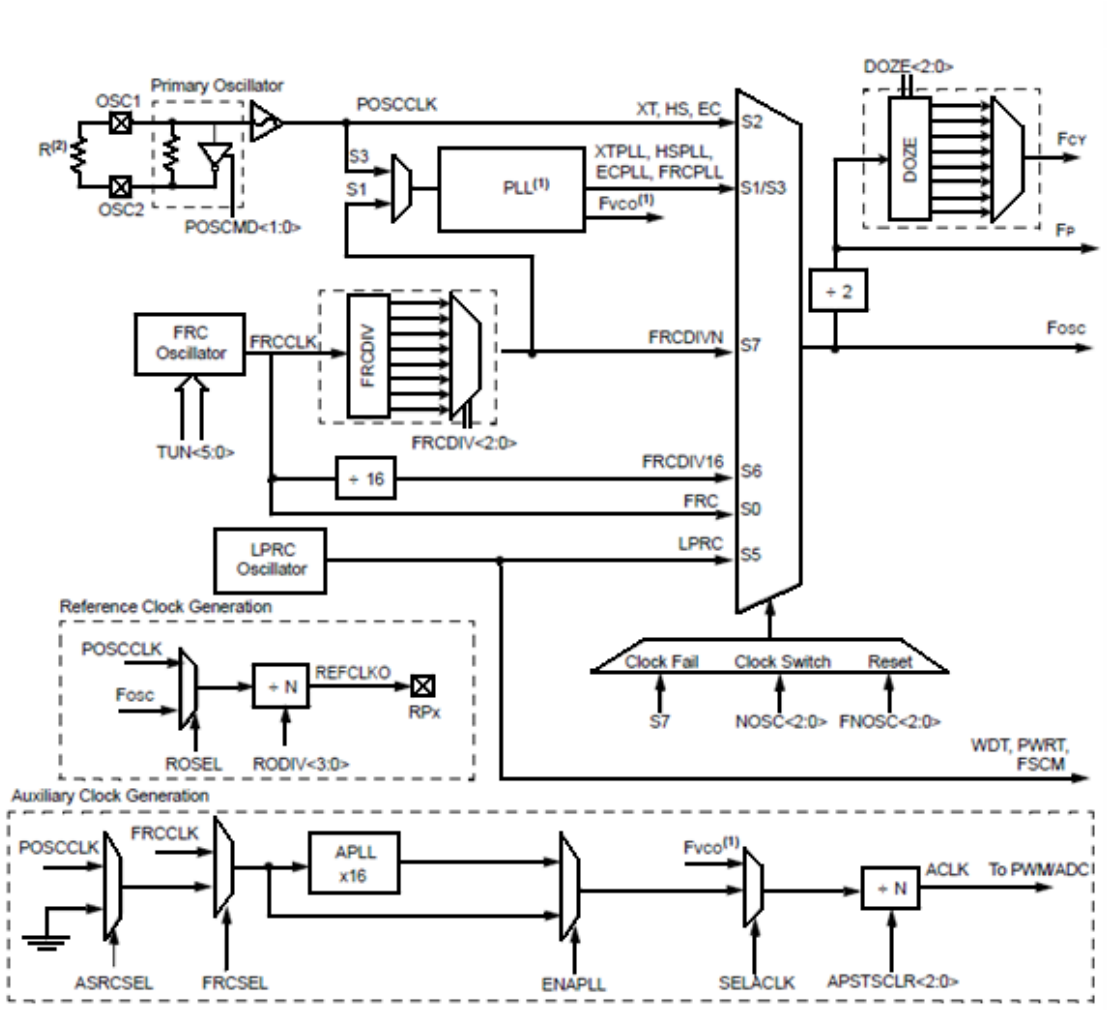

Figure 2.20: Oscillator System for the dsPIC33FJ16GS504 PIC Microcontroller

Six clock options are available, including fast RC oscillator, FRC oscillator with PLL, primary oscillator, primary oscillator with PLL, low power RC oscillator, and FRC oscillator with postscaler. The primary oscillator may consist of (XT) crystal and ceramic resonators from 3 MHz to 10 MHz, (HS) high-speed crystals from 10 MHz to 40 MHz, or (EC) an external clock signal applied to the OSC1 pin. The low power RC oscillator runs at 32.768 kHz and is utilized by the Watchdog Timer and Fail-Safe Clock Monitor. There are a total of twelve possible clock modes, outlined in Table 2.15.

Oscillator Mode	Oscillator Source	POSCMD <1:0>	FNOSC <2:0>
Fast RC Oscillator with Divide-by-N (FRCDIVN)	Internal	xx	111
Fast RC Oscillator with Divide-by-16 (FRCDIV16)	Internal	xx	110
Low-Power RC Oscillator (LPRC)	Internal	xx	101
Reserved	Reserved	xx	100
Primary Oscillator (HS) with PLL (HSPLL)	Primary	10	011
Primary Oscillator (XT) with PLL (XTPLL)	Primary	01	011
Primary Oscillator (EC) with PLL (ECPLL)	Primary	00	011
Primary Oscillator (HS)	Primary	10	010
Primary Oscillator (XT)	Primary	01	010
Primary Oscillator (EC)	Primary	00	010
Fast RC Oscillator with PLL (FRCPLL)	Internal	xx	001
Fast RC Oscillator (FRC)	Internal	xx	000

Table 2.15: Oscillator Clock Modes for the dsPIC33FJ16GS504 PIC Microcontroller

The PLL can be used by the primary oscillator and the internal FRC oscillator to reach increased operation speeds. The output of the primary or FRC oscillator is designated F_{IN}. Figure 2.21 shows the PLL block diagram.

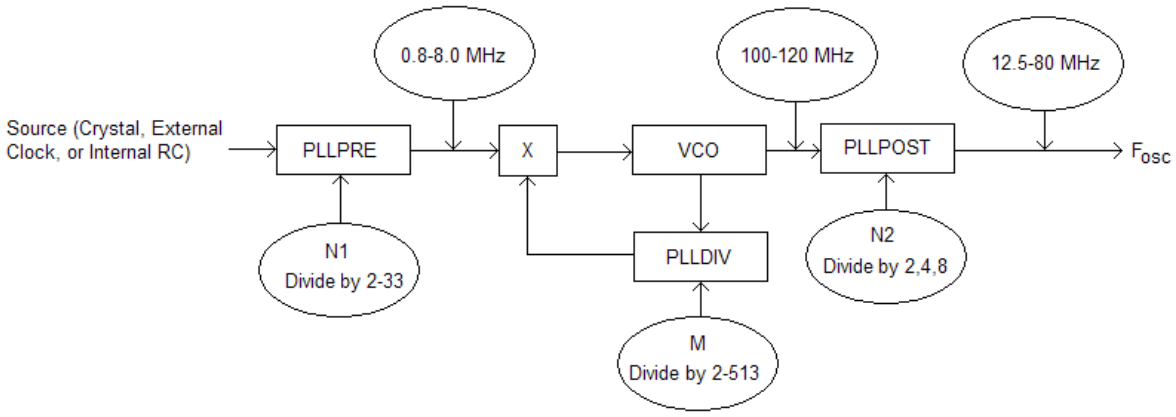

Figure 2.21: PLL Block Diagram for the dsPIC33FJ16GS504 PIC Microcontroller

The factors N1, M, and N2 are used to control the frequency, maintaining a specified range. The output of the PLL, designated F_{OSC}, is given by Equation 2.2.

$$F_{OSC} = F_{IN} \times \left(\frac{M}{N1 \times N2}\right) \quad (2.2)$$

The device operating frequency is given Equation 2.3.

$$F_{CY} = \frac{F_{OSC}}{2} \quad (2.3)$$

2.2.7 Op-Amps

Op-amps, or operational amplifiers, are high-gain voltage amplifiers. Figure 2.22 shows the internal circuitry that is contained in a typical op-amp. This circuitry is defined by three stages. The first, a differential amplifier, provides high input impedance and low noise amplification. The second, a voltage amplifier, provides high voltage gain. The third, an output amplifier, provides high current driving capability and low output impedance [10].

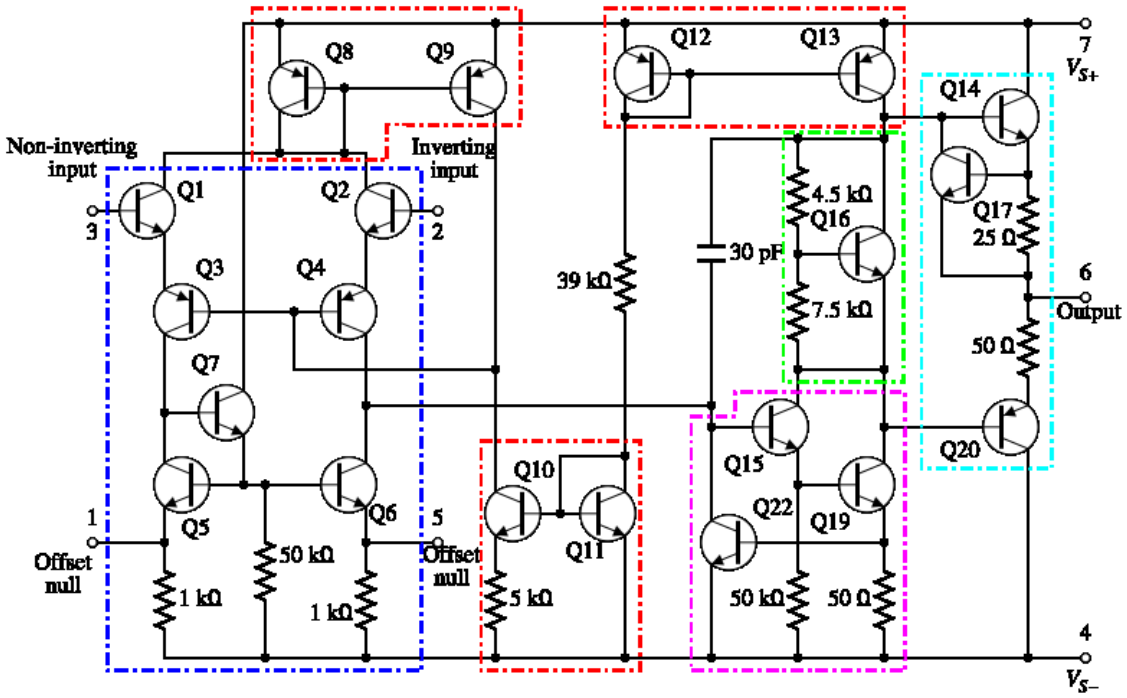

Figure 2.22: Operational Amplifier Internal Circuitry. Reprinted under terms of license [11]

This circuit diagram identifies the current mirrors, outlined in red; the differential amplifier, outlined in blue; the class A gain stage, outlined in magenta; the voltage level shifter outlined in green; and the output stage, outlined in cyan.

2.2.7 Power Factor Correction

The power factor is given by a ratio of the real power to the apparent power. The value of the power factor can range from 0 to 1, and this value can result in significant harmonic distortion. If the load is pure resistance, the power factor will be equal to 1 and no harmonic distortion will occur. If the load is less than 1, harmonic distortion will occur. A power factor of 0.999 corresponds to 3% harmonic distortion, while a power factor of 0.95 corresponds to 30% harmonic distortion [12]. Clearly, the highest power factor possible is desirable.

A boost regulator has advantages for active power factor correction because of its continuous input current, which minimizes noise conducted and produces the optimal input current waveform. However, it requires high output voltage. The VIENNA rectifier is able to convert variable amplitude and variable frequency voltage to a DC voltage, and also controls the input current, producing a sinusoid in phase with the input voltage. Thus, the VIENNA rectifier is sufficient for power factor correction with a power factor very close to one.

2.2.8 Global Positioning System

The wave generator and power management circuit were designed to be placed on a buoy in the middle of the ocean. The buoy was to be tethered to the underwater components. However, if the tether were to break, the buoy would float off aimlessly in the ocean. So, research was conducted into the prospect of a Global Positioning System (GPS) module to determine if the buoy became disconnected from its tether. If so, the GPS would help engineers locate the wandering buoy. There are many GPS units to choose from. A GPS module that uses a standard protocol and can be easily interfaced to a microcontroller is a must. Currently, the standard protocol for GPS units is the NMEA 0183 protocol. A NMEA 0183 message begins with $GP and ends with a carriage return. Data elements are separated by commas and terminated by the * character. Each message ends with the checksum and hex value of the calculated checksum. A GPS module will immediately begin acquiring satellites after power is supplied. After it acquires at least 3 satellites, it will begin reporting its position. The satellite tracking status is reported by the module using two commands. The GSA command includes a field that indicates whether or not there are enough satellites to get a signal. To obtain positional data, two other commands must be used. These commands are GGA and RMC. The GGA command provides you with the time, position and fix type. The RMC command provides you with the time, date, position, course and speed. To receive all the necessary information, both commands must be used. The longitude and latitude can be obtained from either, but only GGA will report the altitude and fix type. The RMC command will be used to obtain the course and speed. The command formats are listed in detail below:

GGA: Global Positioning System Fixed Data

Field 1, UTC Time in the format of hhmmss.sss
Field 2, Latitude in the format of ddmm.mmmm
Fields 3, N/S Indicator (N=North, S=South)
Field 4, Longitude in the format of dddmm.mmmm
Field 5, E/W Indicator (E=East, W=West)
Field 6, Position Fix Indicator (0=No Fix, 1=SPS Fix, 2=DGPS Fix)
Field 7, Satellites Used (0-12)
Field 8, Horizontal Dilution of Precision
Field 9, MSL Altitude
Field 10, MSL Units (M=Meters)
Field 11, Geoid Separation
Field 12, Geoid Units (M=Meters)
Field 13, Age of Diff Correction in seconds
Field 14, Diff Reference

RMC: Recommended Minimum Specific GNSS Data

Field 1, UTC Time in the format of hhmmss.sss
Field 2, Status (A=Valid Data, B=Invalid Data)
Field 3, Latitude in the format of ddmm.mmmm
Fields 4, N/S Indicator (N=North, S=South)
Field 5, Longitude in the format of dddmm.mmmm
Field 6, E/W Indicator (E=East, W=West)
Field 7, Speed over ground in knots
Field 8, Course over ground in degrees
Field 9, Date in the format of ddmmyy
Field 10, Magnetic Variation in degrees
Field 11, Mode (A=Autonomous, D=DGPS, E=DR)

The EM-406A, EM-408, Etek, Copernicus and Holux GPSSlim 236 modules all support the NMEA 0183 protocol and can interfaced to a microcontroller. The EM-406A is manufactured by USGlobalSat. It has an optional development board that well suited for interfacing to a PC.

EM-406A Specifications:

- 20 Channel Receiver
- Built-in antenna
- High sensitivity: -159dBm
- 30’ Positional Accuracy / 25’ with WAAS
- Supports WAAS in default mode.
- Hot Start : 8 seconds
- Warm Start : 38 seconds
- Cold Start : 42 seconds

- 70mA power consumption
- 4.5 – 6.5 volt operation
- Outputs NMEA 0183 and SiRF binary protocols
- Small foot print : 30mm x 30mm x 10.5mm
- Built-in LED status indicator
- 6-pin interface cable included

The EM-408 module is also manufactured by USGlobalSat. This module doesn't have its own evaluation board. It does have a built-in antenna and a MMCX connector for attaching an external antenna. Both the EM-406A and the EM-408 outputs its data at 4800 baud, 8N1.

EM-408 Specifications:

- 20 Channel Receiver
- Built-in antenna
- High sensitivity: -159dBm
- 30' Positional Accuracy / 25' with WAAS
- Supports WAAS in default mode.
- Hot Start : 8 seconds
- Warm Start : 38 seconds
- Cold Start : 42 seconds
- 75mA power consumption
- 3.3 volt operation
- Outputs NMEA 0183 and SiRF binary protocols
- 30gram weight
- Built-in LED status indicator
- 5-pin interface cable included
- External MMCX antenna connector

NAVIBE 611 Sport GPS

The NAVIBE 611 is a small GPS module that operates off 2 AA Batteries. It can also be powered via the rear connector. It features a small connector that provides both a serial and USB interface. It also has data logging capabilities.

NAVIBE 611 Sport GPS Specifications:

- Durable orange rubberized housing
- 12 parallel channels for fast acquisition and reacquisition
- Supports standard NMEA 0183 protocol
- Water resistant housing
- LCD display shows distance, average/max speed
- Operates on two (2) AAA batteries
- Can also be used as a USB GPS receiver

The Holux GPSlim236 shown supports a Bluetooth wireless interface and has a built-in battery that will power the module for 10 hours. The connector is a noninverting TTL serial interface that can be used when interfacing with a microcontroller.

Holux GPSlim236 Specifications:

- Dual function (Bluetooth GPS+ G-mouse)
- 20 parallel satellite-tracking channels for fast acquisition and reacquisition
- Compatible with Bluetooth Serial Port Profile (SPP) completely
- Built-in rechargeable Lithium ion battery without external power supply for at least 10 hours operation.
- Built-in 850mAh rechargeable battery for memory and RTC backup and for fast Time To First Fix (TTFF).
- Support NMEA0183 v2.2 data protocol or SiRF binary code
- FLASH based program memory
- New software revisions upgradeable through serial interface

2.3 Software Research

As mentioned previously, the software used in this project was to be limited to PC software and controller software. In today's fast emerging market, there are various options and hence it was necessary to research them in detail. Under PC software, there are few important components that need to be researched:

2.3.1 User Interface

It was established that the user interface would need to be a powerful graphical user interface (GUI) application for debugging and logging data purposes. While the user interface did not have any impact on the functional performance of the project, it provided several particularly useful features. These included the observation of the completed converter's operation and the display of system operation for the purposes of debugging as the converter is being perfected.

Furthermore, the GUI was intended to provide capability for the software to be updated in the field. This would allow for modification as deemed necessary in the future, or for the correction of potential errors that may be discovered.

2.3.2 PC Communication

One of the ways to establish long communication between the PC and digital controllers is via a serial. Although, the serial connection requires a large voltage

swing i.e. ±12V, it still is one of the easiest way to transfer data. A serial connection only requires three wires – receive, transmit, and ground.

Another method of communication could be though a Wi-Fi port. A Wi-ranger is already in place inside the DAQ box of the sensor package. It should not be too difficult to integrate

2.3.3 Digital Controller

The control system controllers can be classified in four main types:

1. Proportional Controllers (P Controllers) – These controllers are simple controllers that are used to provide stable gain. Supplying a proportional gain is one of the main features of such controller. This is achieved by overshoot compensation and ripple voltage minimization. The proportional gain achieved by such systems is fairly low. Hence, P Controllers alone are not a desired option for control systems requiring high proportional gain.
2. Proportional-Derivative Controllers (PD Controllers) – These controllers basically are used to compensate for some future error value. For highly varying output systems, such controllers are desired as they provide a proportional derivative gain. Although such systems greatly reduce overshoot and ripple, they are inefficient as a small amount of high frequency noise can have a large distortion in the system. Hence, it is possible for the PD Controllers to set a value that is far from the desired output value.
3. Proportional-Integral Controllers (PI Controllers) – Opposing to the PD Controllers, the PI Controllers are used to compensate for some past value errors. By taking an integral of the output value minus the desired value, this controller compensates for the steady-state error by minimizing it to zero, unlike the P Controller. Also, unlike the PD Controller, the PI Controller maintains a steady signal in case of high frequency noise due to the lack of derivative action. However, such controllers are much slower and less responsive and hence undesirable for the project.
4. Proportional-Integral-Derivative Controller (PID Controller) – A PID Controller is a combination of all three – Proportional, Integral and Derivative Controller. This controller takes a proportional constant and adds it to the current output. Then, the error generated from it will be integrated and added on to the system which makes the system steady-state. Finally, the derivative action is provided in order to control the output for any change or disturbance. Such controllers are flexible and can be programmed to achieve desirable outputs with high accuracy. Hence, a PID Controller is the most suited option for the project.

A proportional-integral-derivative (PID) controller can be used as a feedback controller. A simple algorithm can be created for controlling the different voltages and currents. Figure 2.23 shows a block diagram image of a PID controller.

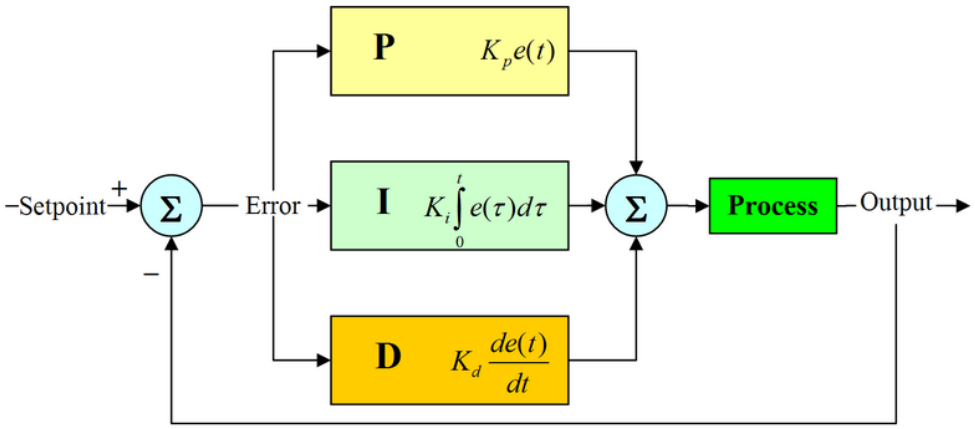

Figure 2.23: Block Diagram of a PID Controller (Reprinted under CC-BY-2.5; Released under the GNU Free Documentation License)

2.3.4 PIC Microcontroller

In order to efficiently program the PIC microcontroller, a software program needed to be chosen that could provide professional results and be easy to troubleshoot. A suitable compiler would not only determine the productivity of the microcontroller but also overall efficiency of the system. The software packages were examined by looking at its programming language, availability of GUI and the built-in libraries. Cost of the software was also be a factor in determining the most appropriate software package.

After rigorous research, the options were narrowed down to MicroChip's MPLAB, MikroC Pro by MikroElektronica and HI-Tech owned by MicroChip which are reviewed below.

MikroC Pro – MikroC Pro is a product of MikroElektronica. This product has applications to a wide variety of dsPIC microcontrollers, just short of 250 different families including dsPIC 12/16/18/24/30/33. The company also offers products with different programming languages such as MikroBasic and MikroPascal that offers the programmer to program in Basic and Pascal environments respectively. However, it was predetermined to program in C language and hence MikroC was the best choice out of the other products. This software package introduces new and innovative ways of programing the microcontroller. These features include a powerful compiler, extended in-built libraries including hardware interfacing and DSP libraries, an IDE with various environments including a preview window in flash screen, a software simulator, and a powerful In-Circuit Debugger (ICD) called MikroICD which allows the user execute real-

time programs to debug code. MikroElektronica encourages consumers to purchase their hardware along with the software utility package in order to receive a discounted price. The price of the software package alone is $249.99. They also provide a free trial version that could be used except there is a code limit on it.

MPLAB — Microchip supplies three editions of MPLAB C compilers for dsPIC33F DSC line of microcontrollers. Each are ANSI x3. 159-1989-compliant Windows applications that serve as a platform for the development of C code. The compiler also includes a command-line driver program that enables application programs to be compiled, assembled, and linked with one step. The Standard compiler must be purchased, and it features all optimization levels. The free Standard Evaluation compiler features all optimization levels for 60 days before downgrading to level one optimization. The free Lite compiler offers only optimization level one. While higher optimization levels could reduce the amount of code or increase the speed to an extent, the dsPIC33FJ12GS504 microcontroller has a significant amount of flash memory and should not suffer for a low optimization level. Considering that the MPLAB compiler is free, and that it is offered by Microchip specifically for use with their microcontrollers, it seems the most logical choice for this project.

HI-TECH – (now owned by Microchip) offers a freestanding, optimizing ANSIC compiler that supports PIC and dsPIC devices. The compiler is available for all popular operating systems both 32-bit and 64-bit. As well as being a stand-alone console application, it is fully compatible with Microchip's MPLAB IDE. This allows a user to develop in MPLAB and compile with HI-TECH. The compiler includes many built in functions and it produces highly efficient machine code. The retail cost of this complier places it outside of the budget of this project. However, they do offer a LITE version of the complier for free at htsoft.com. The compiler also integrates into HI-TIDE. This is an IDE based on Eclipse. The HI-TECH compiler produces small, tight, fast code. However, it isn't as user-friendly as its MikroC and MPLAB counterparts are.

Chapter 3: Design

3.1 Hardware

The Hardware system for this project was divided into four different parts:

1. Input Circuit (AC-DC Rectifier)
2. Buck Converter (DC-DC Converter)
3. Battery Charging Controller
4. Microcontroller

Figure 3.1 shows the block diagram of the Power Management Circuit which will be discussed in detail in the following sections.

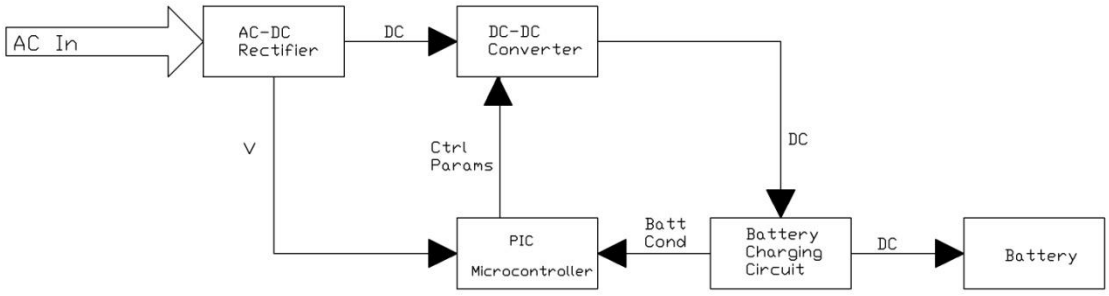

Figure 3.1: Complete Block Diagram of Power Management Circuit

3.1.1 Input Circuit

The mechanical engineering team designed a turbine to drive a Ginlong permanent magnet generator. This generator produced a 3-phase output of variable frequency, current, and voltage. This output was rectified to a constant DC voltage. That DC voltage was stepped down to 15.6 volts. The 15.6 volt output was used to charge a battery and power the internal circuitry. Both the rectifier and converter were realized with digital control mechanisms. In particular, a DSP microcontroller ran simple control algorithms to monitor the input voltage and conditionally disable the converter. The latter helped elucidate how the system operates as a whole. The arrows indicate signal flow and direction. Lastly, signals within the blocks are digital and signals between the blocks are analog.

There are many designs for accomplishing AC to DC rectification. The Ginlong generator is designed to produce a 500W of output power. For high power applications, a three-phase input helps lower the stress on components and reduce component size. Originally, our design was going to be a three-phase non-isolated VIENNA rectifier. However, the total power consumption of the sensors was only 15 watts. Additionally, the mechanical teams only reported

being able to generate a maximum of 250 RPMs. The latter corresponds to an open circuit voltage of only 25 volts. We chose to implement a simple full wave bridge rectifier with a large 150µF reservoir capacitor. This design was simple and worked at varying AC frequencies. We converted to a single phase output from the generator by only connecting to one hot leg and a neutral. The other two disconnected terminals didn't have any effect because no current could be drawn from them. Thus, they don't add any torque to the generator.

We wanted a visual indicator of when the generator was producing electricity. So, the first part of circuit consisted of an LED indicator. Then, the varying amplitude AC from the generator was converted to varying amplitude DC with an AC-DC converter. The system needed to be self powered. So, we also included two fixed output voltage regulators to drop the 12 volt output of the battery down to 5 volts and 3.3 volts. The block diagram of the input circuit is shown in Figure 3.2.

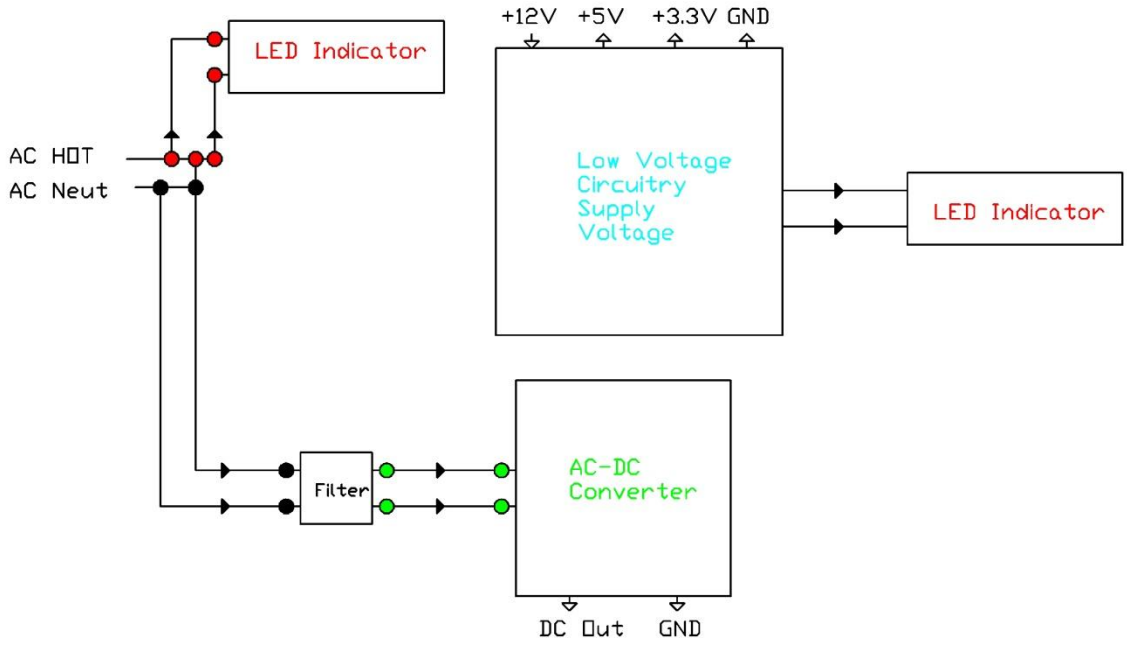

Figure 3.2: Input Circuit Block Diagram

The LED indicator circuit used a 1MΩ resistor to drop the voltage down to an acceptable value. The voltage drop across the resister only occured when the LED was connected. The latter was because the LED draws 30mA of current. Without this current draw, there is no voltage drop across the resistor and the open circuit voltage at the LED terminals would be much higher than the LED could handle. Therefore, the LED was always connected to the indicator circuit. Two diodes were used to block the negative portion of the AC waveform. A fairly large reservoir capacitor was used to smooth the positive waveform into a steady DC voltage with a slight ripple. With a 30mA current draw, the maximum output

voltage across the LED was around 2.0 VDC. A 2.6 volt 30mA red 5mm LED was chosen. Figure 3.3 shows the complete schematic of the LED indicator circuit.

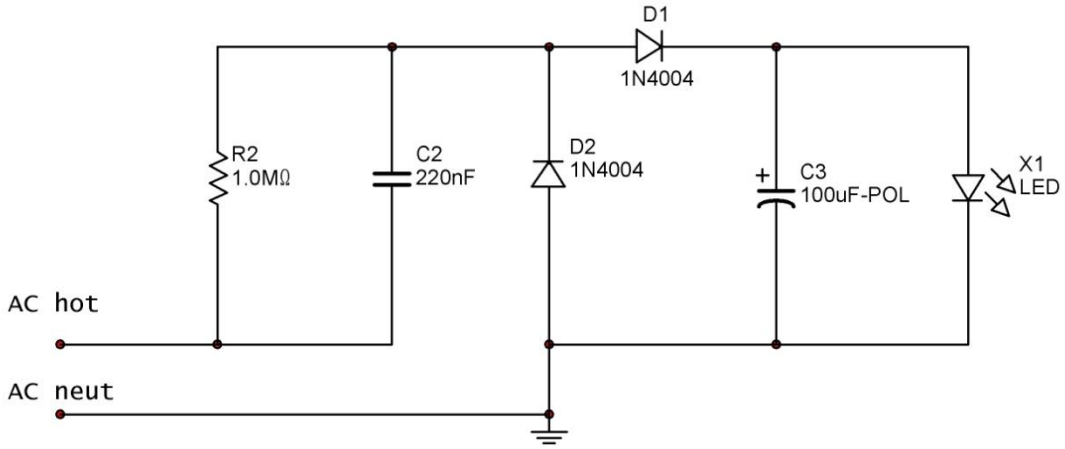

Figure 3.3: LED Indicator Circuit

The next stage of the input circuit was a full wave bridge rectifier. This circuit is very simple and doesn't require any explanation. A low pass filter consisting of two capacitors and an inductor was placed in front of the bridge rectifier to block high resonant frequencies. A large 150uF smoothing capacitor was placed at the output. The generator will produce an AC voltage at different frequencies for different RPMs. The large smoothing capacitor will still effectively convert the rectified AC to DC. At lower frequencies, the voltage ripple will be higher.
Figure 3.4 shows the complete schematic of the AC-DC converter circuit.

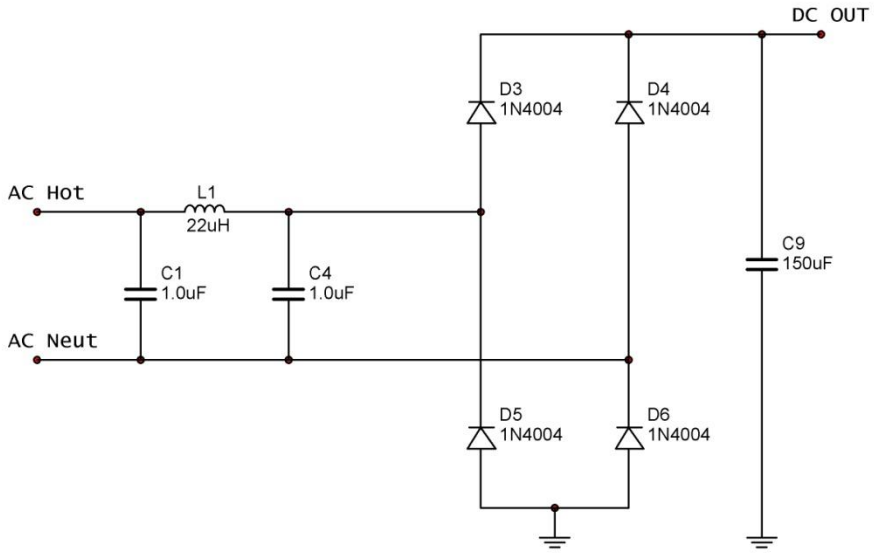

Figure 3.4: AC-DC Rectifier with Smoothing Output Capacitor

The last portion of the input circuit is composed of two fixed output voltage regulators. These regulators are used to convert 12 VDC from the lead acid battery to 5 volts and 3.3 volts. First, to regulate the voltage down to 5 volts, we used a LM340AT-5 3 terminal fixed output regulator. The TO-220 package was chosen without a heatsink because total current drawn through the regulator was less than 500 mA. The LM340AT-5 can supply a current in excess of 1 amp.

This regulator features thermal overload protection, internal short circuit protection, and output transistor safe area compensation. Thermal overload protection shuts down the circuit when subjected to an excessive power overload condition. Internal short circuit protection limits the max current the circuit will pass, and output transistor safe area compensation reduces the output short circuit current as the voltage across the pass transistor is increased. We bypassed the regulator input with a capacitor. Although some designers choose not to bypass the input when used with low current applications, we felt it was better to design the circuit for easy modification at a later date. If other low voltage components need to be added to the system, the current requirements will increase. The 5 volt output was used to power our 2x16 LCD display.

The output was also connected to the LM3940 regulator. The LM3940 is a low dropout regulator for 5 V to 3.3 V conversion. Because the LM3940 is a true low dropout regulator, it can hold its 3.3V output in regulation with input voltages as low as 4.5V. The T0-220 package of the LM3940 means that in most applications the full 1A of load current can be delivered without using an additional heatsink. The 3.3 volt output was used to power our PIC24 microcontroller. The datasheet for the LM3940 stated an external output capacitor was critical to maintain regulator stability. The datasheet called for a minimum capacitance of 33 uF. We used a 47 uF capacitor that met the minimum ESR requirements specified in the datasheet. Figure 3.5 shows the complete schematic of the low voltage supply circuit.

We wanted a visual indicator of when the system was actively charging the battery. Therefore, a 2N4401 general purpose NPN transistor was connected to a 3.6 V blue 5mm LED. The base leg of transistor was connected to the enable line of the buck converter. Therefore, when the microcontroller sends a logical high (3.3 VDC), the transistor will pass current from the collector to the emitter. The collector was connected to the 3.3 volt bus. The emitter was connected to the positive side of the blue LED. The negative side of the LED was connected to ground. The 2N4401 is rated for up to 600 mA.

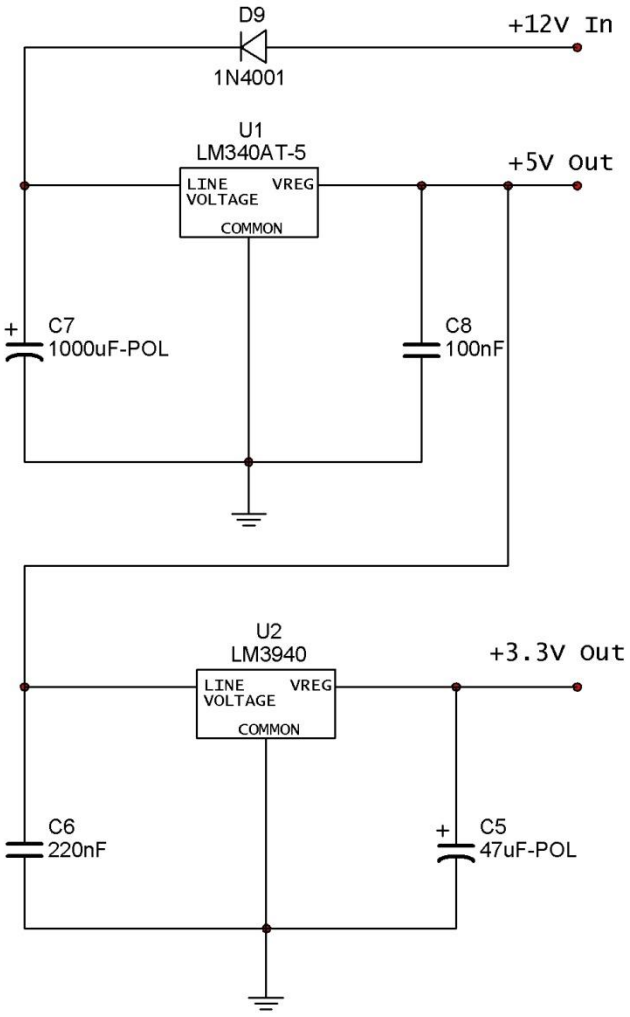

Figure 3.5: Low Voltage Supply Circuit

3.1.2 DC-DC Converter

The output of the Input circuit used as the input for the DC-DC Converter. The goal was to convert a varying DC signal to a steady DC output to power the sensor package. It was determined in the research section that a synchronous Buck Converter would be the most appropriate option. Based on the output of the Input Circuit, a proper DC-DC buck converter had to be used to produce desirable outputs. The DC-DC converter for this project had to take voltages up to 60V (peak) and be able to operate with low input current. The converter had to be able to produce a steady output voltage of 12V and an output current of 2A. After researching various DC-DC Buck Converters that fit above characteristics, the TPS54260 3.5V to 60V input, 2.5A, step down converter by Texas Instruments was found to be the most appropriate. The features for this component are given in Table 3.1 [13].

Parameters	Values	Unit
I_{OUT} (max)	2.5	A
V_{IN} (min)	3.5	V
V_{IN} (max)	60	
V_{OUT} (min)	0.8	
V_{OUT} (max)	58	
I_Q (typ)	0.138	mA
Switching Frequency (max)	2500	kHz
Switch Current Limit (typ)	3.5	A
Regulated Outputs	1	#
Duty Cycle (max)	98	%
Operating Temperature Range	-40 to 150	°C
Thermal Shutdown	182	
Topology	Buck, Inverting Buck/Boost	

Table 3.1: Parameters of the TPS54260 Buck Converter

As seen in the specifications table, the TPS54260 Step Down Converter operates at voltage up to 65V which is higher than the desirable 60V. Figure 3.6 shows a functional block diagram of the TPS54260 Step Down Converter. Figure 3.7 shows the functional diagram of TPS54260. The different applications of this converter could be derived by understanding the block diagram.

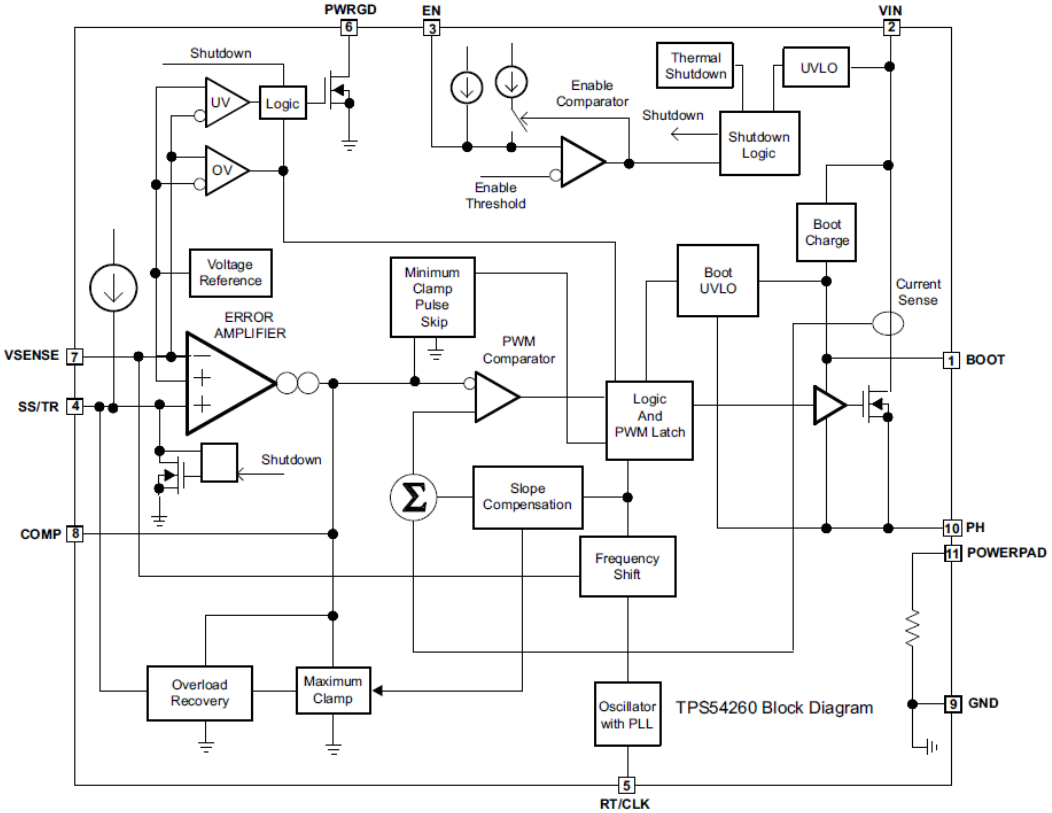

Figure 3.6: Functional Block Diagram of the TPS54260 Step Down Converter (Courtesy of Texas Instruments)

200-mΩ High-Side n-channel MOSFET – is one of the features embedded inside this converter. This MOSFET allows high efficiency which makes the regulator capable of delivering 2.5A of continuous current to a load.

Error Amplifier – TPS54260 comes with an inbuilt transconductance error amplifier. The COMP pin (pin 8) is driven by the output of the error amplifier. This amplifier compares the output voltage and the internal reference voltage. The output of the error amplifier is compared to the high side power switch circuit. The voltage on the COMP pin increases or decreases as the output current increases or decreases. Once the power switch current reaches the level set by the COMP voltage, the power switch turns off. Additionally, the amplifier compares the V_{SENSE} voltage to the voltage set by the SS/TR pin or the internal 0.8V voltage reference. During normal operation, the transconductance (gm) of the amplifier is 310µA/V. The transconductance of the amplifier changes with the change in the voltage level. During the slow start operation, the transconductance is a fraction of the normal operating gm and is 70µA/V when the V_{SENSE} pin falls below 0.8V.

Low Dropout Operation and Bootstrap Voltage (BOOT) – The TPS54260 is equipped with an integrated boot regulator. This regulator provides a gate drive voltage to the high side MOSFET when used with a small ceramic capacitor (0.1µF, 10V, X5R/X7R), as shown in Figure 3.7. In order to maintain the maximum duty cycle (100%) for drop out improvement, the voltage between the BOOT pin and PH pin must remain above 2.1V. This voltage drives the high side MOSFET. When the voltage drops below 2.1V, the high side MOSFET turns off using an UVLO circuit and the low side diode conducts. This refreshes the BOOT capacitor charge. However, for this design, caution had to be taken since the design is made for light/no load situations. During such situation, the V_{IN} stop voltage is supposed to be greater than BOOT UVLO trigger condition. This can be done by replacing resistors on the EN pin using the V_{IN} UVLO feature.

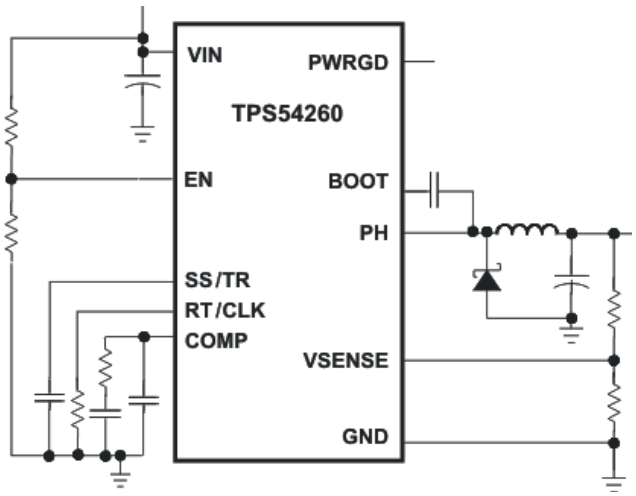

Figure 3.7: Functional Diagram of the TPS54260 Step Down Converter (Courtesy of Texas Instruments)

Equations 3.1 and 3.2 are used to calculate the resistor values on the EN pin.

$$R1 = \frac{V_{START} - V_{STOP}}{I_{HYS}} \quad (3.1)$$

$$R2 = \frac{V_{ENA}}{\frac{V_{START} - V_{ENA}}{R1} + I_1} \quad (3.2)$$

Where, V_{START} = Start voltage for hysteresis
V_{STOP} = Stop voltage for hysteresis
I_{HYS} = Hysteresis current
I_1 = internal pull-up current for EN pin (0.9µA)
V_{ENA} = Voltage at enable pin

Figure 3.8 shows the external resistors R1 and R2 that could be replaced in order to set the undervoltage lockout.

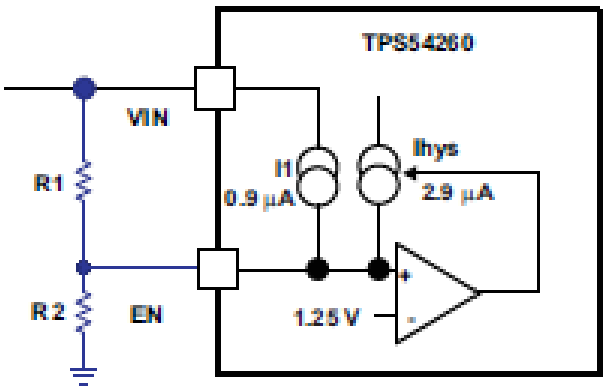

Figure 3.8: Adjustable Undervoltage Lockout (UVLO)
(Courtesy of Texas Instruments)

Enable – This is an optional feature of the TPS54260. This feature shuts down the regulator in case the enable pin (Pin 3) is high. The microcontroller was programmed in order to monitor the input voltage of the system. If the input falls below 15V, the enable pin is pulled and the regulator shuts down. The specifications of the Enable pin are show in Table 3.2. The workings of the Enable pin are provided in the microcontroller section in detail.

Slow Start/Tracking Pin (SS/TR) – was used to regulate the output. In order to implement slow start, a capacitor needed to be used on the SS/TR pin to ground. A 2µA internal pull up current is provided by the TPS54250 in order to charge the slow start capacitor. Equation 3.3 was used to calculate the value for the slow start capacitor (C_{SS}).

$$C_{SS} = \frac{T_{SS} \times I_{SS}}{V_{REF} \times 0.8} \ (nF) \quad (3.3)$$

Here, T_{SS} is the time for slow start in ms,
I_{SS} is the slow start current (2µA)
V_{REF} is the voltage reference (0.8V)

According to the above equation, the value for the Slow Start Capacitor (C_{SS}) for the design was 0.01µF.

Thermal Shutdown – The TPS54260 regulator will shut down when the junction temperature exceeds 182°C. Once the temperature drops below 182°C, the regulator powers up by discharging the SS/TR pin.

Parameters		**Values**	**Unit**
Input Voltage	V_{IN}	-0.3 to 65	V
	EN	-0.3 to 5	
	Threshold EN	1.15 to 1.36	
	BOOT	73	
	V_{SENSE}	-0.3 to 3	
	COMP	-0.3 to 3	
	PWRGD	-0.3 to 6	
	SS/TR	-0.3 to 3	
	RT/CLK	-0.3 to 3.6	
Output Voltage	BOOT-PH	8	V
	PH	-0.6 to 65	
	PH, 10-ns Transient	-2 to 65	
Voltage Difference	PAD to GND	±200	mV
Source Current	EN	100	µA
	BOOT	100	mA
	V_{SENSE}	10	µA
	PH	Current Limit	A
	RT/CLK	100	µA

Table 3.2: Pin Specific Parameters for TPS54260

TPS54260EVM-597 – For this project, the TPS54260EVM-597 was used. This is an evaluation module which was available for purchase from Texas Instruments. This module was already populated as shown in Figure 3.9. Table 2 shows the Performance Specification Summary of TPS54260EVM-597.

As shown in Table 3.3, the EVM was maximized for an input voltage range of 10.8V to 13.2V. This left the output voltage to at 3.3V. According to the specifications of the project, the input range of the buck converter needed to be 0V to 60V and the output voltage to be minimum 15V which was to be fed into the battery charging circuit.

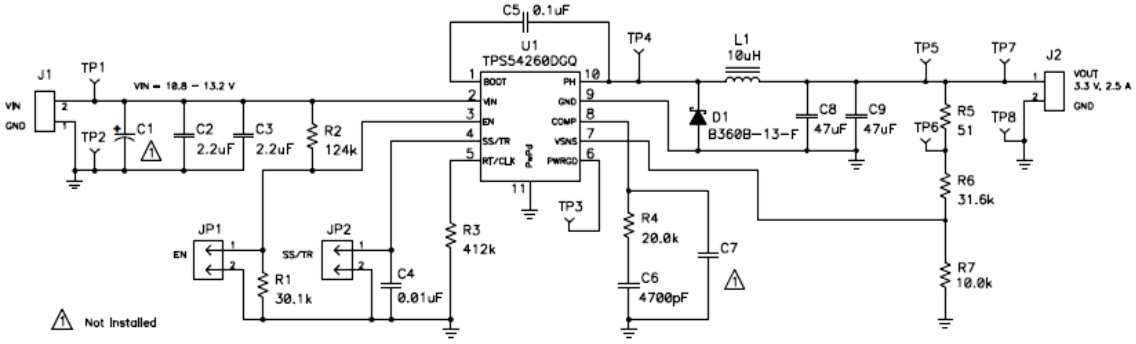

Figure 3.9: TPS54260EVM-597 Schematic
(Courtesy of Texas Instruments)

However, since this is a buck converter, the input voltage would have to be greater than 15V. (This problem could be easily fixed in the future generation by the use of a SEPIC topology instead of a buck topology.) Hence, the input voltage range was changed to 16V to 56V. In order to implement the necessary changes, certain components had to be replaced from the EVM. The new components were chosen as follows:

Output Voltage Set Point: The most important change in the EVM was to change the resistor value R_6. This was calculated by using Equation 3.4.

$$R_6 = 10k\Omega \times \frac{V_{OUT} - 0.8V}{0.8V} \quad (3.4)$$

For V_{OUT} = 16V, R_6 = 190kΩ. However, the closest value to that was 187kΩ which changed to V_{OUT} to be 15.7V which was acceptable for the design.

Specifications	Values			Unit
	Min	Typ	Max	
Input Voltage (V_{IN})	10.8	12	13.2	V
Output Voltage (V_{OUT})		3.3		V
Output Current (I_{OUT})	0		2.5	A
Operating Frequency		300		kHz

Table 3.3: Specifications for TPS54260EVM-597

Output Capacitors: Another important change that was needed for the design was that of the output capacitors. The two 47µF output capacitors C_8 and C_9 that were already populated in the EVM could have worked as the capacitance of both was high enough. However, the voltage rating on both of them was 10V which was much lower than the output voltage and hence needed to be changed. Keeping the switching frequency (f_{SW}) of the circuit at 300kHz. For a 5% transient load response the change in V_{OUT} for a load step of ΔI_{OUT} = 1A, gives us ΔV_{OUT} = 0.69V. Using Equation 3.5, the minimum value for C_{OUT} was calculated.

$$C_{OUT} > \frac{2 \times \Delta I_{OUT}}{f_{SW} \times \Delta V_{OUT}} \quad (3.5)$$

After calculating, the value for C_{OUT} was found to be 9.66µF. In order to account for the DC bias loss and to give some margin for calculation, the total value for C_{OUT} was set to 100% of its initial value. Hence, the two 47µF capacitors were replaced by two 10µF capacitors.

The edited version of the schematic was then introduced into SwitcherPro Desktop which is analysis based software provided by Texas Instruments. Figure 3.10 shows the efficiency of the TPS54260EVM.

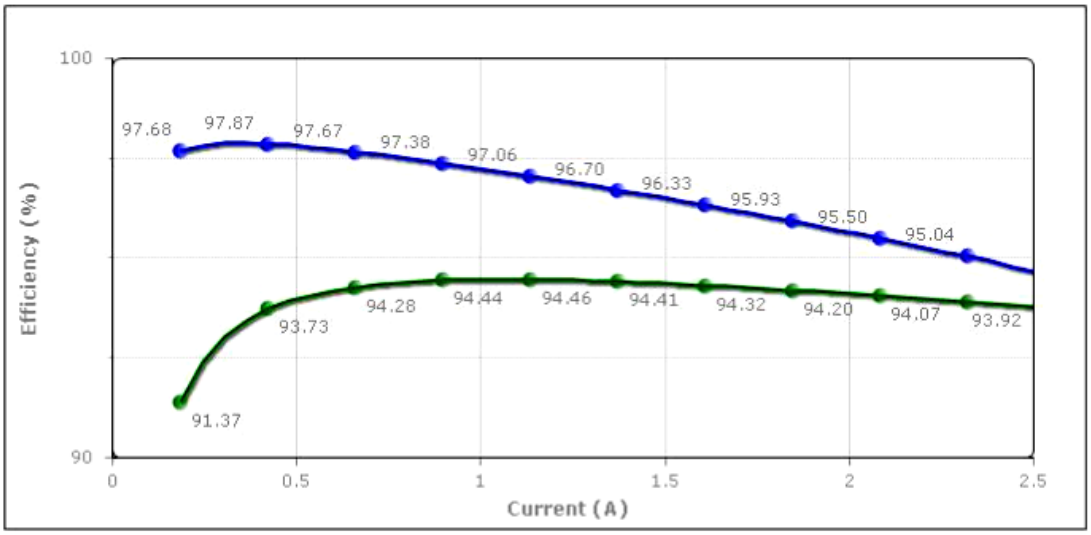

Figure 3.10: TPS54260EVM Efficiency vs. Output Current

3.1.3 Battery Charging Circuit Design

For this project, a BQ24450 integrated charge controller for lead-acid batteries was chosen. This controller regulates both voltage and current during charging which ensures safety and charging efficiency. This also helps maximize the battery charging capacity and battery life. Figure 3.11 shows a simplified block diagram of the BQ24450 controller.

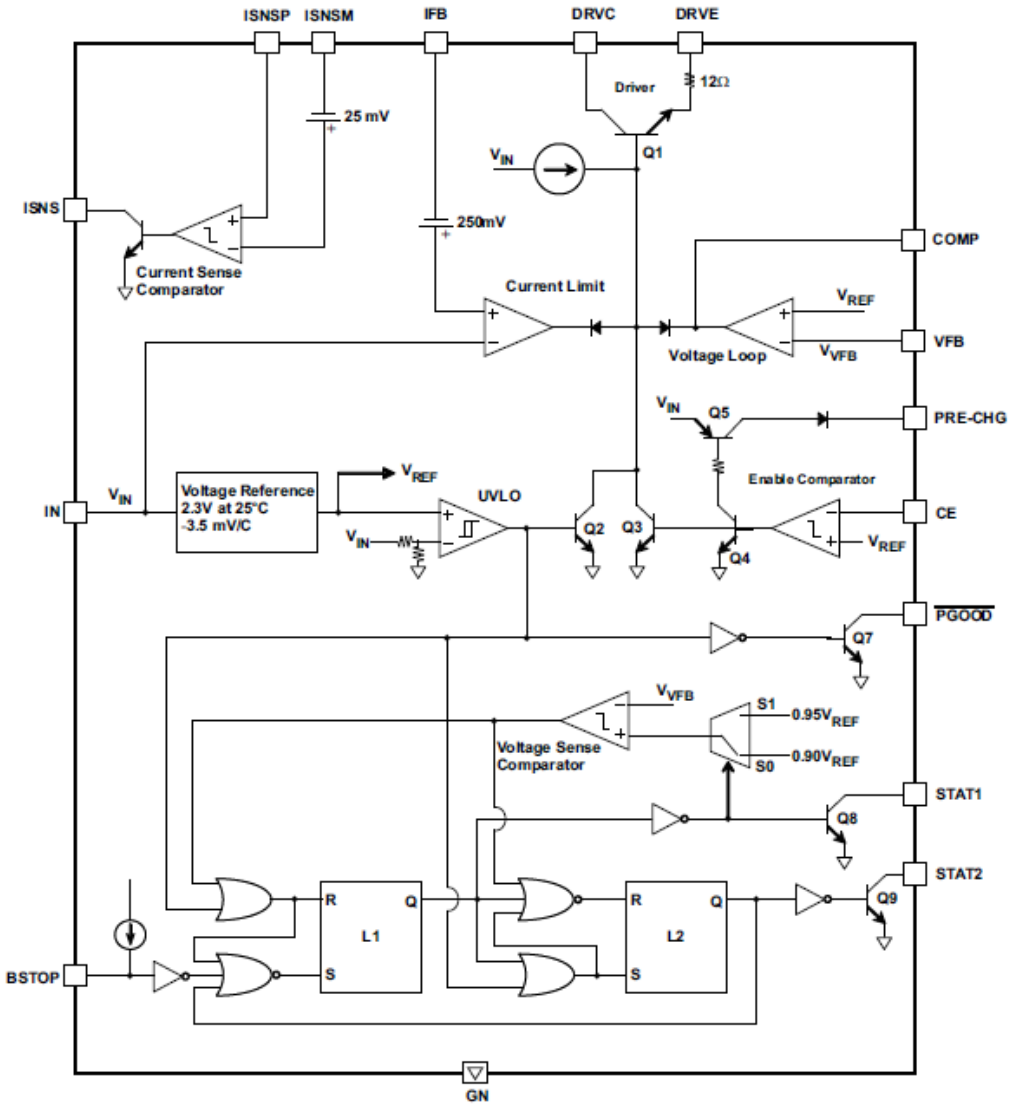

Figure 3.11: BQ24450 Block Diagram
(Courtesy of Texas Instruments)

As seen in the block diagram, the IC features built-in precision voltage reference. This is temperature-compensated which allows the IC to track the characteristics of lead-acid cells providing optimum charge without the use of any external components. Also, the low current consumption capability of the IC helps maintain higher accuracy for temperature monitoring as it minimizes the self-heating effects.

There are different ways the IC could be configured: constant-voltage float charge, dual-voltage float-cum-boost charger or dual step current charger. For this design, an improved dual-level float-cum-boost charger with pre-charge configuration was chosen. This configuration allows the charger to pre-charge the battery till the voltage levels rise to levels safe enough to permit charging at

maximum current ($I_{MAX-CHG}$) [14]. This is a very important feature as it ensures battery safety when the batteries are deeply discharged.

As shown in Figure 3.12, the CE pin (pin12) was used to detect the voltage of the battery. If the voltage at the CE pin is below V_{REF}, the comparator turns ON Q3 and Q4. As this turns OFF Q1, Q5 is turned ON. This lets the pre-charge current (I_{PRE}) to flow from PRE-CHG pin (pin11) through R_T into the battery. If the voltage of the battery is above the safe threshold V_{TH}, the enable comparator is turns OFF Q3 and Q4 which turns ON Q1. This turns OFF Q5 and provides $I_{MAX-CHG}$ through Q_{EXT}. The circuit then resumes its normal operation.

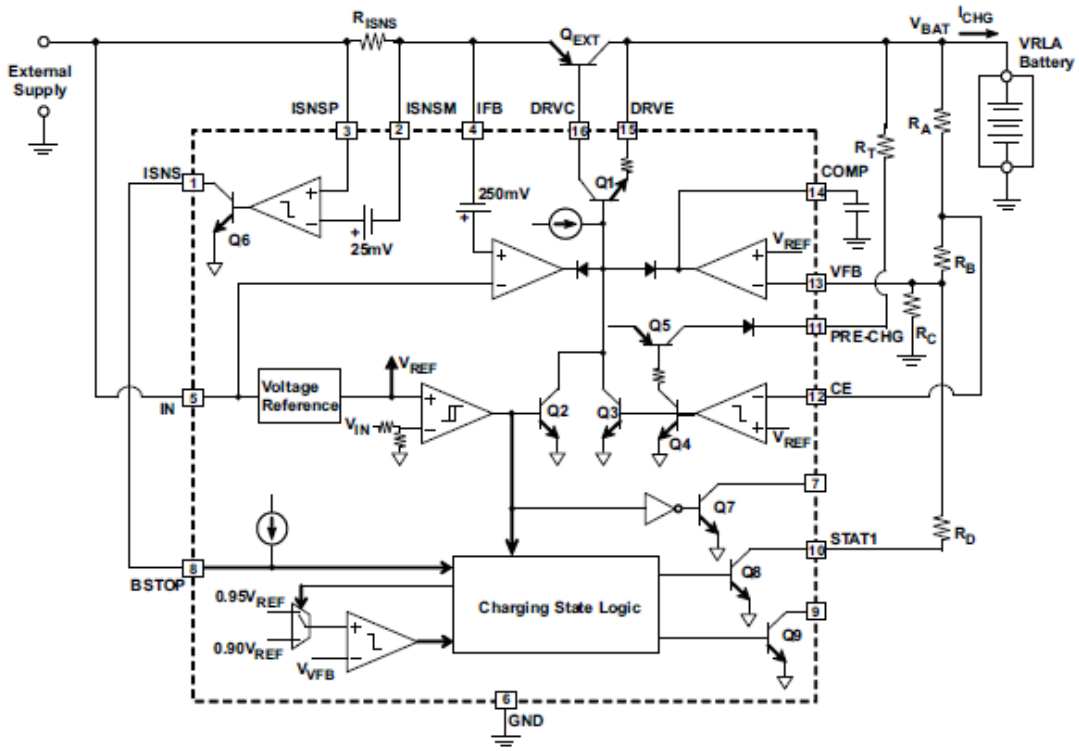

Figure 3.12: Improved Dual-Level Float-Cum-Boost Charger with Pre-Charge (Courtesy of Texas Instruments)

In order to charge the sealed acid-batteries with the BQ24450, an external pass transistor was required in the circuit. The circuit was able to support NPN as well as PNP pass transistors. There were a variety of external pass-transistor circuits available for this design: Common-Emitter PNP, PNP in a Quasi-Darlington with Internal Driver, External Quasi-Darlington, and NPN Emitter-Follower. However, before implementing an external pass-transistor circuit, certain factors were needed to be taken into account:

1. The external pass circuit needs to have sufficient voltage rating for the application.
2. Must have necessary current and power handling capabilities to charge the battery at desired rate.

3. Must have enough current gain in order to keep the drive current below 25mA.

Keeping the above factors in mind, the external pass-transistor circuit was chosen as the Common-Emitter PNP as shown in Figure 3.13.

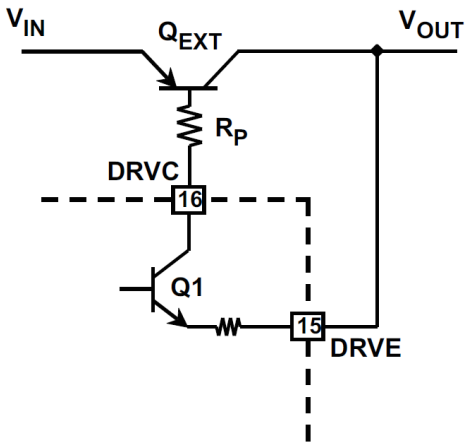

Figure 3.13: Common-Emitter PNP External Pass-Transistor Circuit
(Courtesy of Texas Instruments)

The above mentioned circuit has the $I_{MAX\text{-}CHG}$ range of 25mA to 1000mA. This was a critical specification as our goal was to keep the $I_{MAX\text{-}CHG}$ between 600mA and 800mA. Additionally, the input to output differential for the design was 1.5V. Common-Emitter PNP was the only fit to this specification as the minimum differential voltage ΔV was 0.5V. Initializing this external pass-transistor circuit required compensation capacitor at the COMP pin. For stable operation under all conditions, the value of C_{COMP} was chosen as 0.1µF. Also, the IC's power dissipation was calculated using Equation 3.6.

$$P_D = \left(V_{IN(MIN)} - 0.7V\right) \div h_{FE} \times I_{MAX-CHG} - (I_{MAX-CHG})^2 \div (h_{FE})^2 \times R_P \quad (3.6)$$

In the above expression, h_{FE} is the current gain of the external transistor. In order to minimize IC's self heating and share some power dissipation, an external resistor, R_P, could also be used. Equation 3.7 below was used to calculate the value for R_P.

$$R_P = (V_{IN(MIN)} - 2.0V) \div I_{MAX-CHG} \times h_{FE(MIN)} \quad (3.7)$$

BQ24450EVM – For this design, a BQ24450EVM was chosen. This Evaluation Module (EVM) from Texas Instruments was suitable for the project as it was populated with all the necessary components. The EVM features all the necessary characteristics that were needed for the project's design. There were a couple important features that were worth mentioning: Programmable charge current and pre-charge for deeply discharged lead-acid batteries. The schematic for the BQ24450EVM is shown in Figure 3.14.

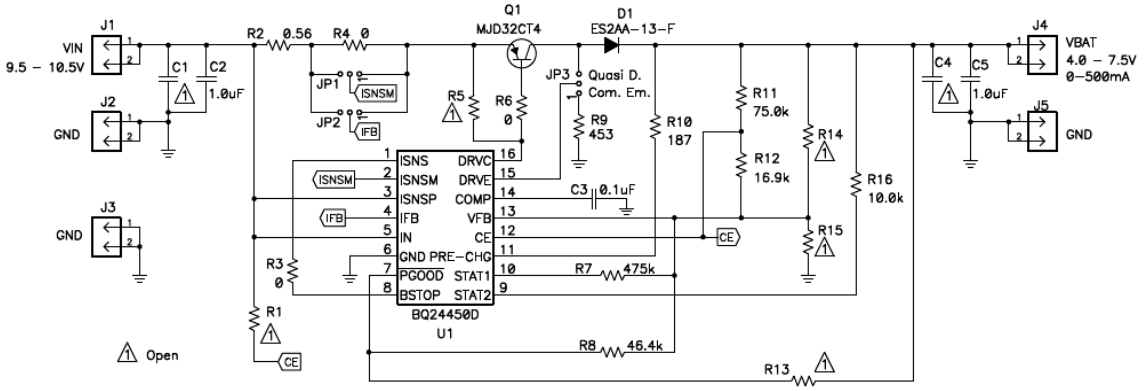

Figure 3.14: BQ24450EVM Schematic
(Courtesy of Texas Instruments)

As shown in Figure 3.13, the BQ24450EVM was initially populated for the specifications as shown in Table 3.4.

Specifications	Values			Unit
	Min	Typ	Max	
Input Voltage (V_{IN})	9.5	10	10.5	V
Output/Battery Voltage (V_{BAT})	4		7.5	V
Supply Current (I_{IN})	0		0.5	A
Output/Charge Current (I_{OUT})	0		0.5	A

Table 3.4: BQ24450EVM Specifications

Hence, it was necessary to replace some components in the design to achieve the following specifications as shown in table 3.123.

Specifications	Values			Unit
	Min	Typ	Max	
Input Voltage (V_{IN})	13.8	15.6	16.4	V
Output/Battery Voltage (V_{BAT})		13.8		V
Supply Current (I_{IN})	0		0.5	A
Output/Charge Current (I_{OUT})	0		0.7	A

Table 3.5: Required BQ24450EVM Specifications

According to the BQ24450EVM user's guide, the output voltage could be changed by replacing some on-board resistors (R_7, R_8, R_9, R_{11}, and R_{12}). The voltage reference, V_{REF}, on the V_{FB} pin (pin 13) is 2.3V and the leakage current in the STAT1 pin (pin 10) is 50µA. V_{TH}, V_{FLOAT}, and V_{BOOST}, for the system is 10.5V, 13.8V, and 14.4V respectively. Equations 3.8 – 3.12 were used to calculate the necessary values:

$$R_C = 2.3V \div 50\mu A = 46k\Omega\ (46.4k\Omega) = \mathbf{R_8} \quad (3.8)$$

$$V_{BOOST} = V_{REF} \times (R_A + R_B + R_C \parallel R_D) \div R_C \parallel R_D$$

$$\rightarrow R_D = 661.259k\Omega\ (665k\Omega) = \mathbf{R_7} \quad (3.9)$$

$$V_{FLOAT} = V_{REF} \times (R_A + R_B + R_C) \div R_C \rightarrow R_A + R_B = 5 \times R_C = 230k\Omega \quad (3.10)$$

$$V_{TH} = V_{REF} \times (R_A + R_B + R_C \parallel R_D) \div (R_B + R_C \parallel R_D) \rightarrow R_B = 16.9k\Omega = \mathbf{R_{12}} \quad (3.11)$$

$$R_A = 92.8k\Omega - R_B = 213.1k\Omega\ (215k\Omega) = \mathbf{R_{11}} \quad (3.12)$$

The value for R_9 was kept the same as that of the EVM (453Ω).

3.1.4 Battery

For the purpose of the prototype, a lead-acid battery was needed. After research, the Enercell 12V 7AH sealed lead acid battery was chosen to implement in the design. Figure 3.15 shows the picture of the battery while Table 3.6 shows the battery characteristics.

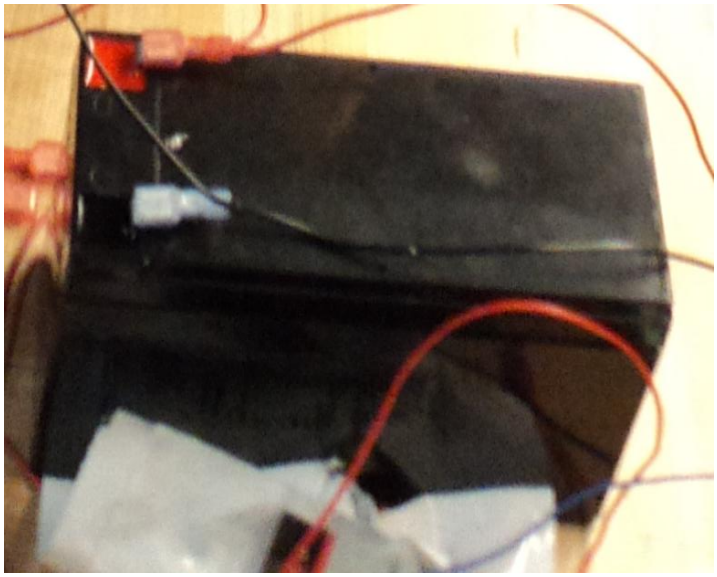

Figure 3.15: Enercell 12V 7AH Sealed Lead-Acid Battery

Characteristics & Features	Values
Product Height	3.84 inches
Product Width	5.94 inches
Product Depth	2.56 inches
Chemistry	Sealed Lead Acid

Capacity	7000 mAH
Voltage	12 V
Rechargeable	Yes
Normal Charge	14.4 V – 15 V
Stand By/Trickle Charge	13.5V – 13.8 V
Max Initial Charging Current	2.1 A

Table 3.6: Battery Characteristics and Features

As shown in Table 3.6, the Enercell 12V 7AH Sealed Lead-Acid Battery was a perfect match for the prototype. It was also a good fit due to its 7000 mAH capacity. For a load current of 1mA, the battery would last for 7 hours with no waves in the gulf. Hence, it would be suitable for the initial prototype.

3.1.5 Microcontroller

In order to provide a degree of control over the overall system, it was decided that a microcontroller should be used. The intended goals of the microcontroller were to take measurements of both the input voltage and the battery voltage and to use the input voltage measurements to perform hysteresis and overvoltage protection of the system. In order to accomplish this, the mikroe LV 24-33 v6 development tools from MikroElektronika were used to program a PIC24FJ96GA010 microcontroller. The PIC24 microcontroller came pre-mounted on an MCU card with the development tools. Other microcontrollers were researched, but continued experimentation with the PIC24 microcontroller demonstrated that it would be more than sufficient for the intended applications. The microcontroller mounted on its MCU card is shown in Figure 3.16.

Figure 3.16: PIC24FJ96GA010 Mounted on an MCU Card

In order to take measurements of the system input voltage and battery voltage, two of the microcontrollers sixteen 10-bit analog to digital conversion (ADC) pins were used. Because the input voltage was expected to vary from 0 to 60V DC, and the battery voltage was expected to be roughly 12V DC, the voltages needed to be scaled down before they could be read by the microcontroller. To do so, simple voltage dividers were used. For the input voltage, a 1kΩ resistor and a 20kΩ resistor were used to create a ratio of 1:21, such that a maximum input of

60V would be reduced to approximately 2.85V before being fed into the microcontroller. For the battery voltage, a 10kΩ resistor and a 30kΩ resistor were used to create a ratio of 1:4, such that a battery voltage of 12V would be reduced to 3V before being fed into the microcontroller.

The method of using a voltage divider to scale down the voltages being read by the microcontroller initially led to some errors in measurement. While the voltage dividers worked reasonably well at low voltages, higher voltages resulted in loading effects. In order to adjust for these effects, two LM324n operational amplifiers were used as unity gain buffers to prevent current from feeding into the microcontroller from the voltage dividers. This resulted in significantly more accurate readings for the microcontroller which was necessary for proper functionality and control. Further error in the voltage readings was noticed as a small difference between the measured voltage after the voltage divider and the expected voltage. This error was a linear function of input voltage and was therefore easily compensated for in the microcontroller code.

Once the input voltages were converted from analog to digital by the microcontroller, the tens, ones, and tenths digits were extracted and displayed to the liquid crystal display (LCD). This was accomplished by taking the ADC reading, dividing by 1023 (2^{10} – 1 for the 10-bit ADC) and multiplying by 5000 to scale to a 5V range. The individual digits were then extracted by dividing through by a derived scaling term specific to the voltage divider used.

After the voltage dividers and unity gain buffers were implemented, a slight disparity in the range of hundredths of a volt was found between the expected and measured voltages after the voltage divider. This led to a reasonably small error in measured voltage which increased linearly with input. This error was negligible for the battery voltage which peaked at about 12V, but for the system input voltage which peaked at about 60V, a slightly larger error occurred. Because this error varied linearly with input, a simple correction sequence was implemented in the code. This ensured that the LCD displayed a value reflecting the actual input voltage as opposed to the slightly erroneous divided voltage.

3.1.6 C Language Code

The code that was developed and used to program the microcontroller is given below in bold text. Lines beginning with // are actual in-code comments. Additional commentary not found in the code is supplied intermittently.

The first segment of code establishes the necessary connections between the PIC microcontroller and the LCD.

```
// LCD module connections
sbit LCD_RS at LATB2_bit;
sbit LCD_EN at LATB3_bit;
```

```
sbit LCD_D4 at LATB4_bit;
sbit LCD_D5 at LATB5_bit;
sbit LCD_D6 at LATB6_bit;
sbit LCD_D7 at LATB7_bit;

sbit LCD_RS_Direction at TRISB2_bit;
sbit LCD_EN_Direction at TRISB3_bit;
sbit LCD_D4_Direction at TRISB4_bit;
sbit LCD_D5_Direction at TRISB5_bit;
sbit LCD_D6_Direction at TRISB6_bit;
sbit LCD_D7_Direction at TRISB7_bit;
// End LCD module connections
```

This section of code defines the variables that were used to calculate and convert the measured voltages, and to display the measurements to the LCD. The variable i is simply a counter, while ch3 and ch4 represent the tens and ones places of the system input voltage, respectively, in the internal calculations. The characters chA, chB, and chC represent the tens, ones, and tenths places of the system input voltage, respectively, in the LCD display. The value adc_read and adc_read2 represent the ADC readings of the system input voltage and battery voltage, respectively. The strings text and text2 were used to write text to the LCD. The values tlong and tlong2 were used in the internal calculations of the system input and battery voltages, respectively. The value x was used to compute a correction term for higher input voltages.

```
int i, ch3, ch4;
unsigned char chA, chB, chC, ch2, x;
unsigned int adc_rd;
unsigned int adc_rd2;
char *text;
char *text2;
long tlong;
long tlong2;
```

The code first defines the AN pins of the microcontroller as digital input/output pins, defines Port A as output, and sets Port A initially to one. Port A was connected to the blue LED through a FET device, causing the LED to illuminate momentarily once the microcontroller was turned on.

```
void main() {
  ADPCFG = 0xFFFF;                // Configure AN pins as digital I/O
  TRISA = 0;                      // Initialize PORTA as output
  LATA = 1;                       // Set PORTA to one
```

The code then cleared the LCD of any residual text from previous use of the device.

```
 LCD_Init();
 LCD_Cmd(_LCD_CURSOR_OFF);     // send command to LCD (cursor off)
 LCD_Cmd(_LCD_CLEAR);          // send command  to LCD (clear LCD)
```

This section of code served no particular purpose in terms of the intended goals of the project, but ensured that the message “Senior Design Spring 2011” would be displayed each time the microcontroller was turned on. “Senior Design” was assigned to text and sent to the first row, first column of the LCD. “Spring 2011” was then assigned to text and sent to the second row, first column of the LCD. The message was displayed for two seconds before the code progressed.

```
 text = "Senior Design";              // assign text to string
 LCD_Out(1,1,text);                   // print string on LCD, 1st row, 1st
collumn
 text = "Spring, 2011";               // assign text to string
 LCD_Out(2,1,text);                   // print string on LCD, 2nd row, 1st
collumn
 Delay_ms(2000);
```

After the two second delay, the text written to the LCD was replaced with “V in: ” on the top row and “Batt V: ” on the second row.

```
 text  = "V in: ";                    // assign text to string
 text2 = "Batt V: ";
```

The remainder of the code was written inside of an intentionally eternal while loop. As long as the microcontroller remained on, the loop would continue to cycle indefinitely. ADC readings were first taken from pins RB10 and RB11 on the microcontroller.

```
while (1) {
   adc_rd  = ADC1_read(10);           // get ADC value from 2nd channel
(Pin 23)
   adc_rd2 = ADC1_read(11);              // get ADC value from 3rd channel
(Pin 22)
   LCD_Out(1,1,text);                 // print string on LCD, 1st row, 1st
collumn
   LCD_Out(2,1,text2);                // print string on LCD, 2nd row, 1st
collumn
```

The values ch3 and ch4, used to take average voltage measurements every second, needed to be reset with each iteration.

```
   ch3 = 0;
   ch4 = 0;
```

Contained within the while loop was a for loop which repeated 500 times in succession, terminating in a 2ms delay, equating to a one second loop.

```
for(i=0;i<500;i++)
{
```

The system input voltage was first converted to a 5V scale by multiplying by 5000 and dividing by 1023 ($2^{10} - 1$).

```
tlong = (long)adc_rd * 5000;        // convert adc reading to millivolts
tlong = (tlong / 1023);             // 0...1023 -> 0-5000mV
```

Next, the individual digits of the voltage measurement were extracted and stored in chA, chB, and chC. The denominator for the tens volt digit was first computed based on the voltage divider ratio of 1:21. Subsequent denominators were derived by dividing by ten and rounding to the nearest integer value.

```
chA = (tlong / 767);                // extract 10 volts digit
chB = (tlong / 77) % 10;            // extract volts digit
chC = (tlong / 8) % 10;             // extract 0.1 volts digit
```

To compensate for a small error in the measured voltage after the voltage divider, which initially resulted in a display undershoot error of roughly 12.5%, the value x was stored with the actual measured input voltage (with tens digit chA multiplied by ten) and then divided by eight to acquire 12.5% of the measured value.

```
x = ((10 * chA) + chB);             //Correction term of 12.5%
x = (x / 8);
```

The correction term x was then added to the measured voltage. Assuming an input less than 72V, the correction term was guaranteed to be 9V or less. As such, for the case when x added to the ones digit raised the ones digit to a value of nine or less, the tens digit did not need to change. For the case when x added to the ones digit raised the ones digit above nine, the tens digit was incremented by one and the ones digit was decremented by (10 − x).

```
if((x + chB) <= 9)                  //Add correction term to displayed voltage
chB = (chB + x);
else
{
chA = (chA + 1);
chB = (chB + x - 10);
}
```

Once the tens, ones, and tenths place digits of the system input voltage were established, they were written to the LCD. The tens digit was written to row one, column seven, the ones digit at the subsequent cursor point, followed by a decimal point and the tenths digit. The symbol V for voltage was then displayed, followed by two forced blank spaces to ensure any random erroneous displays to the LCD would be distinguishable from the voltage measurements.

```
   LCD_Chr(1,7,48+chA);              // write ASCII digit at 1st row, 7th
collumn
   LCD_Chr_CP(48+chB);               // write ASCII digit at cursor point
   LCD_Chr_CP('.');
   LCD_Chr_CP(48+chC);               // write ASCII digit at cursor point
   LCD_Chr_CP('V');
   LCD_Chr_CP(' ');
   LCD_Chr_CP(' ');
```

The process used to convert the system input voltage was also used for the battery voltage. The denominator term was computed separately based on the voltage divider used for the battery voltage input. Because the battery voltage was significantly lower than the maximum system input voltage, no correction term was required to adjust the displayed values. After calculation, the tens, ones, and tenths digits were written to the bottom row of the LCD.

```
   tlong2 = (long)adc_rd2 * 5000;    // convert adc reading to millivolts
   tlong2 = tlong2 / 1023;           // 0...1023 -> 0-5000mV

   ch2 = tlong2 / 3800;              // extract 10 volts digit
   LCD_Chr(2,9,48+ch2);              // write ASCII digit at 2nd row, 9th
collumn

   ch2 = (tlong2 / 380) % 10;        // extract volts digit
   LCD_Chr_CP(48+ch2);               // write ASCII digit at cursor point
   LCD_Chr_CP('.');

   ch2 = (tlong2 / 38) % 10;         // extract 0.1 volts digit
   LCD_Chr_CP(48+ch2);               // write ASCII digit at cursor point
   LCD_Chr_CP('V');
   LCD_Chr_CP(' ');
   LCD_Chr_CP(' ');
```

To perform hysteresis, an average system input voltage was calculated each second to compensate for DC ripple. Every 2ms, the value of the tens and ones digits of the system input voltage was accumulated for 500 iterations.

```
   ch3 = ch3 + chA;
```

```
   ch4 = ch4 + chB;
   Delay_ms(2);
      }
```

At the end of the one second for loop, the accumulated tens and ones digits of the system input voltage were divided by 500 to determine the average voltage over the previous second. This value was used to perform hysteresis.

```
                                    // HISTORESIS
   ch3 = (ch3 / 500);               // Average 10 volts digit after 0.5
seconds
   ch4 = (ch4 / 500);               // Average volts digit after 0.5
seconds
```

The tens digit was first compared to 5, and the ones digit to 5, to see if the system input voltage was in the range of 55-59V. The tens digit was then compared to 6 to see if the input voltage was greater than 59V. If either case was true, Port A was set to zero, disabling the buck converter and turning off the blue LED.

```
   if((ch3 == 5 && ch4 >= 5) || ch3 > 5)
   LATA = 0;                        // Set PORTA to 0, disable Buck over
55V
```

The tens digit was then compared to 1 and the ones digit to 5 to see if the system input voltage was in the range of 10-15V. Then tens digit was then compared to 0 to see if the input voltage was less than 10V. If wither case was true, Port A was set to zero, disabling the buck converter and turning off the blue LED.

```
   if((ch3 == 1 && ch4 <= 5) || ch3 < 1)
   LATA = 0;                        // Set PORTA to 0, disable Buck
under 15V
```

The tens digit was then compared to 2 and 5, and the ones digit to 5, to see if the system input voltage was in the range of 25-50V. If it was, Port A was set to one, enabling the buck converter and turning on the blue LED.

```
   if((ch3 == 2 && ch4 >= 5) || (ch3 > 2 && ch3 < 5))
   LATA = 1;                        // Set PORTA to 1, enable Buck for
25V−50V

  }
}
```

3.1.7 LCD Connections

The connections between the microcontroller MCU card and the LCD are depicted below in Figure 3.17. These connections were labeled on the development board, with the exception of V_O, which was initially connected to ground. Investigation of the circuit diagram for the LV 33-24 v6 development board showed that V_O was the connection for the LCD contrast. The pin was connected to a resistor to ground. Several resistor values were tried, with contrast darkening with higher resistor values, until an ideal resistor value of 4.2kΩ was found.

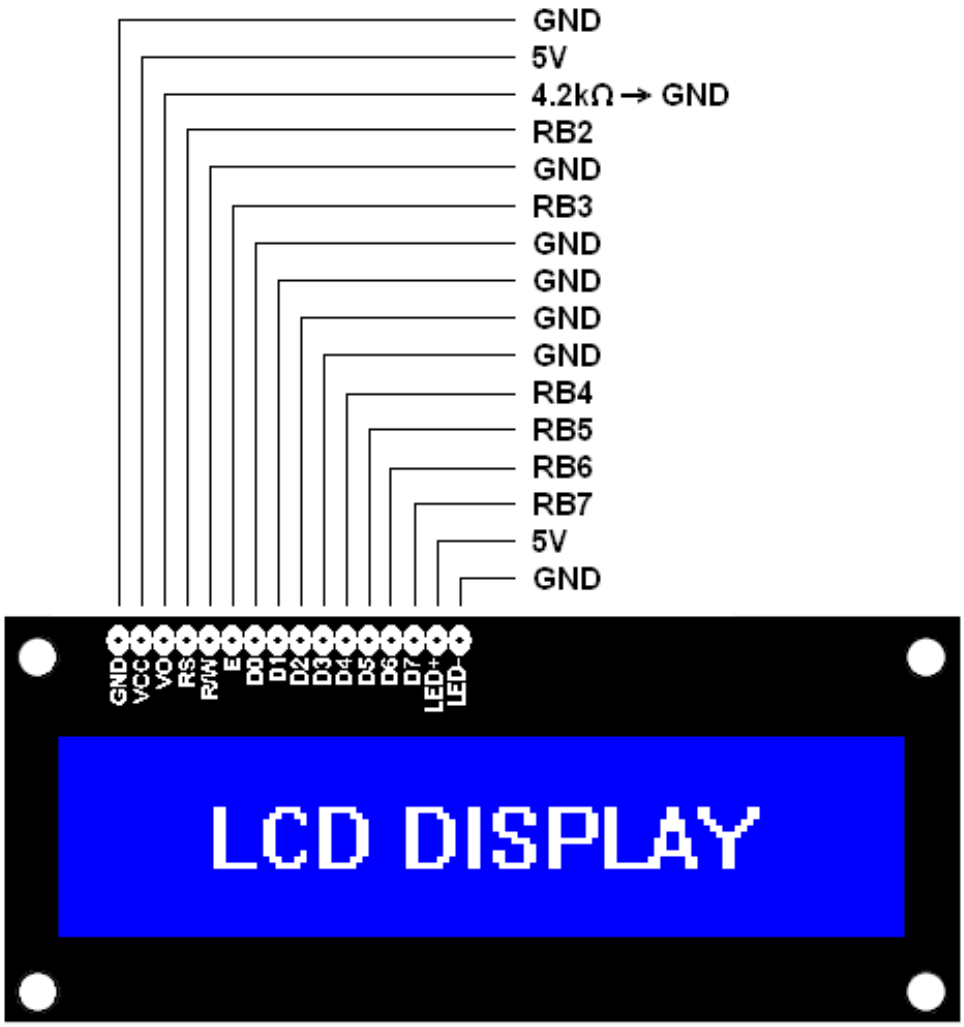

Figure 3.17: LCD Connections to MCU Card

3.1.8 System Packaging

Because this project is being designed for use at sea, it will need to be adequately protected from a number of physical threats. These include potentially harsh winds, corrosive seawater, marine animal activity, or possibly human manipulation. In order to help ensure the safety of the project, it will not only be treated with an epoxy coating, but it will also be housed in a secure, weatherproof enclosure. This enclosure will need to be comprised of a durable yet non-corroding material if it is to protect the project adequately.

The non-metallic NEMA 4X line of protective enclosures offered by AutomationDirect will provide ideal protection for the project. Figure 3.18 shows a typical non-metallic NEMA 4X enclosure. Features of the NEMA 4X enclosures include:

- Fiberglass construction
- Polyurethane seamless gasket for watertight seal
- Chemical and corrosion resistance
- Rounded edges with minimal protrusions or exposed pocket area for accumulation of debris
- Impact resistance and physical strength greater than that of ABS and PVC

Figure 3.18: System enclosure

3.1.9 Suggested Future Design Improvements

GPS – The EM-408 GPS module is a good choice because it easily interfaces with 3.3V microcontrollers. The actual supply voltage range is from 3.2 V to 3.6 V. The latter is identical to the 16-bit microcontroller utilized in the system. The average current draw of the device is 45mA. This is after the device has acquired

satellites. On startup, the device has an average draw of 75 mA with a peak draw of 90mA. The GPS can also operate in a standby mode that drops the current draw to 0.4 mA. The module can also draw up to 8mA of current to charge a capacitor used for memory storage. This storage feature helps the module to quickly lock onto satellites by storing last location and time information. Additionally, a more sensitive external antenna may be added to decrease satellite tracking time and provide the ability to place the antenna away from the electronics. There are five connections to the module. Two are for power, two are for data and one is used for enable/disable. The enable is active high, so bringing it high will enable the module. Sleep mode is accomplished by bringing it low. If this pin is left floating, it will go low. So, a resistor should be used to pull the pin high. Of the two data connections, one is used for transmit and the other is used for receive. Both of these connections use the standard serial protocol implemented in microcontroller UARTs. So, we can directly connect these pins to the microcontroller. See Figure 3.19.

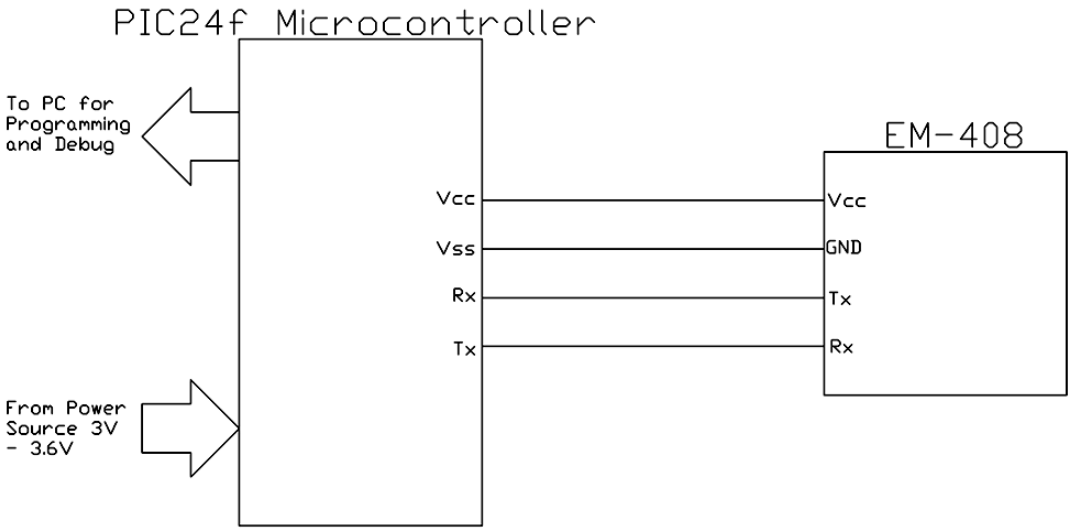

Figure 3.19: Interfacing EM-408 GPS Module to PIC24f Microcontroller

Some documentation stated the receive line must be brought high to work. However, this is false because an internal resistor pulls the line up to the supply voltage. The only issue that might occur is obtaining an error free data stream because of marginal voltage thresholds. Fortunately, our PIC microcontroller has comparators built in and one can be used to clean up the signal before sending it to the chip's UART. The module transmits data as NEMA messages at 4800 baud with 1 stop bit and no parity. The default NEMA messages outputted are GSA, GSV and RMC. Each line is terminated with a Carriage Return (CR) and Line Feed (LF) pair of characters. The NEMA standard states that the maximum number of characters between the starting $ and the CR/LF pair should be 80 characters. So, the typical output from the module upon startup should resemble the list below.

$PSRFTXT,Version:GSW3.2.4_3.1.00.12-SDK003P1.00a
$PSRFTXT,Version2:F-GPS-03-0701301
$PSRFTXT,WAAS Enable
$PSRFTXT,TOW: 0
$PSRFTXT,WK: 1399
$PSRFTXT,POS: 6378137 0 0
$PSRFTXT,CLK: 96250
$PSRFTXT,CHNL: 12
$PSRFTXT,Baud rate: 4800
$GPGGA,235947.050,,,,,0,00,,,M,0.0,M,,0000*5D
$GPGSA,A,1,,,,,,,,,,,,,,*1E
$GPRMC,235947.050,V,,,,,,,281006,,*29
$GPGGA,235948.057,,,,,0,00,,,M,0.0,M,,0000*55
$GPGSA,A,1,,,,,,,,,,,,,,*1E
$GPRMC,235948.057,V,,,,,,,281006,,*21
$GPGGA,235949.042,,,,,0,00,,,M,0.0,M,,0000*50
$GPGSA,A,1,,,,,,,,,,,,,,*1E
$GPRMC,235949.042,V,,,,,,,281006,,*24
$GPGGA,235950.042,,,,,0,00,,,M,0.0,M,,0000*58
$GPGSA,A,1,,,,,,,,,,,,,,*1E
$GPRMC,235950.042,V,,,,,,,281006,,*2C
$GPGGA,235951.042,,,,,0,00,,,M,0.0,M,,0000*59
$GPGSA,A,1,,,,,,,,,,,,,,*1E
$GPGSV,3,1,12,20,00,000,43,10,00,000,,31,00,000,,27,00,000,*7B
$GPGSV,3,2,12,19,00,000,,07,00,000,,04,00,000,,24,00,000,*76
$GPGSV,3,3,12,16,00,000,,28,00,000,,26,00,000,,29,00,000,*78
$GPRMC,235951.042,V,,,,,,,281006,,*2D
$GPGGA,235952.042,,,,,0,00,,,M,0.0,M,,0000*5A
$GPGSA,A,1,,,,,,,,,,,,,,*1E
$GPRMC,235952.042,V,,,,,,,281006,,*2E
$GPGGA,235953.042,,,,,0,00,,,M,0.0,M,,0000*5B
$GPGSA,A,1,,,,,,,,,,,,,,*1E
$GPRMC,235953.042,V,,,,,,,281006,,*2F
$GPGGA,235954.042,,,,,0,00,,,M,0.0,M,,0000*5C
$GPGSA,A,1,,,,,,,,,,,,,,*1E
$GPRMC,235954.042,V,,,,,,,281006,,*28

After locking onto enough satellites, the module should obtain the correct position and output the data below:

$GPGGA,043356.000,3158.7599,S,11552.8689,E,1,05,3.4,25.0,M,-29.3,M,,0000*56
$GPGSA,A,3,23,20,13,11,32,,,,,,,,4.7,3.4,3.4*31
$GPRMC,043356.000,A,3158.7599,S,11552.8689,E,0.24,54.42,101008,,*20
$GPGGA,043357.000,3158.7598,S,11552.8691,E,1,05,3.4,24.6,M,-29.3,M,,0000*58

$GPGSA,A,3,23,20,13,11,32,,,,,,,,4.7,3.4,3.4*31
$GPRMC,043357.000,A,3158.7598,S,11552.8691,E,0.32,57.59,101008,,*27
$GPGGA,043358.000,3158.7597,S,11552.8692,E,1,05,3.4,24.0,M,-29.3,M,,0000*5D
$GPGSA,A,3,23,20,13,11,32,,,,,,,,4.7,3.4,3.4*31
$GPRMC,043358.000,A,3158.7597,S,11552.8692,E,0.33,58.17,101008,,*20
$GPGGA,043359.000,3158.7597,S,11552.8693,E,1,05,3.4,24.4,M,-29.3,M,,0000*59
$GPGSA,A,3,23,20,13,11,32,,,,,,,,4.7,3.4,3.4*31
$GPGSV,3,1,12,11,75,324,36,01,59,146,27,32,58,161,34,20,56,209,30*75
$GPGSV,3,2,12,23,52,301,40,25,42,101,,13,23,311,23,17,19,237,23*72
$GPGSV,3,3,12,31,12,136,,19,08,358,13,14,06,136,,27,05,350,*72
$GPRMC,043359.000,A,3158.7597,S,11552.8693,E,0.29,58.06,101008,,*2B
$GPGGA,043400.000,3158.7598,S,11552.8693,E,1,05,3.4,25.0,M,-29.3,M,,0000*58
$GPGSA,A,3,23,20,13,11,32,,,,,,,,4.7,3.4,3.4*31
$GPRMC,043400.000,A,3158.7598,S,11552.8693,E,0.20,72.85,101008,,*25

A program will be written on the dsPIC33f Microcontroller to parse the GGA, RMC, GSV, and GSA NMEA commands. The main program will be called parNMEA. This program will call four functions (parGGA, parRMC, parGSV and parGSA) that will parse each of the GGA, RMC, GSV and GSA commands respectively. Each function populates a set of global variables as shown in table 3.7.

Function	Populated Variable
parGGA	GGA_UTCTime
	GGA_Latitude
	GGA_NS
	GGA_Longitude
	GGA_EW
	GGA_FIX
	GGA_FIXtxt
	GGA_Sats
	GGA_HDOP
	GGA_AltValue
	GGA_AltUnit
	GGA_Sep
	GGA_SepUnits
	GGA_Age
	GGA_Diff
parRMC	RMC_UTC
	RMC_Status

	RMC_Latitude
	RMC_NS
	RMC_Longitude
	RMC_EW
	RMC_SOG
	RMC_COG
	RMC_Date
	RMC_Variation
	RMC_Mode
parGSV	GSV_SATSINVIEW
	GSV_NOM
	GSV_MSG
	GSV_SATIDS(x)
	GSV_SATELE(x)
	GSV_SATAZ(x)
	GSV_SATSNR(x)
parGSA	GSA_SATMODE
	GSA_SATCOUNT

Table 3.7: GPS Functions and Populated Global Variables

The data from the module was been taken care of. However, it might also be useful to send commands from the microcontroller to the device. One such command is shown below:

$PSRF104,00,00,00,00,00,00,12,08*29

This command resets the module to its factory default configuration. If this command is sent at 4800 baud, it will be received by the device even if the module was placed into the wrong baud rate. The command must be terminated with a CR/LF pair. After being reset to its “factory fresh” state, this module can take at least twelve minutes to determine its location. The latter is because GPS satellites transmit information that enables the module to calculate the satellite’s orbit. After determining the orbit details of enough satellites, the module can calculate its own position. Luckily, this data will be saved in memory. The weather can also affect the satellite acquisition time. The EM-408 is equipped with an MMCX connection that can be used to connect an external antenna. This allows a more sensitive antenna to be used. Also, this antenna can be placed in a better position away from the electronics. The GPS-00464 antenna is a magnet mount antenna that has a voltage standing wave ratio of less than 2.0. It is powered off 3.3V and has a gain of 26 dB while only drawing 12mA of current.

The antenna uses a standard SMA connector. So, an interface cable like the one in Figure 3.20 would need to be purchased.

Figure 3.20: MMCX to SMA Interface Cable

Overall, adding a GPS module to the microcontroller is simple and inexpensive. Having a GPS onboard will help determine that the buoy remains tethered to the rest of the system.

Power Factor Correction – The power factor is given by a ratio of the real power to the apparent power. The value of the power factor can range from 0 to 1, and this value can result in significant harmonic distortion. If the load is pure resistance, the power factor will be equal to 1 and no harmonic distortion will occur. If the load is less than 1, harmonic distortion will occur. A power factor of 0.999 corresponds to 3% harmonic distortion, while a power factor of 0.95 corresponds to 30% harmonic distortion [12]. Clearly, the highest power factor possible is desirable.

For future design, a SEPIC topology instead of a Buck topology could be implemented. Such a topology uses a buck/boost converter. For voltages above 16V, the SEPIC converter would perform similar to the TPS54260 regulator where it will buck the voltage to the necessary amount. For voltages lower than the necessary output, the SEPIC converter would act as a boost converter and boost the input to the necessary output. During this operation, the Power Factor Correction algorithm could be implemented. The boost regulator has advantages for active power factor correction because of its continuous input current, which minimizes noise conducted and produces the optimal input current waveform. However, it requires high output voltage. By implementing a VIENNA rectifier in the output circuit, one is able to convert variable amplitude and variable frequency voltage to a DC voltage, and also control the input current, producing a sinusoid in phase with the input voltage. Thus, the VIENNA rectifier with a SEPIC topology is sufficient for power factor correction with a power factor very close to one. A recommended SEPIC converter for future design is a TPS40210 from Texas Instruments. The specifications of this converter are given in the Table 3.8.

Parameters	Values
Vin (min)	4.5V
Vout (max)	52V
Vout (min)	5V
Vout (max)	260V
Regulated Outputs	1
Iout (max)	6A
Switching Frequency (max)	1000kHz
Duty Cycle (max)	95%

Table 3.8: Specifications for TPS40210

Additionally, there is an EVM available for the TPS40210 converter. The schematic for the TPS40210EVM is shown in Figure 3.21. Although the EVM is pre configured for a 24V output, necessary results could be achieved by replacing a few components.

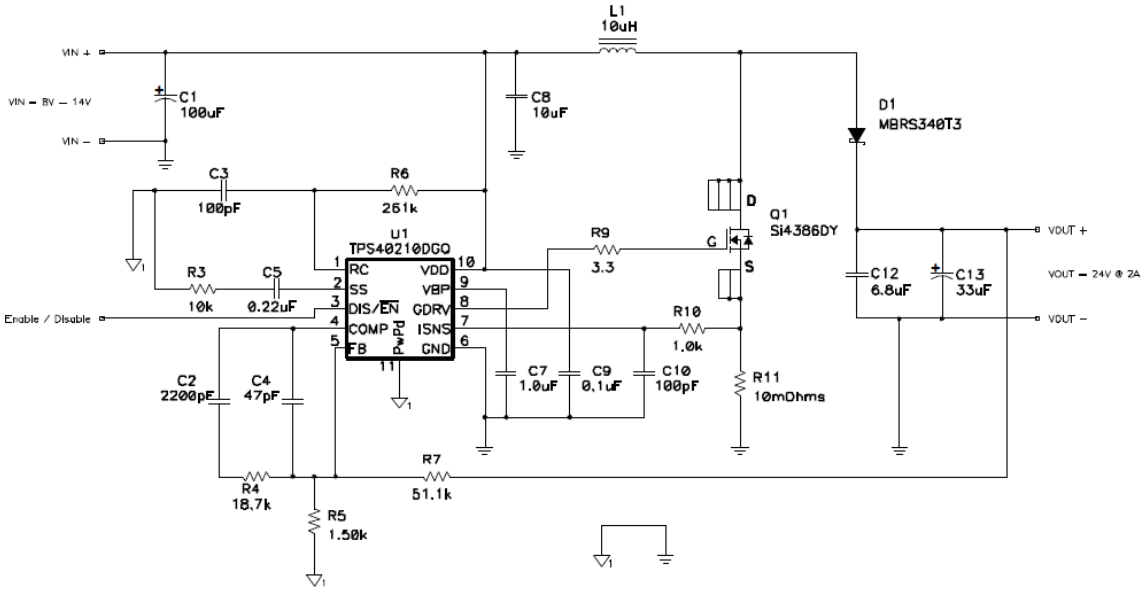

Figure 3.21: TPS40210EVM Schematic

Epoxy Potting – The most significant threat to the electrical components of this project in an environment at sea is the constant presence of seawater. Seawater is corrosive, threatening the integrity of any metallic electrical components. It was proved to be necessary to utilize some form of waterproofing in order to protect the project from the waves, rain, and sea spray. In order to accomplish this, it was determined practical to utilize an epoxy potting. The team was not able to use the Epoxy Potting for the electrical circuits in the design, as intended, due to time constraints. After the circuitry was completely assembled, the entire project was to be coated in an epoxy coating. However, for future designs, the Epoxy Potting should be implemented. Further advantages of epoxy potting include electrical isolation and protection from shock and debris.

Ellsworth Adhesives' Resinlab offers a two-part formula EP 1305 LV Black epoxy potting compound, which would offer excellent protection for the electrical components of this project. Features of the EP 1305 LV Black epoxy that would contribute to the safety of the project include:

- Resistance to water, acids, bases, and most organic solvents
- Shore durometer value of 70 D
- Service temperature of -40° to 150° C
- Volume resistivity of 5.7 x 10^{15} Ω/cm

Chapter 4: Prototype Construction

4.1 Test Facility

The research testing for this project will primarily take place in the laboratory facilities located on the University of Central Florida main campus in the Engineering I building. The facility offers a variety of resources, including professional assistance, desk space, computer access with features available for simulation, and test equipment, including a hydraulic wave simulator and a Ginlong generator.

4.2 Testing Procedures

Although UCF has developed a platform to simulate deep ocean waves, the mechanical energy team was still working on the turbine design. Therefore, another method of testing the power management circuit was needed. A bench top variac was used instead.

Before getting to that stage, the hardware and software was tested individually. Hardware components were tested with an oscilloscope, multimeter and signal generator. The microcontroller code was tested with a circuit emulator and debugger to step through faulty code. The temperature was varied to exteremes to test the circuit's ability to withstand harsh environmental conditions.

The rectifier output was verified with an oscilloscope. The output signal was analyzed over the entire range of expected generator RPMs. This produced an input signal of many frequencies and amplitudes. The input voltage was sharply increased and decreased to simulate the sudden rise and fall of ocean waves. Particular attention was given to ensure the hardware was functioning correctly. This included verifying that the power management algorithm was working as expected. Microcontroller speed affects the control algorithm that handles power management. We developed a more efficient algorithm rather than replacing the microcontroller. The algorithm could have been improved by compiling it on a more advanced compiler. However, the price of more advanced compliers and the debugging difficulties wasn't worth the marginal increase in algorithm effiecieny.

The step down DC to DC converter was tested by varying its input voltage from 20 V to 55 V and verifying a steady output of 15.6 V. There are a plethora of parameters to verify a DC to DC converter is operating correctly. Equations 4.1-4.5 were used to ensure that the DC to DC converter was functioning in a normal manner.

Output Voltage Accuracy = $\left[\frac{V_{ON}-V_O}{V_O}\right] * 100\%$ (4.1)

Regulated Line Regulation = $\left[\frac{V_{ON}-V_D}{V_{ON}}\right] * 100\%$ (4.2)

Unregulated Line Regulation = $\left[\frac{\left(\frac{V_{ON}-V_D}{V_{ON}}\right)}{\Delta V_{IN}\%}\right] * 100\%$ (4.3)

Load Regulation = $\left[\frac{V_{OM}-V_{OF}}{V_{OF}}\right] * 100\%$ (4.4)

Efficiency = $\left[\frac{V_{ON}I_{ON}}{V_{IN}V_{IN}}\right] * 100\%$ (4.5)

The hardest parameter to measure was the output ripple and noise. The ripple was measured in peak-to-peak millivolts. The output ripple was measured with a 20 MHz oscilloscope because the output ripple is a series of small pulses with high frequency content. The measurement itself had to be made with great care and with special high frequency probes. Even the conventional ground clip couldn't be used because it acted as an antenna and induced an erroneous voltage that wasn't part of the output noise of the converter. Ultimately, the goal was to obtain all the significant harmonics of ripple spikes.

The charging circuit was first tested without a battery connected. Instead an electronic model of a battery was used. A battery can be modeled as a voltage source with capabilities for both current sourcing (discharge) and current sinking (charge), in series with a resistor representing the battery's internal resistance. Then, the voltage and current of the resistor was measured to determine the efficiency of the circuit. The output voltage should remained steady and the charging circuit performed well. So, the model was replaced with a sealed lead acid battery. The charging circuit's ability to prevent overheating and overcharging was tested by connecting a fully charged battery to the circuit and monitoring the current and temperature. The current decreased to a trickle charge and wasn't applied constantly. Rather, it was applied off and on in long pulses. This method of charging prevents overheating. A short circuit test was performed by disconnecting the battery and connecting the positive and negative terminals directly to one another. The controller immediately stopped the flow of current.

Before the final assembly of the finished product, the various components needed to be tested to make certain that they were all in proper functioning order. Initial testing of the microcontroller was performed on the development board, depicted in Figure 4.1. The input circuit, buck converter, and battery charging circuit each needed to be tested on their breadboard prototypes before PCB layouts could be finalized.

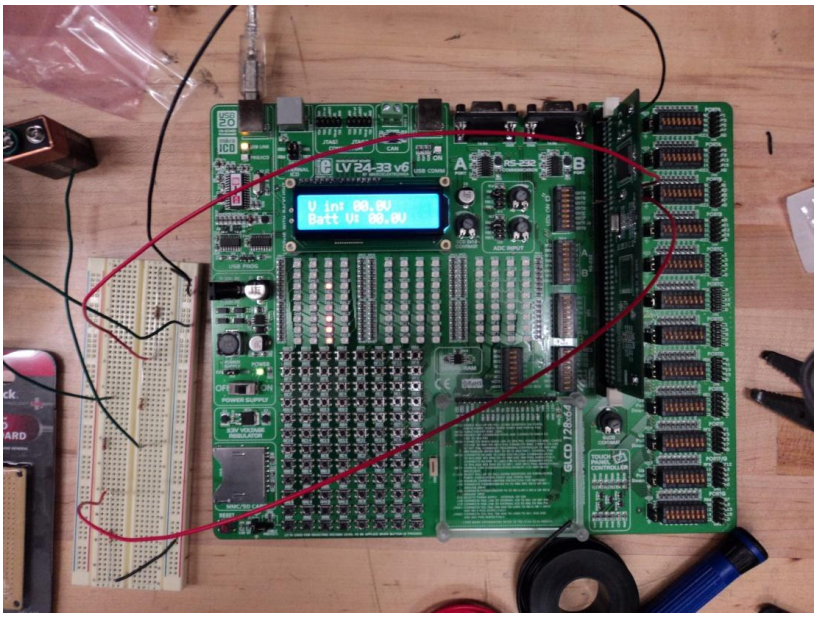

Figure 4.1: Development Board with Microcontroller and LCD

Once the microcontroller was programmed, in order to ensure that proper measurements were being taken, a 9V battery was used to simulate both the battery voltage and the system input voltage. Initially, both inputs were tied to ground to confirm that the microcontroller was taking voltage measurements. Figure 4.2 depicts the LCD when both inputs were tied to ground.

Figure 4.2: LCD Display of Grounded Inputs to the Microcontroller

At this point, the 9V battery was connected to the battery input, and the resulting display on the LCD is shown in Figure 4.3. The battery was then connected to the system input pin to show that V in displayed the same value as Batt V, even though the scaling was different for the two measurements. The resulting display on the LCD is shown in Figure 4.4.

Figure 4.3: LCD Display of Batt V Measurement of a 9V Battery

Figure 4.4: LCD Display of V in Measurement of a 9V Battery

With the components connected inside the enclosure, further testing of the entire system was conducted to confirm that each of the components was functioning correctly. Figure 4.5 shows the measurement of the 12V lead acid battery voltage, on the LCD as well as on a digital multimeter, both displaying 12.7V. The red LED in the lower left corner of the enclosure was illuminated, indicating that the input circuit was functioning and that there was system input voltage. The LCD shows this voltage to be 3.5V. The blue LED in the lower right corner was not illuminating, indicating that the microcontroller had disabled the buck converter, and that the battery was not being charged because the input voltage had not yet reached 25V.

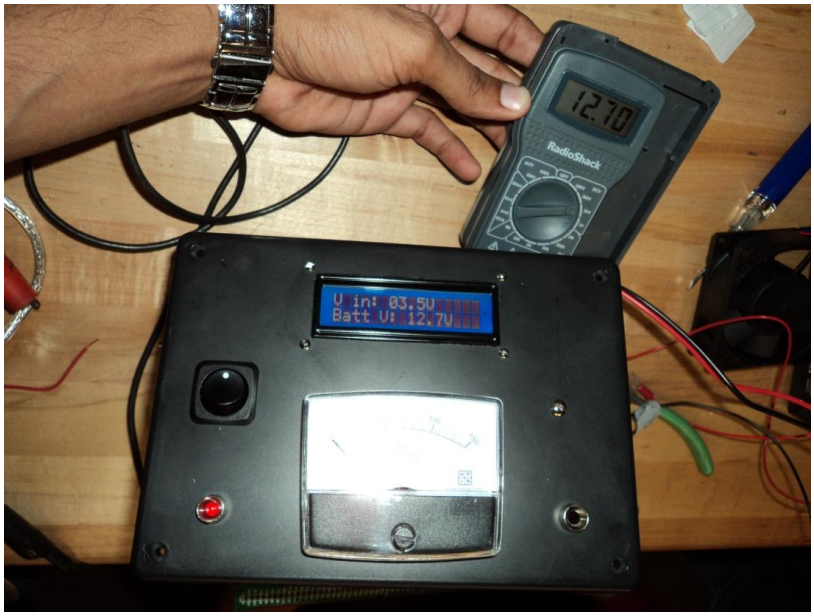

Figure 4.5: Confirmation of Battery Voltage Reading

Figure 4.6 shows the system with an input voltage of 38.8V. The red LED was on, indicating input voltage, and the blue LED was also on, indicating that the battery was being charged. The battery voltage was shown to have increased to 12.9V, confirming that the buck converter was active and that the battery charging circuit was functional.

Figure 4.6: Active System Charging the Battery

Figure 4.7 shows the system with an input voltage reduced to 11.9V. The red LED is on, indicating input voltage, but the blue LED is off, indicating that the battery is not being charged. This agrees with the programmed hysteresis which

turned off the buck converter when the input voltage dropped below 15V. The battery voltage had been drained back down to 12.7V.

Figure 4.7: Inactive System Not Charging the Battery

4.3 System Test

The entire system was built so that it could be tested on a test rig. The test is very close to a real world simulation. The test rig, which was built by the sensors team, used long enough to observe how the system performed under different environmental factors such as temperature, wind and humidity variations. The system test was developed to help discover flaws in the system that didn't appear during the individual stages and software. A slight variation in temperature would be easily manifested itself in unexpected areas.

4.4 PCB Layouts

Input Circuit – The entire input circuit was designed with software from ExpressPCB. The board was kept under 3.8" x 2.5" because of a pricing promotion by ExpressPCB. The miniboardPRO service was selected because it included 3 identical boards with a silkscreen and soldermasks. All traces were made to be 0.050" wide. The latter ensured that the input circuit could handle up to 2 amps of current. The entire PCB layout is shown in Figure 4.8.

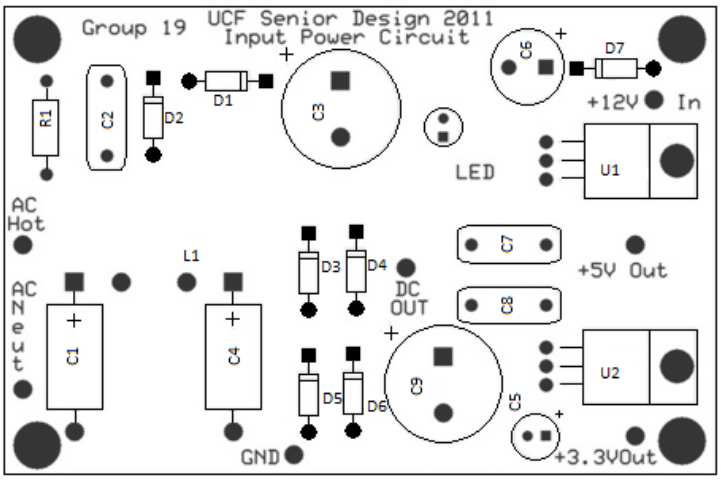

Figure 4.8: PCB layout of Input Circuit

TPS54260EVM-597 – For the TPS54269EVM, the components used were surface mounts. The two-sided layer of the EVM is a typical PCB application. The top layer includes the main power traces for V_{IN}, V_{OUT}, and V_{PHASE}. This layer also contains a large area for ground. The bottom layer consists of BOOT capacitor and ground. Although this EVM was pre populated by Texas Instruments, it will be easy to implement the same layout for future designs. The PCB layout for the TPS54260EVM-597 is shown in Figure 4.9.

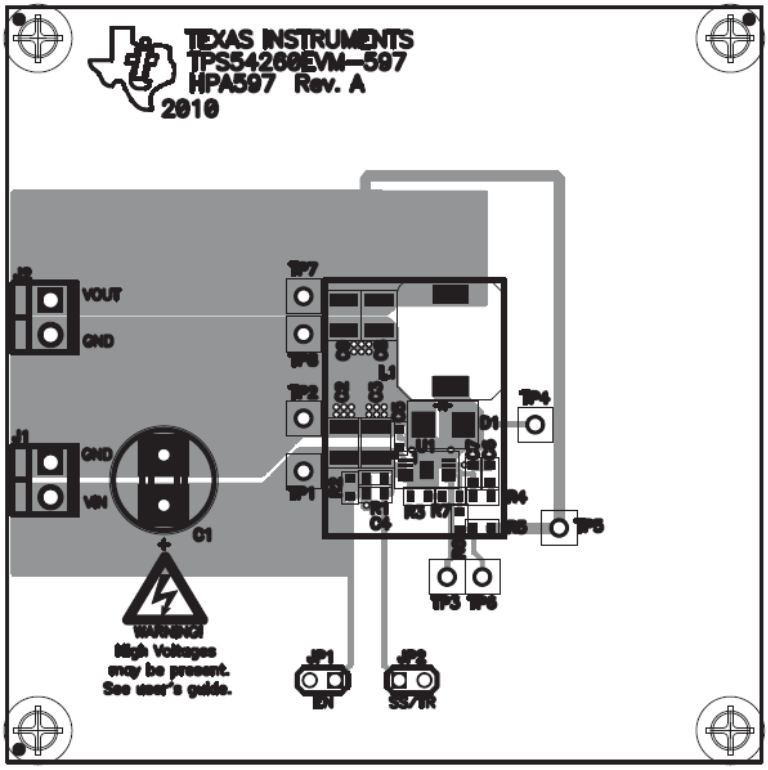

Figure 4.9: Top assembly layer of TPS54260EVM-597
(Courtesy of Texas Instruments)

BQ24450EVM-691 – The BQ24450EVM was purchased from Texas Instruments. Few changes as described in section 3.1.3 were made as per the project specifications. The PCB layout was made using some guidelines as mentioned in the BQ24450EVM user's guide [41]:

1. All low-current GND connections must be kept separate from the high-current charge or discharge paths from the battery. Use a single-point ground technique incorporating both the small signal ground path and the power ground path.
2. The high current charge paths into IN pin and from the OUT pin must be sized appropriately for the maximum charge current in order to avoid voltage drops in these traces.

Although this EVM was pre populated by Texas Instruments, it will be easy to implement the same layout for future designs. Figure 4.10 shows the PCB layout of the BQ24450EVM.

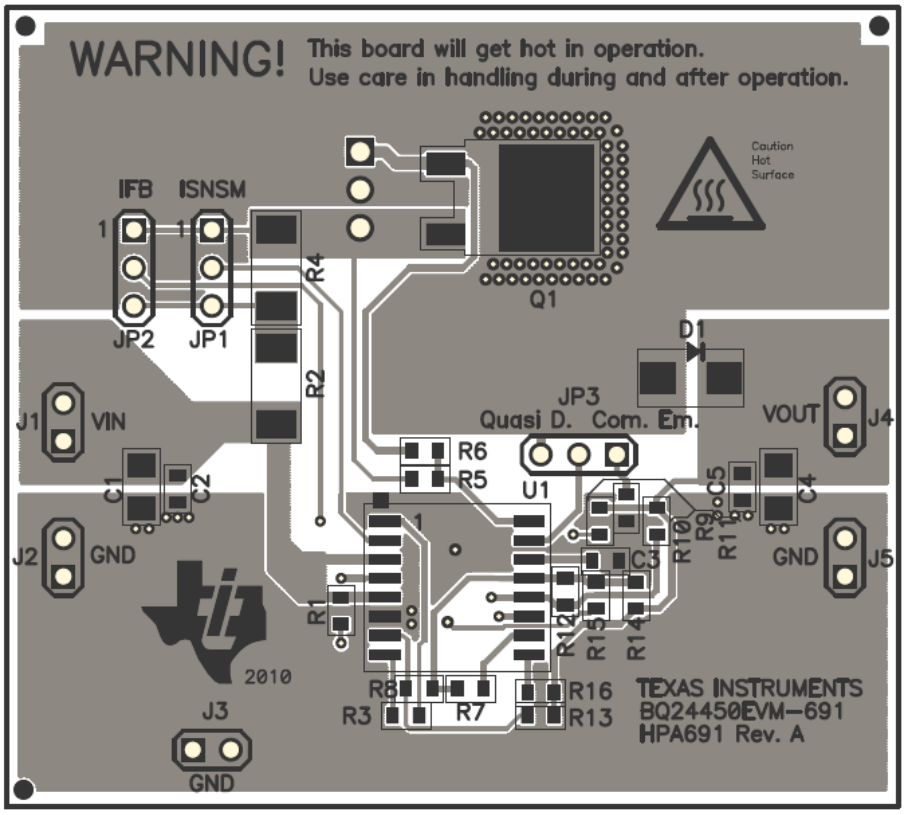

Figure 4.10: Top assembly layer of BQ24450EVM-691
(Courtesy of Texas Instruments)

Chapter 5: Project Operation

Following steps need to be taken in order to perform operations with the Electrical Unit. Figure 5.1 shows the Electrical Unit with appropriate markings.

1. As an input to the system, a varying input source is needed. This could be a generator or a variac. The input voltage needs to be between 0VAC and 60VAC.
2. Plug in the input (A) of the Electrical Unit to the output of the Power Source.
3. Attach a 12V lead acid battery to the output (B) of the Electrical Unit.
4. The sensor package needs to be attached to the output of the lead acid battery.
5. Once the above connections are made, turn on the power source and make sure that the input voltage is in the accepted range.
6. Next, turn on the switch (C) which is placed on the electrical unit.
7. The LCD screen (D) should turn on and the analog AC panel (E) on the electrical unit should show the AC input from the power source. Also, the blue LED on the right (F) should turn on for two seconds.
8. The red LED on the left (G) turns on if there is power coming in and turns off when there is no input power.
9. The blue LED (F) is for the purpose of hysteresis. The LED turns on when the input reaches 25VDC and remains on until the voltage drops to 15VDC. Also, it will turn off when the power reaches 55VDC and turns back on under 50VDC.
10. To turn off the device, simply turn off the power switch (C) on the unit.

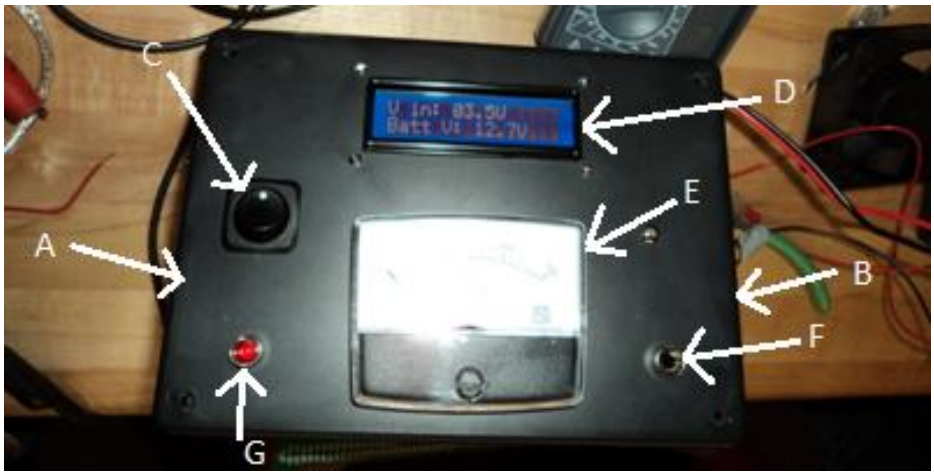

Figure 5.1: System Design

Chapter 6: Summary

6.1 Parts Procurement

The design of various key components such as the Input Circuit, Buck converter, and Battery Charging Circuit were used in order to determine different parts that needed to be acquired. Also, some equipment was readily available for use from either the research lab or other teams. That also included the ginlong generator and the wave turbine.

The other parts that were not readily available were acquired through the market. Wide varieties of individual components such as resistors, capacitors, op-amps, etc. were available for use. These components were produced by reputable manufactures such as Microchip, Texas Instruments, International Rectifier, etc. Digi-Key and Element-14 are two of the largest distributors for such parts. Most of the parts could be easily obtained from Digi-Key and Element-14 and hence they were two of the most valuable suppliers for this project. Throughout the project, technical support and project consultancy were provided by a number of sources including but not limited to Texas Instruments and Amateur Radio Club at the University of Central Florida. Edaboards.com forums were also a good source of support.

Cheapest options were considered during the purchase stage. The final parts list is shown in Table 6.1:

Item Description	Cost	% of Total Projection
Resistors	$5.56	0.39%
Capacitors	$41.34	2.87%
Inductors	$31.92	2.22%
Diodes	$12.51	0.87%
Transistors	$15.35	1.07%
LEDs	$2.98	0.21%
Lead Acid Battery	$18.06	1.26%
Buck Converter EVM	$25.00	1.74%
Battery Controller EVM	$49.00	3.41%
Microcontroller	$3.42	0.24%
Multimeter	$24.50	1.70%
Blank MCU Cards	$56.60	3.93%
Breadboards	$64.89	4.51%
Breadboard Jumper Kits	$38.82	2.70%
PCB	$262.00	18.21%
Development Kit	$467.00	32.45%
Shipping Cost	$320.00	22.24%
Total Cost	**$1,438.95**	**100%**

Table 6.1: Project Budget

6.2 Milestone Chart

Figure 6.1 shows the Milestone Chart associated with this project. Our team followed this chart very closely.

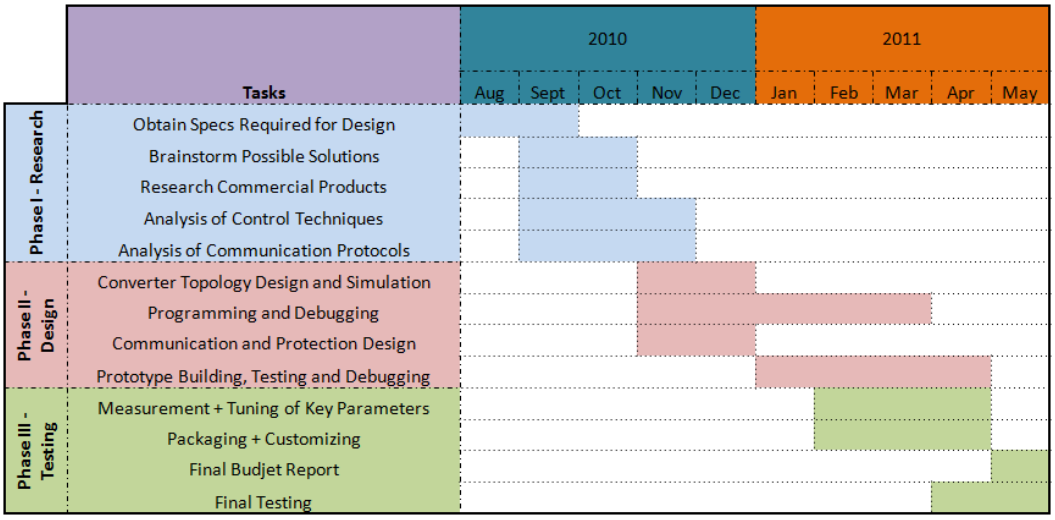

Figure 6.1: Milestone Chart

6.3 Conclusion

This project was geared towards developing a system that could efficiently convert a varying AC signal from the wave turbine generator to a steady 5VDC signal output. The conversion method of this process was presented in this report using various hardware and software components. The entire system was presented using various design elements including multisim simulations, graphs, tables, etc. Finally, the parts list was compiled and formulated in order to adequately prepare the team for the Senior Design II phase.

Project Team Content:

Louis Bengtson will be graduating with B.S.E.E. in May 2011 and plans to pursue a career in the electrical engineering profession.

Jimit Shah will be graduating with B.S.E.E. in May 2011. He plans to join Texas Instruments starting July 2011 as a Technical Sales Associate.

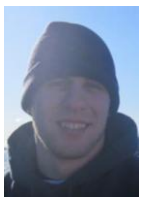

Kaleb Stunkard will be graduating with B.S.E.E. a minor in Computer Science in May 2011. He plans to pursue a career in I.T. or as a patent reviewer for USPTO.

Appendix A: Works Cited

[1] Miller, Christine. "A Brief History of Wave and Tidal Energy Experiments in San Francisco and Santa Cruz." Western Neighborhoods Projects. Western Neighborhoods Project, 03 Sep 2004. 25 Oct 2010. <http://www.outsidelands.org/wave-tidal.php>.

[2] "The untimely death of Salter's Duck." Green Left. Green Left Weekly, 29 Jul 1992. 27 Oct 2010. <http://www.greenleft.org.au/node/3401>.

[3] Kolar, Johann, Uwe Drofenik, and Franz Zach. "Space Vector Based Analysis of the Variation and Control of the Neutral Point Potential of Hysteresis Current Controlled Three-Phase/Switch/Level PWM Rectifier Systems." Proceedings of the International Conference on Power Electronics and Drive Systems. Singapore, 1995. Vol. 1, pp. 22-33.

[4] Drofenik, Uwe. " File:Vienna rectifier schematic.jpg." Wikipedia. 2 Nov 2010. <http://en.wikipedia.org/wiki/File:Vienna_rectifier_schematic.jpg>.

[5] Qiao, Chongming, and Smedley, K.M. "Three-phase unity-power-factor VIENNA rectifier with unified constant-frequency integration control." Power Electronics Congress, 2000. CIEP 2000. VII IEEE International. Acapulco, Mexico, IEEE. 2000. pp. 125-130.

[6] “3A High Voltage High-Side and Low-Side Gate Driver.” National Semiconductor. National Semiconductor, 7 Nov 2010. <http://www.national.com/pf/LM/LM5101A.html#Overview>.

[7] “MOSFET Drivers.” Analog Devices. Analog Devices, 7 Nov 2010. <http://www.analog.com/en/power-management/mosfet-drivers/products/index.html>.

[8] “LTC4440-5 - High Speed, High Voltage, High Side Gate Driver.” Linear Technology. Linear Technology, 2007. 8 Nov 2010. <http://www.linear.com/pc/productDetail.jsp?navId=H0,C1,C1003,C1142,C1041,P9990>.

[9] “PIC microcontroller.” Wikipedia. 11 Nov 2010. <http://en.wikipedia.org/wiki/PIC_Microcontroller#Microchip_programmers>.

[10] “Operational amplifier.” Wikipedia. 11 Nov 2010. <http://en.wikipedia.org/wiki/Operational_amplifier>.

[11] Braun, Daniel. “File:OpAmpTransistorLevel Colored Labeled.svg.” Wikipedia. 11 Nov 2010. <http://en.wikipedia.org/wiki/File:OpAmpTransistorLevel_Colored_Labeled.svg>.

[12] Todd, Philip C. “UC3854 Controlled Power Factor Correction Circuit Design.” Texas Instruments, 1999. 24 Nov 2010 < http://focus.ti.com/lit/an/slua144/slua144.pdf>.

[13] Texas Instruments. TPS54260 Datasheet. <http://focus.ti.com/docs/prod/folders/print/tps54260.html>

[14] Texas Instruments. BQ24450 datsheet. <http://focus.ti.com/docs/prod/folders/print/bq24450.html>

Appendix B: Permissions

The permissions for figures 3.6, 3.7, 3.8, 3.9, 3.11, 3.12, 3.13, 3.14, and 3.21 were granted by Texas Instruments under the following terms: